CENTER *for* MUSCULOSKELETAL RESEARCH

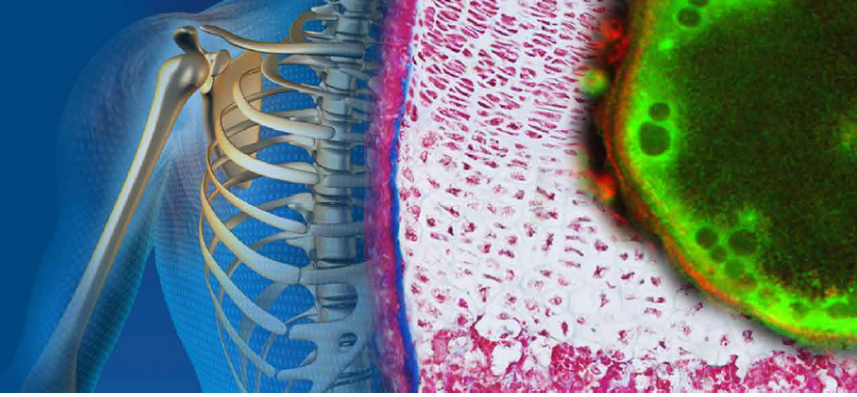

14th Annual CMSR Symposium

Thursday, October 17, 2024

Sponsored By

Department of Orthopaedics and Rehabilitation
University of Rochester Medical Center
&
National Institute of Arthritis and Musculoskeletal and Skin Diseases (NIAMS) Grant T32 AR076950-05

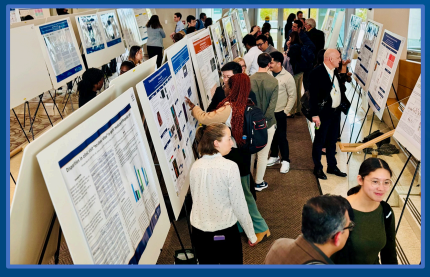

MEDICINE *of* THE HIGHEST ORDER

UR MEDICINE

ROCMSK Training Program

The Annual Center for Musculoskeletal Research (CMSR) Symposium is the centerpiece of the NIH/NIAMS funded T32 program entitled "Rochester Musculoskeletal (ROCMSK) Training Program" at the University of Rochester Medical Center. This program is designed to provide interdisciplinary didactic and research training in musculoskeletal science.

The overarching goal of ROCMSK Training Program is to develop future generations of interdisciplinary musculoskeletal scientists and leaders of innovations. The program is administered in the CMSR at the University of Rochester and integrates 21 highly collaborative faculty with primary appointments in seven academic and clinical departments.

The CMSR and associated training faculty represent a highly integrated group of mentors that provide research training opportunities in the following disciplines, highlighted by abstracts featured in this Symposium:

- Bone Biology and Disease
- Cartilage Mechanobiology
- Arthritis and Regenerative Therapies
- Tendon Development, Repair, and Regenerative Engineering
- Muscle Biology and Disease
- Drug Delivery
- Fracture Repair and Bone Tissue Engineering
- Musculoskeletal Infection, Stem Cells, and Musculoskeletal Development
- Skeletal Cancer Biology and Therapeutics

The education program ensures a comprehensive understanding of musculoskeletal science that is seamlessly accessible to all CMSR trainees at every academic level. ROCMSK training emphasizes basic and translational science education. The training experience aims to build competency in areas ranging from the most basic molecular and genetic studies to the design and execution of human clinical trials. This year, ROCMSK awarded two pre-doctoral and one post-doctoral training seats.

This Symposium is a celebration of the trainees' accomplishments.

14th Annual Center for MusculoSkeletal Research Symposium

Thursday, October 17, 2024

Zoom Link

https://urmc.zoom.us/j/96380178562

Clinical Hour Presentations

Class of '62 Auditorium (G-9425), URMC

7:00 am	*Welcome & Introduction*	***Paul Rubery, MD***
7:04 am	*Use of Machine Learning for Ultrasound Assessment of the Ulnar Nerve and Diagnosis of Cubital Tunnel Syndrome*	***Akhil Dondapati, MD*** *Constantinos Ketonis, MD, PhD*
7:12 am	*A Quantitative Analysis of Gait in Patients with Lumbar Degenerative Disease*	***Haseeb Goheer, BS*** *Ram Haddas, PhD, MBA*
7:20 am	*The Association of Hospital Volume and Patient Medical Complexity on Length of Stay, Complications, and Readmission Rates After Total Shoulder Arthroplasty*	***Patrick Castle, MD*** *Sandeep Mannava, MD, PhD*
7:28 am	*Predictors of Successful Outcomes Following Revision Carpal Tunnel Release*	***Akhil Dondapati, MD*** *Bilal Mahmood, MD*
7:36 am	*Post-traumatic Hip Osteoarthritis After Pelvic Ring Injuries*	***James Brodell, MD*** *Noah Joseph, MD*
7:44 am	*Cost Analysis of Endoscopic Carpal Tunnel Release with MAC versus Local Anesthesia*	***Thomas Carroll, MD*** *Constantino Ketonis, MD, PhD*
7:52 am	*Utilization of an Artificial Intelligence-Based Documentation System Improves Provider Efficiency in Outpatient Orthopaedic Clinics*	***Eric Davis, BA*** *Benedict DiGiovanni, MD*

Rosier Award Presentations

Class of '62 Auditorium (G-9425), URMC

	9:00 am	*Welcome & Introduction*	***Paul Rubery, MD*** ***Hani Awad, PhD***
Post-Doctoral Fellows	9:10 am	*Unraveling the Nerve: Exploring the Role of Innervation in Aging Osteoarthritis Through Advanced 3D Light Sheet Microscopy*	***Paromita Kundu, PhD*** *Lee Lab*
Post-Doctoral Fellows	9:25 am	*Ca2+ Signaling Through CaV1.2 Ca2+ Channel Regulates Achilles Tendinopathy Development*	***Haiyin Li, MD, PhD*** *Cao Lab*
Post-Doctoral Fellows	9:40 am	*Enhanced Engulfment of Apoptotic Targets by Bone Marrow Stromal Cells Increases Their Senescence, Decreases Bone, and Causes Myeloid Skewing*	***Emily Quarato, PhD*** *Calvi Lab*
Post-Doctoral Fellows	9:55 am	*Lysosomal-associated Protein Transmembrane 5 (LAPTM5) Maintains Osteoblast Formation in Young Mice by Inducing Autophagy in BM-MSCs and Its Degradation Causes Age-related Bone Loss*	***Jun Wu, PhD*** *Boyce Lab*
Pre-Doctoral Trainees	10:10 am	*PRDM16 Maintains Cartilage Homeostasis by Modulating Chondrocyte Phenotypes Break*	***Eloise Fadial, BS, MS*** *Wu Lab*
Pre-Doctoral Trainees	10:25 am	*Local Bone Remodeling Drives Clonal Expansion and Niche Interactions of Hematopoietic Stem Cells*	***Cih-Li (Amy) Hong, DVM*** *Yeh Lab*
	10:40 am	***Break***	
	11:00 am	***Deciding to Participate: Why It's Important?***	***Laura Saxby Lynch*** *MSKI Council Member*
Pre-Doctoral Trainees	11:10am	*Enabling New Insights into the Human Immune Response to Staphylococcus Aureus with a Dual-scale StaphAIR Biosensor*	***Alanna Klose, MS*** *Miller Lab*
Pre-Doctoral Trainees	11:25 am	*Validating Anti-S. Aureus Immunotherapies via Time-Lapse Fluorescent Confocal Microscopy of Neutrophil Survival, Swarming, and Opsonophagocytosis of Bacteria on Metal Implants*	***Sashank Lekkala, MS*** *Schwarz Lab*
Pre-Doctoral Trainees	11:40 am	*Fluid Flow Impacts Endothelial-Monocyte Interactions in a Model of Vascular Inflammatory Fibrosis*	***Isabelle Linares, MS*** *Awad Lab*
Pre-Doctoral Trainees	11:55 pm	*Optimizing Tissue Engineered Periosteum Biochemical Cues to Hasten Allograft Healing*	***Alyson March, BS, MS*** *Benoit Lab*
	12:10 pm	*Three-Minute Teasers (3MT) – Finalists for Best Poster Presentations*	
	12:50 pm	**Annual CMSR Photo**	**Class of '62 Auditorium (G-9425), URMC**
	1:15 pm	**Lunch & Poster Session**	**Sarah Flaum Atrium (G-9500), URMC**

Plenary Session

Class of '62 Auditorium (G-9425), URMC

CMSR Faculty Spotlight

2:30 pm **Veronica Ulici, MD, PhD**
The Role of PI3K/Akt and JNK Signaling Pathways in Long Bone and Axial Skeleton Development

3:00 pm **Andrew Berger, PhD**
Of Mice and Humans: Trying to Prescreen for Osteoporosis Using Infrared Light

3:30 pm **Benjamin Miller, PhD**
Continuous Monitoring of Cytokine Secretion in a Human Tendon on a Chip

Keynote Presentation

4:00 pm **Jennifer J. Westendorf, PhD**
PHLPP1 and Injury-Induced Osteoarthritis

5:30 pm ***Dinner and Rosier Awards Presentation*** **Sarah Flaum Atrium (G-9500), URMC**

MEDICINE of THE HIGHEST ORDER

UR MEDICINE

Keynote Speaker: Jennifer Westendorf, PhD

Professor of Biochemistry and Molecular Biology
Professor of Orthopedics
Chair, Department of Biochemistry and Molecular Biology
Mayo Clinic

Jennifer (Jen) Westendorf, Ph.D., is the *Margaret Amini Professor of Orthopedic Regenerative Medicine Research* and serves as the Chair of the Department of Biochemistry and Molecular Biology at Mayo Clinic in Rochester, MN. Dr. Westendorf directs the Skeletal Development and Regeneration Research Laboratory in Rochester, MN and is enterprise chair of the Department of Biochemistry and Molecular Biology, with faculty in Rochester, MN, Jacksonville, FL and Scottsdale, AZ.

Dr. Westendorf's research interests focus on molecular mechanisms regulating skeletal development, regeneration and repair and aims to improve the care of individuals with skeletal problems such as osteoarthritis, osteoporosis, and musculoskeletal cancers. Her federal funded research is currently focusing on how Phlpp enzymes and other proteins that control skeletal growth, and repair of joint injuries that lead to osteoarthritis.

Dr. Westendorf has directed a NIH-funded training grant (T32) in musculoskeletal research at Mayo Clinic for the last 15 years. She is proud of that any of the trainees on this program, as well as trainees in her laboratory have earned individual fellowship awards (F31, F32, K01) and research grants from the NIH (R01, P01) and other entities. Former trainees are now professors at universities, scientific editors, industry scientists and experts.

Dr. Westendorf is presently the President-Elect of ASBMR and will assume the role of President after the annual meeting in September 2024. She has also served on the Board of Directors of the ORS and the International Federation of Musculoskeletal Research Societies (IFMRS). She has also served on the Advisory Committee (Council) of the National Institute of Arthritis Musculoskeletal and Skin Diseases (NIAMS) and as Deputy Editor of the *Journal of Bone and Mineral Research (JBMR)*.

More background:

Dr. Westendorf received B.A. degrees in biology and chemistry from the University of Minnesota, Morris and a Ph.D. in biomedical sciences-immunology from Mayo Clinic. She received postdoctoral training in tumor biology and biochemistry/molecular biology at St. Jude Children's Research Hospital in Memphis, TN and Vanderbilt University in Nashville, TN. She was an Associate Professor of Orthopedics at the University of Minnesota from 2000-2006 and joined the Mayo Clinic faculty in 2007.

In recognition of her work, Dr. Westendorf has received many honors and awards, including the V Scholar Award from the V Foundation for Cancer Research, the Fuller Albright Award from American Society for Bone and Mineral Research (ASBMR), the Orthopedic Research Society (ORS) Women's Leadership Forum Award, and the Dean's Recognition Award from the Mayo Graduate School. She is Fellow of the ASBMR.

Symposium Papers

Clinical Hour Abstracts

1	Akhil Dondapati, MD	Use of Machine Learning for Ultrasound Assessment of the Ulnar Nerve and Diagnosis of Cubital Tunnel Syndrome
2	Haseeb Goheer, BS	A Quantitative Analysis of Gait in Patients with Lumbar Degenerative Disease
3	Patrick Castle, MD	The Association of Annual Hospital Volume and Patient Medical Complexity on Length of Stay, Complications, and Readmission Rate after TSA, rTSA, and Revision TSA
4	Akhil Dondapati, MD	Predictors of Successful Outcomes Following Revision Carpal Tunnel Release
5	James Brodell, MD	POST-TRAUMATIC HIP OSTEOARTHRITIS AFTER PELVIC RING INJURIES
6	Thomas Carroll, MD	Cost Analysis of Endoscopic Carpal Tunnel Release with MAC Versus Local Anesthesia
7	Eric Davis, MBA	Utilization of an Artificial Intelligence-Based Documentation System Improves Provider Efficiency in Outpatient Orthopaedic Clinics: Reducing the Afterhours Burden of the Electronic Health Record

Rosier Awards Post-Doctoral Trainee Presentations

8	Paromita Kundu, PhD	Unraveling the Nerve: Exploring the Role of Innervation in Aging Osteoarthritis Through Advanced 3D Light Sheet Microscopy
9	Haiyin Li, MD, PhD	Ca2+ signaling through CaV1.2 Ca2+ channel regulates Achilles tendinopathy development
10	Emily Quarato, PhD	Enhanced Engulfment of Apoptotic Targets by Bone Marrow Stromal Cells Increases Their Senescence, Decreases Bone, and Causes Myeloid Skewing.
11	Jun Wu, PhD	Lysosomal-associated protein transmembrane 5 (LAPTM5) maintains osteoblast formation in young mice by inducing autophagy in BM-MSCs and its degradation causes Age-related bone loss

Rosier Awards Pre-Doctoral Trainee Presentations

12	Eloise Fadial, BS, MS	PRDM16 maintains cartilage homeostasis by modulating chondrocyte phenotypes
13	Cih-Li Hong, DVM	Local Bone Remodeling Drives Clonal Expansion and Niche Interactions of Hematopoietic Stem Cells
14	Alanna Klose, MS	Enabling new insights into the human immune response to Staphylococcus aureus with a dual-scale StaphAIR biosensor
15	Sashank Lekkala, MS	Validating Anti-S. aureus Immunotherapies via Time-Lapse Fluorescent Confocal Microscopy of Neutrophil Survival, Swarming, and Opsonophagocytosis of Bacteria on Metal Implants
16	Isabelle Linares, MS	Fluid Flow Impacts Endothelial-Monocyte Interactions in a Model of Vascular Inflammatory Fibrosis
17	Alyson March, BS, MS	Optimizing tissue engineered periosteum biochemical cues to hasten allograft healing

Rosier Award Best Poster Finalists

18	Katherine Escalera-Rivera, MS	Loss of Nr4a1 expression protects cartilage during post-traumatic Osteoarthritis
19	Christina Kaszuba, MS	Taurine Transporter Mediated Regulation of Mesenchymal Stromal Cells
20	Kevin Lee, MS	Compartmentalized Niche and Spatially Heterogenous Inflammatory Landscape Regulate Tet2+/-Mediated Clonal Hematopoiesis
21	Bei Liu, MS, MD	Microfluidic-Based Synthesis of Amorphous Calcium Phosphate Nanoparticles Enables Precise Control of Nanoparticle Characteristics and Enhance Osteogenesis
22	Yiwei Lu, BS	Senescent cells impair fracture repair by promoting ubiquitination and proteasomal degradation of PDGFRb in mesenchymal progenitor cells of aged mice
23	Samantha Muscat, BS	Physiological loading via voluntary wheel running promotes stronger murine Achilles tendons
24	Yue Peng, MS	Identification of Telocytes in the Synovial Lymphatic System and their Roles in Lymphatic Vessel Homeostasis and Function
25	Zachary Sechrist, BS	Ablation of Tumor-Derived IGFBP-3 Attenuates TGFβ-Associated Muscle Catabolism in Two Independent Murine Models of Pancreatic Ductal Adenocarcinoma
26	Eliya Tazreena Tashbib, MS	PRDM16 is required for normal nasal septal cartilage and bone development in mice
27	Cheng Xiang, PhD	Study of the role of neutrophil extracellular traps in age-related bone loss
28	Victor Zhang, BS	Type III collagen supports self-assembly of hiPSC-Endothelial Cells in a vascularized Human Tendon-on-a-Chip

Posters

29	Thomas Carroll, MD	Outcomes of Distal Radius Fractures in Geriatric Patients Following Volar Locked Versus Dorsal Bridge Plating
30	Thomas Carroll, MD	Volar Locked Plating Versus Dorsal Bridge Plating for Complete Articular (AO/OTA Type 23C) Distal Radius Fractures
31	Sandra Castillo, PhD	Neutrophil Attraction and Efferocytosis by Mesenchymal Stromal Cells
32	Sarah Catheline, PhD	Energy metabolism in osteoprogenitors and osteoblasts: prevalence of the pentose phosphate pathway
33	Jordan Cruse, BS	Analyzing the Association of the Area Deprivation Index on Patient-Reported Outcomes after Hip Arthroscopy
34	Eric Davis, MBA	Defining Provider Electronic Health Record Use Profiles for Outpatient Orthopaedic Surgery Encounters
35	Eric Davis, MBA	Quantifying the Burden of Documentation in the Electronic Health Record in Outpatient Orthopaedic Surgery Encounters
36	Akhil Dondapati, MD	Clinical and Radiographic Outcomes of Distal Radius Fractures Following Dorsal Bridge Fixation to the Second Versus Third Metacarpal
37	Akhil Dondapati, MD	Machine Learning Utilization to Predict Osteoporosis Status from Plain Hand Radiographs
38	Renae Duncan, BS	Role of Mitochondrial Genetics in the Response of Bone Marrow Stromal Cells to Mechanical Stimulation
39	Phu Duong, PhD	CUT&Tag applied to zebrafish adult tail fins reveals a return of embryonic H3K4me3 patterns during regeneration
40	Chris Dussik, MD	Patient-Specific Factors Impact Outcomes Following Flexor Tendon Repair

41	Edgardo Franco, BS	Endothelial Cell Remodeling in an Idh2 Mutant Murine Model
42	Dylan Greif, MD	Rotator Cuff Tear Adversely Induces Articular Cartilage Thickening and Subchondral Bone Remodeling in Mice in a Sex-Dependent Manner
43	Paul Guirguis, BS	Efficacy of Transcatheter Arterial Embolization in Traumatic Pelvic Fractures: A Systematic Review and Meta-Analysis
44	Johannes Hasler, MS	Stiffness and Topography Modulates TRPV4 Activation in AF Mechanotransduction
45	Cih-Li Hong, DVM	The Bone Marrow Stromal Network Communicates Through Intercellular Calcium Waves and is Disrupted via Gap Junction Inhibition and Single-cell Deactivation of the Hub Cells
46	Mark James, MS	Young and Aged Quiescent Joint Tissues Fail to Repair DNA Efficiently, Implications for Chronic Knee Pain After Irradiation
47	Kyle Jerreld, BS	Raman Spectroscopy of Femoral Neck samples can predict Bone Mineral Density and preliminarily classify patients as Osteoporotic
48	Kade Kaufmann	The Lower Extremity Impacts a Spine Patient's Balance and Cone of Economy
49	Elizabeth Kogan	Anti-diabetic drugs and risk of tendinopathy---A TriNetX analytic network-based study
50	Richard Lander, MD	Injury-Specific Factors Impact Outcomes Following Flexor Tendon Repair
51	Haiyin Li, MD, PhD	Dose-dependent association between hypertensive drugs and the risk of tendinopathy in a US population-based study
52	Kevin Li, BS	The Effect of CCL3 on T Cell Populations in Acute Myeloid Leukemia Bone Marrow Microenvironment
53	Melissa MacLiesh, MS	Characterizing bone marrow interstitial pH by two-photon ratiometric imaging
54	Michaela Malin, BA	PROMIS Scores Inferior in Patients Undergoing Arthroscopic Rotator Cuff Repair with C-Spine Conditions
55	Alexander Mathewson, BS	Involvement of S100a4 in post-operative abdominal adhesion formation
56	Katya McDonald, BA	T cell dysfunction during Staphylococcus aureus osteomyelitis in humanized mice
57	Himanshu Meghwani, MBBS, PhD	IL-27 is Mediated by IL-17 to Elicit Sustained Protection Against Staphylococcus aureus Osteomyelitis
58	Hayley Miller, BS	StretchToC: a tendon-on-a-chip platform for investigating the role of mechanical stimulation in fibrotic tissues
59	Jonathan Minto, MD	Can Total Shoulder Arthroplasty Save More Than Just Your Shoulder?
60	Swachi Patel, BS	Enhanced Efferocytosis by Bone Marrow Stromal Cells Decreases Support for the Hematopoietic Stem Cell Lineage
61	Amy Phan, MD	Surgery-Specific Factors Impact Outcomes Following Flexor Tendon Repair
62	Henna Purewal, BS	Outcomes and Complications of Selected Intercarpal Fusions Using Various Fixation Devices
63	Mumin Sabha, BS	Regional Augmentation of PIEZO1 Expression in Human Humeral Head Cartilage
64	Emily Schillinger, MS	Comparison of Kinematics between Markerless and Conventional Marker-Based Upper Extremity Analysis in Clinical Patients
65	Azmeer Sharipol, PhD	Validating 3D Bone Marrow Microenvironment Models: Pivotal for Advancing In Vitro Models in Preclinical Acute Myeloid Leukemia Studies
66	Chutamath Sittplangkoon, PhD	Lysosomal Degradation of TRAF3 in T Cells Causes Immunosenescence, Associated with Age-Related Bone Loss

67	Gilbert Smolyak, BS	Analyzing the Predictive Capability of PROMIS for Management of Carpal Tunnel Syndrome
68	Levy Sominsky, BA	Optimization of an In Vitro Model of Staphylococcal Abscess Communities to Study Bactericidal Mechanisms
69	Arvind Srivatsava, MS	Development of an in vitro µSiM Platform to Study Bacterial Invasion of the Osteocyte Lacuno-Canalicular Network (OLCN)
70	Churou Tang	Quantitative Diagnosis of Murine Osteoarthritis by Geometric Indices of Micro-CT
71	Allie Jia Hui Tay, BS	Real-Time Confocal Microscopy Assessment of PAD4-Mediated NETosis by S. aureus on Implants
72	Kismat Touhid, BA	ADI Is Associated with Depression Disparities at Minimum 1-Year Post-rTSA
73	Kismat Touhid, BA	Area Deprivation Index (ADI) Predicts Patient Reported Outcomes Following Total Shoulder Arthroplasty
74	Kismat Touhid, BA	Piloting ChatGPT in Summarizing Postoperative Rehab Progress Following Flexor Tendon Repair: A Validation Study
75	Jonathan Umelo, MD	Does preoperative serum glucose control affect the incidence of postoperative complications in diabetic patients undergoing primary total hip and total knee arthroplasty?
76	Giap Vu, MD	Is Socioeconomic Status Associated with Patient-Reported Outcomes Following Thumb Basal Joint Arthroplasty for Thumb Basal Joint Osteoarthritis?
77	Hannah Wang	Effects of hydroxybisphosphonate-conjugate sitafloxacin on fracture healing and skeletal growth in mice
78	Sarah Wegman, BA	Femoral Head Osteochondral Allograft Transplantation with Simultaneous Periacetabular Osteotomy for Femoral Head Undercoverage – A Case Series
79	Sarah Wegman, BA	Trends in Female Authorship of Spine Literature from 2002 to 2022
80	Brian Wise, BS, MS	Tendon Impingement Produces Regional Profiles of Intact and Fragmented Aggrecan
81	Brooke Wise, BS	Attraction and efferocytosis of apoptotic neutrophils by mesenchymal stem/stromal cells
82	Justin Wong, BS, MPH	Evaluation of PROMIS Outcomes in Patients Undergoing Cubital Tunnel Release with and without Transposition
83	Justin Wong, BS, MPH	Factors Influencing Ulnar Nerve Transposition in Cubital Tunnel Release and Revision Surgery
84	Hao Wu, BS	Quantification of micro-CT based union ratio to characterize bone graft healing mediated by tissue-engineered periosteum
85	Xiaojie Xing, PhD	NanoString GeoMx Digital Spatial Profiling of Auto and Allo Bone Graft Healing in a Murine Segmental Femoral Bone Defect Model
86	Phillip Yang, BS	Do Patients with Lumbosacral Radiculopathy Require Different Ergonomic Accommodations? A Biomechanical Lifting Analysis
87	Tony Yosick, BS	Assessing Major Osteoporotic Fracture Risk through Metacarpal Cortical Index in a Human Cadaveric Model
88	Chen Yu, MS	Mitochondrial Metabolism Determines Mesenchymal Stem Cell Fate
89	Jane Zhang, BS	TAM Inhibitor LDC1267 Blocks Bone Marrow Stromal Cell Efferocytosis and Rescues Osteoblastic Differentiation

Clinical Hour Abstracts

Disclaimer

14th Annual Center for Musculoskeletal Research Symposium
October 17, 2024

Title: Use of Machine Learning for Ultrasound Assessment of the Ulnar Nerve and Diagnosis of Cubital Tunnel Syndrome

Presenting Author: Akhil Dondapati MD

Co-Author(s): Thomas Carroll MD, Andrew Rodenhouse MD, Gilbert Smolyak BS, Jeffrey Lillie PhD, Ajay Anand PhD, Lisa Pink MS, David Mitten MD

Lab PI / Mentor: Constantinos Ketonis MD PhD

ABSTRACT

Introduction: Recent studies have established ultrasound, specifically ulnar nerve cross-sectional area (CSA), as a promising tool in the diagnosis of cubital tunnel syndrome (CuTS). The purpose of this study was to develop a machine learning algorithm trained on ultrasound images of the cubital tunnel that can be used to automatically identify and segment the ulnar nerve about the elbow and measure its CSA.

Methods: Healthy control patients were scanned using a Fujifilm-SonoSite ultrasound system, equipped with a high-frequency linear array probe [SLAx with bandwidth 6-13 MHz] by a trained technician or physician. The ulnar nerve was identified and segmented in individual frames from these videos by physicians using a custom graphical user interface application developed in-house. A convolutional neural network (YOLO8) was trained on these images to automatically segment the ulnar nerve, resulting in a binary map. The CSA and dice score was then computed using the binary map of the nerve outline from the prediction and the ground-truth to assess the prediction accuracy.

Results: In total, 34 subjects (11 patients and 23 controls) were imaged with ultrasound, and 2,011 ultrasound grayscale images were segmented from these scans: 1,286 images from 23 subjects (7 patients, 16 controls) were used to train the model, 425 images from 5 subjects (2 patients, 3 controls) were used for validation, and 300 images from 6 subjects (2 patients, 4 controls) for testing. The machine learning model resulted in an average dice score of 0.90 with 296 images (99%). When comparing the CSA predictions from the machine learning model to the area derived from the ground-truth, the mean and mean absolute difference was 1.78 (13.76%) mm2 and 2.08 mm2 (16.02%), respectively.

Discussion/Conclusions: Ultrasound is an emerging non-invasive modality in the diagnosis of CuTS. We present a novel machine learning algorithm that can accurately identify the ulnar nerve on ultrasound imaging and measure its CSA. Future directions will seek to continue to improve the accuracy of the algorithm and to generate a diagnosis of CuTS through correlation with electrodiagnostic studies, with a goal of implementation in the clinical setting for earlier detection.

14th Annual Center for Musculoskeletal Research Symposium
October 17, 2024

Title: A Quantitative Analysis of Gait in Patients with Lumbar Degenerative Disease

Presenting Author: Haseeb Goheer

Co-Author(s): Gabriel Ramirez, Andrew Megas, Ashley Rogerson, Varun Puvanesarajah, Ram Haddas

Lab PI / Mentor: Ram Haddas

ABSTRACT

INTRODUCTION: Lumbar degenerative diseases (LD) are the leading cause of low back pain and the primary leading cause of disability in adults aged 45 or older. Furthermore, LD-associated concerns and back pain are the second most common reasons for primary healthcare visits. Although patients with LD present with back pain, patients also experience altered gait patterns which contribute towards disability, reduced quality of life, and/or impairment of daily activities. For this reason, gait analysis has been explored for patients with spinal disorders. Clinical gait analysis is the process by which quantitative information is collected to aid in understanding the etiology of gait abnormalities. There is a scarcity of literature comparing LD and healthy patients using gait analysis. Further understanding of gait differences compared to healthy controls will enable clinicians to better understand the impact of LD on patients. The aim of this study was to evaluate LD, including radiculopathy and stenosis, on an individual's gait.
METHODS: Degenerative lumbar spine patients (LD) and healthy controls without spine complaints who underwent motion analysis between 2023 and 2024 at a single institution were retrospectively reviewed. Patient-reported outcomes measurement information system (PROMIS), Oswestry Disability Index (ODI), and Tampa Scale of Kinesiophobia (TSK) questionnaires were collected prior to testing. Participants were fitted with a full-body external reflective marker set for three-dimensional analysis of their gait through five 10 meters over-ground walking trials at a self-selected speed. Spatiotemporal and joint range of motion were compared between the cohorts using linear mixed-effects regression models. Groups were then compared using post-estimation comparisons using Stata 16.1, StataCorp, College Station TX. Statistical significance was set at $p < 0.05$.
RESULTS: Overall, a total of 93 participants were identified. 32 had lumbar radiculopathy and 26 had lumbar stenosis while 35 were identified as healthy controls. Patients with symptomatic lumbosacral degenerative disease presented with a statistically significant increase in ankle dorsiflexion (Right: S: 17.8° vs R: 15.9° vs H: 12.2°, $p<0.001$; Left: S: 16.3° vs R: 15.0° vs H: 12.0°, $p<0.001$), reduced ankle plantar flexion (Right: S: 7.4° vs R: 8.0° vs H: 12.5°, $p<0.001$; Left: S: 8.8° vs R: 9.3° vs H: 13.3°, $p<0.001$), reduced hip extension (Right: S: -1.3° vs R: 3.6° vs H: 11.7°, $p<0.001$; Left: S: -1.4° vs R: 4.0° vs H: 12.3°, $p<0.001$), and increase in hip flexion (Right: S: 37.4° vs H: 30.2°, $p<0.001$; Left: S: 37.2° vs H: 29.4°, $p<0.001$) during walking in comparison to controls. Moreover, larger anterior and posterior pelvic tilts were observed (S: 16.8° vs R: 11.6°; $p=0.009$ and S: 20.1° vs R: 14.6°; $p=0.003$). Additionally, significantly increased lumbar spine extension (S: 4.9° vs R: 1.0°, $p=0.015$) and lumbar flexion (S: 8.2° vs R: 4.4°, $p=0.021$) were observed in symptomatic stenosis patients when compared to radiculopathy patients. DISCUSSION: Preliminary analysis of this retrospective dataset demonstrates patients with symptomatic lumbosacral degenerative disease have significantly altered gait compared to healthy controls. Furthermore, observable differences were noted between patients with lumbar radiculopathy and lumbar stenosis. This study quantifies the impact of LD on an individual's gait. The dataset enables the continuous pre-operative and post-operative comparison of gait in patients with LD. This also potentially provides clinicians with valuable insight on kinetic changes their patients may experience to help inform discussions on managing expectations with daily living activities. Additionally, gait analysis also provides an opportunity for interdisciplinary collaboration with the rehabilitation team to guide non-operative management, including physical and occupational therapy. SIGNIFICANCE/CLINICAL RELEVANCE: Our findings demonstrate ga

14th Annual Center for Musculoskeletal Research Symposium
October 17, 2024

Title: The Effect of Annual Hospital Volume and Patient Medical Complexity on Length of Stay, Complications, and Re-Admission Rate after TSA, rTSA, and Revision TSA

Presenting Author: Patrick Castle, MD

Co-Author(s): Dylan N. Greif, M.D, Gabriel Ramirez, M.S; Patrick Castle, M.D; Caroline Thirukumaran, MBBS, MHA, PhD; Ilya Voloshin, M.D; Sandeep Mannava, M.D, Ph.D

Lab PI / Mentor: Sandeep Mannava, M.D., Ph.D

ABSTRACT

Introduction: Total shoulder arthroplasty (TSA) volume has increased over the last several decades. The ability to perform such procedures in outpatient or low volume hospital facilities is increasingly becoming necessary to offset demand. With low incidence of complications and all cause 90 day readmission rates attributed primarily to medical causes, medical stratification of patients is becoming more important in driving where patients undergo surgery. There is limited contemporary analysis on the effect of annual hospital volume and patient medical complexity on anatomic TSA (aTSA), rTSA, and revision shoulder arthroplasty procedures. The purpose of this study is to assess the effect of annual hospital volume on post-operative complications, readmissions, and length of stay in patients undergoing TSA, rTSA, and revision TSA, and if complex patients are better served in higher volume facilities.

Methods: After acquiring IRB approval, we used the 2016-2022 Statewide Planning and Research Cooperative System Database (an all-payer dataset derived from billing records in healthcare facilities in New York State) to query demographic information, procedure type, outcomes/complications, and length of stay (LOS) for patients who underwent the above procedures. Hospital volume was divided into quartiles, with quartile four the highest performing. In descriptive analysis, chi-squared tests were used for categorical variables and Kruskal-Wallis tests for continuous variables. Multivariable logistic regression was performed to determine the effect of hospital volume on odds of complications or length of stay. Elixhauser Comorbidity Sum (ECS) was used to categorize medical complexity.

Results: There were 11,388 aTSA, 19,328 rTSA, and 95 primary revision TSA patients included. In our descriptive analysis, LOS decreased by up to one and two days respectively with increasing hospital volume in TSA and rTSA patients. Patients with higher ECS undergoing revision procedures were typically clustered in higher volume facilities, yet LOS was shortest in higher volume facilities and the percentage of complications were lower in higher volume facilities. All-cause readmission did not differ for revision cases. Logistic regression demonstrated that odds of complication in patients undergoing a TSA were not affected by hospital volume, yet LOS increased (1.38, $p < 0.05$). Medicare/Medicaid patients were at increased risk of re-admission and LOS for aTSA and rTSA. Male gender increased risk of complications but lowered LOS for aTSA and rTSA. Odds of complication increased with patients undergoing rTSA in lower volume facilities (1.75, $p < 0.05$), though this trend was not seen in the lowest quartile. ECS predicted higher odds of complication and LOS for both procedures ($p < 0.05$). When comparing the probability of re-admission or post-surgical complication based on ECS and annual hospital volume, only LOS in rTSA patients was adversely affected by lower volume facilities (1.68, $p < 0.05$).

Discussion: The main finding of this study is that the odds of re-admission or complication irrespective of underlying medical complexity is similar across facilities of varying annual volume. Only LOS for rTSA patients was adversely affected based on lower annual hospital volume. As indications for aTSA and rTSA continue to expand, stratification of patients based on medical complexity may affect LOS, however patients with higher ECS scores may not need to be prioritized in higher volume facilities. Despite more complex patients undergoing revision procedures in higher volume facilities, LOS and complication rates did not change, suggesting revisions should be concentrated in higher

volume facilities. Overall, aTSA and rTSA are very safe procedures and with proper medical management can be performed in facilities of varying annual volume, though it may be cheaper to perform them in higher volume facilities based on LOS if surgery must be done inpatient.

14th Annual Center for Musculoskeletal Research Symposium
October 17, 2024

Title: Predictors of Successful Outcomes Following Revision Carpal Tunnel Release

Presenting Author: Akhil Dondapati MD

Co-Author(s): Thomas J Carroll MD, Warren Hammert MD

Lab PI / Mentor: Bilal Mahmood MD

ABSTRACT

Purpose: Carpal tunnel syndrome is the most common compressive peripheral neuropathy encountered in the general population. Many studies suggest that outcomes are generally less favorable after revision carpal tunnel release (CTR), with upwards of 40% of patients dissatisfied with their outcomes. This study sought to identify predictors of successful revision CTR and compare long-term patient-reported outcomes to individuals who underwent primary CTR. We hypothesized that patients undergoing revision CTR would have worse patient-reported outcomes scores compared to primary CTR at 1-year follow-up.

Methods: We retrospectively compared 521 primary CTR and 57 revision CTR patients. Patients with minimum one-year follow-up, including PROMIS and Patient Acceptable Symptom State (PASS) scores, were included. PASS and PROMIS Upper Extremity (UE), Pain Interference (PI), and Physical Function (PF) were compared at pre-operative and 1-year post-operative timepoints. Demographic and surgical data were compared using bivariate and multivariable analysis.

Results: Compared to the primary CTR group, the revision group had a higher BMI, was more likely to be male, have their dominant hand affected, have diabetes, undergo endoscopic CTR, and have concurrent cubital tunnel syndrome (CuTS) ($p<0.05$). A chief complaint of pain (OR 0.23, $p<0.05$), tobacco use (OR 0.11, $p<0.05$), or diabetes (OR 0.22, $p<0.05$) were less likely to have a positive PASS response, while having an interval steroid injection (OR 6.2, $p<0.05$) was a predictor of a positive PASS response. PROMIS UE and PI were better in the primary group at both pre-op and 1-year post-op visits ($p<0.05$). PROMIS PF improved in the primary group at 1-year ($p<0.05$). All PROMIS modalities did not significantly improve at 1-year follow-up in the revision group compared to pre-op ($p>0.05$). However, final PROMIS scores were improved in the primary CTR group compared to revision group in all categories ($p<0.05$). Positive PASS response in the revision group was lower pre-operatively and 1-year post-operatively
($p<0.05$).

Discussion/Conclusions: Steroid injections, lack of diabetes and tobacco use, and chief complaint of paresthesias or weakness, rather than pain, are predictors of satisfactory outcomes after revision CTR. Patients undergoing revision demonstrated worse PROMIS scores than primary CTR at 1-year follow-up. Our findings can help supplement surgeons' discussions with their patients regarding risk factors and expectations after revision CTR.

14th Annual Center for Musculoskeletal Research Symposium
October 17, 2024

Title: Post-Traumatic Hip Osteoarthritis after Pelvic Ring Injuries

Presenting Author: James D. Brodell., Jr., M.D.

Co-Author(s): Hashim J.F. Shaikh, M.D.; Thomas F. Rodenhouse, M.D.; Brian D. Giordano, M.D.; John P. Ketz, M.D.; Sandeep P. Soin, M.D.

Lab PI / Mentor: Noah M. Joseph, M.D.

ABSTRACT

OBJECTIVES:
Pelvic ring injuries typically result from a high energy mechanism and usually present with considerable associated morbidity and mortality. Unstable fracture patterns necessitate operative stabilization of the pelvic ring. Pelvic ring injuries are themselves associated with significant hemorrhage, particularly with volume-expanding injuries of the pelvis. Long-term sequelae following pelvic ring injury has been described only sparingly, though available studies describe primarily clinical outcomes including complications, ambulation, revision surgery, adjacent joint disease, and symptomatic hardware. However, there remains a paucity of literature describing the effect of pelvic ring trauma on the natural progression of arthrosis of the hip joint. Much of the existing literature concerning post-traumatic osteoarthritis after pelvic trauma has focused on acetabulum fractures. No attention has been dedicated to determining the rate of post-traumatic hip osteoarthritis after pelvic ring injuries. Therefore, the aim of this study was to describe the rate of progression of osteoarthritis in the hip following pelvic ring injury. We hypothesized that pelvic ring injury would result in a significant incidence of rapidly progressive post-traumatic hip osteoarthritis. METHODS:
Design: Retrospective Cohort
Setting: Urban/Suburban Academic Level I Trauma Center
Patient Selection Criteria: Subjects were identified using a retrospective search for pelvic ring injuries. Patients were included if they were age 18 or greater, had a pelvic ring injury, and one year or more of radiographic follow-up. Patients were excluded if they had prior total or hemi-arthroplasty of either hip, femoral neck fracture, acetabulum fracture, femoral head fracture, or inadequate radiographic follow-up.
Outcome Measures and Comparisons: Both hips were graded using the Tönnis classification at the time of injury and available follow-up pelvis films. Comparison was made between stable and unstable pelvic ring injury patients, as well as severity of injury using the Young-Burgess classification.
RESULTS:
In total, 211 patients were included for final analysis with mean follow up of 3.1 years (SD = 1.2 years). The average age of the cohort was 58.8 years (SD 28.1 years). The observed frequencies of the Young Burgess injury patterns were as follows: LC I (68.7%), APC II (13.2%), LC II (8.1%), APC I (1.8%), LC III (4.4%), and APC III (3.8%). For the Young-Burgess classification, the ICC was 0.995 with 95CI (0.991, 0.997) and p-value < 0.001. For the Tönnis classification, the ICC was 0.914 with 95%3 CI (0.854, 0.950), p-value < 0.001.Multivariable logistic regression analysis demonstrated that patients with APC III (OR 1.89; 95CI: 1.15-2.01; p = 0.01) or LC II injuries (OR 1.12; 95CI:1.05-3.01; p = 0.03) had a statistically significant risk in the progression of OA within their ipsilateral hip when referenced against patients with an LC I injury. In the regression model, neither age, ISS, CCI, nor obesity were predictive of OA progression. There was a significantly greater percentage of patients within the unstable group who demonstrated OA progression compared to patients who had stable pelvises (35.7% vs. 6.2%, p < 0.001). CONCLUSIONS:
This investigation is the first of its nature to examine the relationship of post-traumatic hip osteoarthritis in pelvic ring injury patients. We found a significant, previously unrecognized incidence of post-traumatic osteoarthritis after pelvic ring injuries. Additonal work is needed to better determine the incidence of hip OA after pelvic ring injury and possible interventions to address this asscoiated pathology.

14th Annual Center for Musculoskeletal Research Symposium
October 17, 2024

Title: Cost Analysis of Endoscopic Carpal Tunnel Release with MAC Versus Local Anesthesia

Presenting Author: Thomas Carroll

Co-Author(s): Akhil Dondapati, Andrew Park

Lab PI / Mentor: Constantinos Ketonis

ABSTRACT

Purpose: The purpose of this study was to analyze differences in the costs associated with ECTR under local and MAC anesthesia.

Methods: We retrospectively compared the surgical costs of 844 patients undergoing isolated ECTR between 2018-2024. Surgeries were performed at a surgical center associated with a large academic medical practice. Patients undergoing isolated ECTR were identified using Current Procedural Terminology (CPT) code 29848. This included 187 patients undergoing ECTR with MAC and 657 with local anesthesia. The total hospital billed procedure cost, anesthesia cost, supply cost, and post-operative care cost was calculated for each group of patients. Total time spent at the surgical center, as well as insurance type, were also recorded. Univariate analysis was completed using T-test and Chi-square analysis and statistical significance was set at $p=0.05$.

Results: ECTR under local anesthesia was associated with shorter overall time spent in the surgical center compared to MAC (148.12 minutes vs 224.41 minutes; $p<0.05$). Total hospital billed procedure cost was significantly lower in the local only group ($5,643 vs $9,073; $p<0.05$), representing an overall cost reduction of $3,430.15 in the local group. For the local group, there was also an overall lower cost of supplies ($725 vs $811; $p<0.05$), anesthesia cost ($0 vs $994; $p<0.05$), medication cost ($10 vs $69.50; $p<0.05$) and operating room/recover room time cost ($4844 vs $6822; $p<0.05$). The insurance type distribution between the two groups was significantly different, with the local group having a higher percentage of private insurance ($p<0.05$).

Conclusion: Patients undergoing ECTR with local anesthesia demonstrated overall shorter time spent in the surgical center with reduced total hospital billed procedure cost, anesthesia cost, medication/supply cost, and operating room/recovery room cost. ECTR with local only anesthesia was associated with an overall cost reduction of $3,430.15 compared to MAC and local.

14th Annual Center for Musculoskeletal Research Symposium
October 17, 2024

Title: Utilization of an Artificial Intelligence-Based Documentation System Improves Provider Efficiency in Outpatient Orthopaedic Clinics: Reducing the Afterhours Burden of the Electronic Health Record

Presenting Author: Eric Davis, MBA

Co-Author(s): Andrew Rodenhouse, MD; Philomena Burger, BA; Benedict DiGiovanni, MD

Lab PI / Mentor: Benedict DiGiovanni, MD

ABSTRACT

Introduction:

Despite recent technological advancements including smart-text phrases, note templating, and "speech recognition systems," documentation within the electronic health record (EHR) remains an arduous, monotonous task within orthopaedic surgery and may contribute to provider inefficiency, prolonged work hours, and increased burnout. The purpose of this pilot study was to determine whether the utilization of an artificial intelligence (AI)-based, ambient documentation system could improve provider efficiency in the EHR during outpatient encounters.

Methods:

A retrospective, quality improvement study was conducted. EHR metrics from providers within the Department of Orthopaedics at an urban, academic medical center and satellite facilities were collected. The EHR Epic Signal database, which provides detailed provider-level information was queried for metrics pertaining to the documentation process including the average number of appointments per day, progress note length, time in notes per day, pajama time, time on unscheduled days, time outside 7am – 7pm, time outside scheduled hours, and percent of appointments closed same day. Pajama time is defined as the average number of minutes a provider spends on charting activities on weekdays outside the hours of 7am – 5:30pm or outside scheduled hours on weekends or non-scheduled holidays. Post-utilization months (4-month interval December 2023 to March 2024) were compared to the same 4-month interval from the previous calendar year (pre-utilization) as a control to calculate the difference and percent change for each metric. Data were subclassified based on provider utilization thresholds. Additionally, the highest utilization provider's metrics were analyzed over time.

Results:

19 providers including attending physicians (n=11), advanced practice providers (n=5), and podiatrists (n=3) were included. There was no statistically significant difference in the average number of appointments per day in the pre and post-utilization periods. The average AI-tool utilization rates ranged from 24.0% to 31.4% of encounters per month in the post-utilization period. Compared to the pre-utilization period, provider use of the AI-tool improved provider efficiency across nearly all metrics analyzed. In particular, the afterhours burden parameters all had a marked reduction. The pajama time, time on unscheduled days, time outside 7am – 7pm, and time outside scheduled hours decreased 15.9 (41%), 22.3 (31%), 23.6 (61%), and 9.0 minutes (24%) respectively. The average progress note length decreased 590.5 characters (15%) and the average time in notes per day decreased 16.9 minutes (31%). However, there was no improvement seen in the percent of appointments closed same day. Interestingly, primary outcome metrics (time in notes per day, pajama time, time outside 7am – 7pm) had pronounced efficiency improvements at higher utilization thresholds. Similarly, using the highest utilization provider as an example, primary outcome metrics continued to improve over time suggesting that increased efficiency savings can be achieved with extended use.

Use of an ambient, AI-based documentation system markedly improved orthopaedic provider efficiency as measured by Epic Signal data metrics in this pilot, quality improvement study. Increased utilization rates and extended use over time allowed for maximum improvements in provider efficiency. The reduction in afterhours time and effort was striking and has the potential to have a significant positive influence on provider wellbeing. More widespread adoption of similar AI-based documentation tools may allow for reduced daily work hours, reduced provider burnout, increased efficiency and thus revenue, and overall improved satisfaction rates. This technology deserves increased attention and warrants further study.

Rosier Award Finalists Post-Doc Abstracts

Disclaimer

14th Annual Center for Musculoskeletal Research Symposium
October 17, 2024

Title: Unraveling the Nerve: Exploring the Role of Innervation in Aging Osteoarthritis Through Advanced 3D Light Sheet Microscopy

Presenting Author: Paromita Kundu

Co-Author(s): Yaxin Zhang, Mark James, Jennifer Jonason, Mark Buckley, Whasil Lee

Lab PI / Mentor: Dr Whasil Lee

ABSTRACT

Introduction: Aging osteoarthritis (OA) is a multifaceted condition characterized by the gradual deterioration of joint structures, leading to pain, stiffness, and reduced mobility. Increasing evidence suggests that nerve involvement plays a crucial role in the pain experienced by individuals with OA. Till date the distribution of nerves in knee joints has been studied using 2D histological images which limits the understanding of the precise nerve distribution. Here we for the first time investigate the 3D regulation of nerves in an aging mouse model. We particularly focused on age-related and sex-dependent changes in the nerve innervation patterns within knee joints by employing advanced imaging technique, iDISCO 3D microscopy.

Methods: Ethical approval was obtained by the institutional UCAR committee (Protocol #2019-008). Male or Female C57Bl/6 mice aged 3-5 months (young) and 20-22 months (aged) were assessed for pain like behavior using Pressure application measurement (PAM), histopathological knee OA was evaluated using SafO stain of the medial knee compartment, nerve innervation was studied by staining the whole knee with pan neuronal marker PGP9.5, sensory marker CGRP using iDISCO 3D imaging in light sheet microscopy, DRGs (L3-L5) were dissected and immunostained with pain sensory neuronal markers CGRP and PIEZO2. Statistical analysis was performed by Unpaired t-test using GraphPad Prism 10.

Results: PAM data indicates pain threshold in the hind limb joints was significantly lower in older males compared to younger mice ($p=0.0037$). However, young and old female mice did not exhibit difference in pain threshold. Additionally, histological evaluation and OARSI scoring of SafO-stained knee cartilage sections demonstrated a significant loss of staining and cartilage degeneration in aged male and female mice. 3D iDISCO immunostaining with PGP9.5, a pan-neuronal marker revealed a dense nerve fibre network around the joint in aged male mice compared to younger ones. To quantify the nerve fibres, 3D manual segmentation of the nerve filament was performed using IMARIS filament tracer software. We observed ~ 3-fold increase in filament length as well as increase in branching points in the aged male mice knee to young mice. 3D staining of the mouse knee with primary sensory nerve marker CGRP also revealed a significantly higher nerve fiber length (~ 1.5-fold) in aged male mice in comparison to young ones. Additionally, no changes in sympathetic innervation were observed in either young or aged mice of both sexes, as indicated by the 3D pattern of TH+ nerve fibers. Immunostaining of the dorsal root ganglia (DRGs), which contain the cell bodies of sensory neurons, using the sensory marker CGRP and the mechanosensory ion channel Piezo2, revealed a significant increase in both the number of CGRP-positive neurons ($p<0.0001$) and the expression of Piezo2 ($p=0.033$) in aged male mice compared to young mice. In contrast, DRGs from both young and aged female mice showed no significant differences in the expression of either CGRP or Piezo2. Discussion: The findings from this study offer important insights into the role of nerve innervation in osteoarthritis (OA) as it relates to aging. The results clearly demonstrate that natural aging is associated with mechanical hyperalgesia and the histopathological progression of OA in aged male mice. 3D staining of the knee reveals significant changes in both total nerve fiber innervation and sensory nerves in the aged male OA knee, further enhancing our understanding of the neural mechanisms driving pain in OA. The increase in CGRP and Piezo2 expression in the DRGs clearly indicates heightened pain sensitivity in the aging OA knee in male mice. This research opens new possibilities for developing targeted therapies to alleviate pain and improve the quality of life for OA patients.

14th Annual Center for Musculoskeletal Research Symposium
October 17, 2024

Title: Ca2+ signaling through CaV1.2 Ca2+ channel regulates Achilles tendinopathy development

Presenting Author: Haiyin Li

Co-Author(s): David J Ciufo, Brendan F. Boyce

Lab PI / Mentor: Chike Cao

ABSTRACT

Introduction: Achilles tendon is most susceptible to acute injury and chronic degeneration known as tendinopathy, a disease often associated with pain and disability. While repetitive overuse and acute injury are factors in the etiology of Achilles tendinopathy, how they contribute to disease pathogenesis at the cellular and molecular level remains largely unknown, hindering therapeutic advancement. We recently demonstrated that CaV1.2, an L-type voltage-gated Ca2+ channel (L-VGCC) is dynamically expressed in tendon and regulates tendon formation during development and postnatal growth, whereas its expression is very limited in healthy adult mice. Moreover, our clinical study using the TriNetX Analytics Network reveals a decreased incidence of Achilles tendinopathy in hypertensive patients with calcium channel blockers (CCBs, specific for L-VGCC) compared with those on non-CCB antihypertensives. It suggests that elevated Ca2+ signaling through aberrant CaV1.2 expression may underlie the development of Achilles tendinopathy. To test this hypothesis, we examined CaV1.2 expression in a mouse model and in human Achilles tendinopathy patients and tested the e ect of upregulated Ca2+ signaling using two CaV1.2 transgenic mouse models on the pathogenesis of Achilles tendinopathy.
Methods: This study used the CaV1.2+/lacZ reporter line (a lacZ reporter under the promoter of CaV1.2 gene), C57BL/6J, and two CaV1.2 transgenic lines: a wildtype (Scx-CaV1.2WT) or a G406R gain-of-function mutant (Scx-CaV1.2G406R). Both male and female mice were included. Partial unilateral Achilles tendon transection (PUAT) was performed on 10~12-week-old CaV1.2+/lacZ or C57BL/6J mice. To monitor CaV1.2 expression, X-gal staining was performed on Achilles tendon 7 days post-surgery (D7) from the LacZ reporter mice upon PUAT. Achilles tendinopathy development was monitored in PUAT C57BL/6J mice on D42 or two CaV1.2 transgenic lines by uCT and Alcian Blue Hematoxylin/Orange G (ABOG) staining. Immunohistochemistry (IHC) was performed in human Achilles tendinopathy samples and CaV1.2 transgenic mice to detect CaV1.2 and Runx2 expression.
Results: We found that PUAT of 10~12-week-old CaV1.2+/lacZ reporter mice (n>3) induces substantial CaV1.2 re-expression, supported by a significant increase of X-gal-stained tendon cells around the injury site on D7 post-injury, compared with the intact contralateral tendon, which has limited CaV1.2 expression. Furthermore, we verified that PUAT induces Achilles tendinopathy on D42 with ectopic bone formation, injury site scar formation and intense chondrocyte transdi erentiation/extracellular matrix degeneration in the neighboring intact portion of Achilles tendon (n>10). In human diseased Achilles tendons (n=3), extensive CaV1.2 was detected in many linearly aligned tendon cells and in the blood vessel cells in the tendon interfascicular matrix. Moreover, we found Achilles tendinopathy was developed in Scx-CaV1.2WT and Scx-CaV1.2G406R mice by 3-4 months of age with 100% penetrance in the absence of injury (n>3). This phenotype is significantly accelerated in Scx-CaV1.2G406R mutant mice with early onset and increased ectopic bone formation. ABOG staining further shows that Achilles tendinopathy is accompanied by chondrocyte (trans)di erentiation in the middle tendon substance and in the lesion of ectopic bone. Ectopic bone formation and tendon degeneration progress with age in both transgenic mouse models. Runx2 by IHC is detected in a subpopulation of linearly aligned tenocytes in both human diseased tendon and the CaV1.2 transgene expressing mice but absent in healthy mouse controls.
Discussion & Conclusion: Our study identifies a novel role of CaV1.2 channel and its mediated Ca2+ signaling which underlies the pathogenesis of Achilles tendinopathy. This finding may warrant future randomized clinical trial to explore novel treatment for Achilles tendinopathy.

14th Annual Center for Musculoskeletal Research Symposium
October 17, 2024

Title: Enhanced Engulfment of Apoptotic Targets by Bone Marrow Stromal Cells Increases Their Senescence, Decreases Bone, and Causes Myeloid Skewing.

Presenting Author: Emily R. Quarato

Co-Author(s): Noah A. Salama, Adam Tyrlik, Roman Eliseev, and Laura M. Calvi

Lab PI / Mentor: Laura M. Calvi

ABSTRACT

Background: Bone marrow stromal cell (BMSC) dysfunction impacts age-induced bone loss and alters support for hematopoietic stem cells (HSCs). One hallmark of BMSC dysfunction is senescence however, the mechanisms inducing BMSC senescence remains unclear. Previously we demonstrated during aging that bone marrow macrophages become deficient in their ability to clear apoptotic cells, a process known as efferocytosis. While macrophages act as the primary efferocytic cells, we've shown that BMSCs can contribute to efferocytic clearance. Thus we hypothesized that excess efferocytosis may contribute to BMSC dysfunction, and represent a novel mechanism of senescence, bone loss and initiation of hematopoietic malignancy.

Methods: Young (3-4m) and aged (22-24m) C57BL/6, Bai1xPrxCre, and Axl–/– mice were bred in house or received from the NIA. Neutrophils were also isolated from the peripheral blood of humans using mono-poly resolving media and then frozen at -80°C for 24hrs. For in vivo experiments, mice were injected retro-orbitally with flourescently labeled end-stage neutrophils, incubated for 18hrs before bone marrow was isolated and analyzed via flow cytometry. Using a similar schematic, BMSCs were isolated using FACS and submitted for scRNAseq at the URMC Genomic Research Core and sequenced using standard operating procedures. Final libraries were constructed with the Illumina NovaSeq6000. To measure colony formation, whole bone marrow was plated at 10e6 cells/well, incubated with complete medium for 10-14 days and stained for colony quantification. To determine bone quantity, mouse femurs were isolated and imaged using a viva CT 40.

Results: Using in vitro and in vivo functional assays and scRNA sequencing in young (3m) and aged (24m) C57Bl/6 mice we found that BMSCs increase their efferocytic burden during aging. Additionally, efferocytic BMSC had increased markers of senescence (p53 & p21) compared to non-efferocytic counterparts. To confirm that increased efferocytic burden induced BMSC senescence, we developed a mouse model of enhanced efferocytosis by BMSCs (Bai1xPrxCre). We confirmed increased rates of efferocytosis (1.2x fold) and senescence via βgal (2x fold) in vitro. Consistent with increased senescence, Bai1xPrxCre mice had a 20% decrease in CFU-F/OB formation, and an 8% reduction in cortical thickness at 3 months, which declined significantly with age (12m). Consistent with BMSC dysfunction we found decreased HSC support via a 40% reduction in colony formation (CFU-C). Analysis of bone marrow from Bai1xPrxCre mice found premature myeloid skewing, a common phenotype of aging. As high levels of efferocytic activity are associated with BMSC dysfunction, we aimed to block BMSC efferocytic activity. Using pharmacological and transcriptional data we identified Axl as the primary efferocytic receptor on BMSCs. In mice with global loss of Axl, BMSCs had decreased efferocytic efficiency in vitro (-1.27x fold) and in vivo (-1.6x fold). In concordance, we found Axl mice had a 25% increase in CFU-F/OB formation, and a 9% gain in cortical thickness at 3 months, which remained significantly higher than WT with aging. To determine if the increased bone was due to a reduction in BMSC senescence, we measure BMSC senescence in vivo via β-gal and found a significant reduction at 24m of age (3x fold).

Conclusion: Collectively, our data support the idea that excess BMSC efferocytosis is a novel mechanism to induce senescence and may be an underappreciated mechanism associated with bone loss and hematopoietic malignancy in settings of defective macrophages, as seen in aging, obesity, and diabetes-induced bone loss. Given the unique reliance of BMSC efferocytosis on Axl, a molecule that can be pharmacologically targeted, this novel mechanism may be leveraged for the treatment of bone loss in aging and in other diseases caused, in part, by BMSC efferocytic excess.

14th Annual Center for Musculoskeletal Research Symposium
October 17, 2024

Title: Lysosomal-associated protein transmembrane 5 (LAPTM5) maintains osteoblast formation in young mice by inducing autophagy in BM-MSCs and its degradation causes Age-related bone loss

Presenting Author: Jun Wu

Co-Author(s): Cheng Xiang, Rong Duan, Lianping Xing, Zhenqiang Yao

Lab PI / Mentor: Brendan F. Boyce

ABSTRACT

Background & Hypothesis: Age-related osteoporosis is characterized by reduced bone volume and strength, associted with dysfunction of bone marrow mesenchymal stromal/stem cells (BM-MSCs). Lysosomes are crucial for cellular aging control, but their roles in osteoporosis are not fully understood. Bioinformatics analysis of RNA-seq data from BM-MSCs of young (3-5 mon) and old (18-22 mon) mice revealed decreased mRNA levels of lysosomal-associated protein transmembrane 5 (LAPTM5, a transmembrane protein in late endosomes/lysosomes) in old BM-MSCs. Single cell sequence analysis also showed that LAPTM5 is mainly enriched in osteoblast/osteocyte lineage subsets of endosteum-associated BM cells, suggesting that LAPTM5 may play a role in osteoblast (OB) formation and/or function. We hypothesize that LAPTM5 enhances autophagic fluxes and supports osteoblastic bone formation in young mice and its over-expression could potentially mitigate age-related osteoporosis.

Experiments & Methods: We analyzed RNA-Seq data to identify differentially expressed genes (DEGs) with a p-value <0.05 and |log FC| >1 cutoff, and used Gene Set Enrichment Analysis (GSEA) to investigate changes in the lysosome pathway. Lysosome tracker treatment confirmed lysosome changes in aged BM-MSCs, and LAPTM5 was the most significantly changed lysosome marker DEG. We measured LAPTM5 mRNA and protein levels in BM-MSCs from young and aged mice using qRT-PCR, Western blot (WB) and immunofluorescence (IF). To determine the cause of LAPTM5 down-regulation, we treated BM-MSCs with proteasome inhibitor, MG132, and lysosome inhibitor, chloroquine. We assessed the effects of LAPTM5 overexpression (OV) and knockdown (Sh) on OB formation using ALP colony assays, and evaluated bone formation in vivo following tail vein injection of LAPTM5-OV and -Sh plasmids every 2 d for 30 d, followed by CT and H&E analyses. We measured OB-related genes (Runx2, ALP, OCN, SP7) in LAPTM5-OV and -Sh mice using qRT-PCR and WB. We assessed autophagic flux in BM-MSCs from both young and old mice by analyzing LC3-II: LC3-I ratio and SQSTM1/p62 levels with WB and IF.

Results: We identified 971 DEGs and found downregulation of the lysosome pathway in old BM-MSCs via GSEA analysis. Lysosome tracker results confirmed decreased lysosomes in old BM-MSCs. We found LAPTM5 was the most significantly changed lysosome marker DEG. LAPTM5 mRNA and protein levels were significantly lower in old (20-mon) BM-MSCs than in young (3-mon) BM-MSCs. IF confirmed that LAPTM5 protein expression was lower in BM of old mice. Treatment of BM-MSCs with MG132, but not chloroquine, rescued LAPTM5 degradation and also reduced midnolin degradation. Overexpression of midnolin accelerated LAPTM5 degradation, and midnolin knockdown inhibited it, suggesting that aging-mediated LAPTM5 degradation in BM-MSCs involves canonical proteazomal and the novel midnolin-proteasome degradation pathway. Treatment of BM-MSCs from young and old mice with LAPTM5 lentivirus for 48 hr accelerated ALP-positive colony formation, while knockdown inhibited it. Tail vein injection of LAPTM5 plasmids for 30 d increased vertebral bone mass in both 3- and 18-mon-old mice, with increased OB numbers, mineral apposition and bone formation rates, and elevated osteogenic-related genes levels. Conversely, LAPTM5 knockdown reduced these indices. LAPTM5 overexpression significantly enhanced autophagic flux in BM-MSCs, as indicated by increased LC3-II/LC3-I ratio and decreased SQSTM1/p62 levels, while knockdown had the opposite effect, suggesting that LAPTM5 promotes bone formation by enhancing autophagic flux. Discussion & Conclusions: Our findings indicate that LAPTM5 acts as an important positive regulator of bone mass in young mice by enhancing autophagic fluxes and promoting osteoblastic markers, while LAPTM5 degradation during aging contributes to age-related bone loss. We conclude that LAPTM5 appears to be a novel target for prevention of age-related osteoporosis.

Rosier Award Finalists Pre-Doc Abstracts

Disclaimer

14th Annual Center for Musculoskeletal Research Symposium
October 17, 2024

Title: PRDM16 maintains cartilage homeostasis by modulating chondrocyte phenotypes

Presenting Author: Eloise Fadial

Co-Author(s): Victoria Hansen, Eliya Tazreena Tashbib, Gulzada Kulzhanova, Alexis Klee, Jennifer Jonason

Lab PI / Mentor: Chia-Lung Wu

ABSTRACT

INTRODUCTION: Cartilage development is a complex process regulated by tightly coordinated transcription and epigenetic networks. Previously, we showed that PRDM16, a histone methyltransferase and zinc finger transcriptional factor, is upregulated during chondrogenesis of human induced pluripotent stem cells (hiPSCs). PRDM16 is also downregulated in the subchondral bone of patients with osteoarthritis (OA). Global knockout (gKO) of Prdm16 in mice results in abnormal osteogenic and chondrogenic differentiation and neonatal lethality. However, the detailed molecular mechanisms by w hich PRDM16 regulates chondrogenesis and joint homeostasis in a cartilage-specific manner remain largely unknow n. Here, we hypothesize that PRDM16 is a positive regulator of chondrocyte phenotypes and postnatal cartilage homeost asis. We aim to elucidate the regulatory mechanisms of PRDM16 by using cartilage-specific, Prdm16 conditional knockout (Col2a1-Cre;Prdm16fl/fl, cKO) mice, hiPSCs models, and single-cell RNA sequencing (scRNA-seq).
METHODS: All animal procedures were approved by IACUC. Surgery to destabilize the medial meniscus (DMM) was performed to induced knee OA on the left knees of 16-wk-old WT and cKO mice. Right knees were used as non-surgery control. Both sexes were investigated. Joints were harvested 12wk-post surgery for uCT and histological anal ysis. hiPSCs with inducible PRDM16 knockdown (KD) or overexpression (OE) were generated, differentiated into chondrocytes, and submitted for scRNA-seq. Gene ontology functional analysis was used to identify and annotate cell subsets. Data were analyzed with either one-way or two-way ANOVA as appropriate.
RESULTS&DISCUSSION: Significantly increased OA severity and osteophyte formation were observed in the DMM joints compared to the non-surgery joints in the WT male mice but not WT female mice, in line with previous finding that male mice are prone to DMM-induced OA. DMM joints also exhibited a decreasing trend in bone mineralization densit y vs non-surgery control. Interestingly, OA severity was comparable between DMM and non-surgery joints in the cKO mice, alt hough Prdm16 cKO mice had similar OA severity vs. WT mice post-DMM surgery. These results indicate that P RDM16 is necessary to maintain knee cartilage homeostasis postnatally. PRDM16 KD hiPSC-derived chondrocytes exhibited severe loss of Saf-O staining, while OE of PRDM16 maintained high staining intensity. Furthermore, w hile decreased DNA concentration was observed in the chondrogenic pellets of both edited lines vs WT pellets, only O E hiPSCs produced significant amount of GAG compared to KD line. Our observations imply a link between PRDM16 and chondrocyte viability and is consistent with previous reports showing that PRDM16 is required for heterochromatin integrity and cell survival. Unsupervised clustering of OE, KD, and WT hiPSC-derived chondrocytes revealed 11 distinct chondrocyte subpopulations. Importantly, PRDM16 KD decreased ACANhigh chondrocytes, while PRDM16 OE promoted COL3A1high fibrotic chondrocytes as compared to WT control. Psuedotime anal ysis further predicts that HMGB2+ proliferative chondrocytes exhibited bifurcated cell fates and may differentiate into eit her fibrotic or mature chondrocytes. Thus, our results indicate that neither KD nor OE PRDM16 is ideal for promoting chondrogenesis, but rather balanced PRDM16 expression may be required for proper cartilage development and homeostasis. Most importantly, scRNA-seq provides essential evidence that PRDM16 is critical for regul ating chondrocyte phenotypes.
CONCLUSION/CLINICAL SIGNIFICANCE: OA is the one of the most prevalent degenerative joint disorders and has been diagnosed in approximately a quarter billion patients worldwide. Currently, there are no disease modifying drugs for OA. Our findings indicate that PRDM16 maintains cartilage homeostasis by modulating chondrocyte phenotypes and will facilitate the development of future therapeutic applications for OA patients.

14th Annual Center for Musculoskeletal Research Symposium
October 17, 2024

Title: Local Bone Remodeling Drives Clonal Expansion and Niche Interactions of Hematopoietic Stem Cells

Presenting Author: Cih-Li Hong

Co-Author(s): Zi Yin, Wimeth Dissanayake, Kevin Lee, Montgomery Whalen, Laura M. Calvi and Shu-Chi A. Yeh

Lab PI / Mentor: Shu-Chi A. Yeh

ABSTRACT

Introduction: Hematopoietic stem cells (HSCs) reconstitute a majority of blood and immune systems. Emergency hematopoiesis is a critical process in which HSCs are rapidly activated to proliferate and boost blood cell production under stress conditions, such as acute inflammation [Olson et. Al., CSH perspectives in medicine, 10(12), (2020)]. However, such activation often compromises stemness. Identifying mechanisms to reserve a steady HSC pool with long-term reconstitution capacity under stress is central to protect HSCs from exhaustion and ensure the continuity of hematopoiesis.

We previously showed that, stressed HSCs expanded within bone marrow cavities (3D inclusion of endosteum, ~200 mm in diameter) that undergo active bone remodeling. In contrast, cells remain solitary in cavities predominately by bone deposition (D-type cavities) [Christodoulou et. Al., Nature 578, 278–283 (2020)]. The finding suggested that the microenvironemnts resided in different cavities are heterogenous; however, the functional significance is poorly understood. It remains unclear as to which cavities and microenvironment cells sustain HSC potency under stress. Here, we hypothesize that resident niche cells within the D-type cavities are hubs to retain HSCs with long-term reconstitution potential. The work aims to identify a universal mechanism that balance HSC activation and self-renewal under emergency hematopoiesis.

Methods: Intravital imaging was used to track native HSCs and progenitors (HSPCs) in live mice. HSPCs are visualized based on GFP expression driven by the Mds1 allele (Mds1GFP+), while the Mds1GFP/+Flt3cre model removes the flanked GFP cassette upon cell differentiation (Flt3 expression), allowing visualization of the long-term HSCs. Lipopolysaccharide (LPS) (35 μg/mouse, IP) was used to induce acute inflammation as a model of stress hematopoiesis. Bone remodeling was tracked using bone front staining delivered 48 hours apart (tetracyline and alizarin red, 35 mg/kg). To further determine HSC interactions with the niche and their functionality, we conducted 3-hour longitudinal tracking. We then harvested bone remodeling or D-type cavities under image guidance, and flow sort the HSCs within this compartment for colony formation assays. Functional changes were evaluated at steady state, after LPS, and after suppressing bone remodeling via zoledronic acid (ZOL, 1.2 ug/mouse/week, IP). Statistical significance was determined using a two-sided Mann-Whitney test.

Results: Our results indicated that HSCs and HSPCs remained expanded at the remodeling sites, whereas HSCs demonstrated quiescent phenotypes in D-type cavities, with a significantly lower cell motility (< 0.1 μm/minute, N=3, $p = 0.0135$). After LPS challenge, HSCs and HSPCs remain minimally expanded in D-type cavities and demonstrate frequent contact with tissue resident macrophages (TRMs), suggesting TRMs as a candidate for HSC retention. Interestingly, this interaction was further enforced after anti-resorptive treatemnt (ZOL), where HSCs remained as singlets with prolong contact with TRMs (N=3). Moreover, HSCs isolated specifically from the D-type cavities had marked elevation of colony formation capability under LPS challenge (N=3, $p=0.058$), confirming the quiescence phenotype observed in vivo.

Discussion and Conclusion: In conclusion, these findings revealed that local bone remodeling defines HSC potency, potentially through interactions with TRMs, which may represent a universal mechanism to preserve HSC potency under stress. Future work will focus on utilizing spatial transcriptomics approach to delineate the underlying HSC-

TRMs communications, and validate via imaging and pathway-specific modulations. One limitation in the current functional analyses is that colony formation assays do not reflect the long-term reconstituion potential. Therefore, competitive transplantaion assays will be further performed to evaluate multi-lineage reconsitution over 4 months.

14th Annual Center for Musculoskeletal Research Symposium
October 17, 2024

Title: Enabling new insights into the human immune response to *Staphylococcus aureus* with a dual-scale StaphAIR biosensor

Presenting Author: Alanna Klose

Co-Author(s): Christopher Beck, Mary Moran, Lisa Beck, Gowrishankar Muthukrishnan, Benjamin Miller

Lab PI / Mentor: Benjamin Miller

ABSTRACT

Introduction: There are approximately 70,000 new *Staphylococcus aureus* infections annually in the U.S.A following orthopedic surgery, costing $22 million to treat. Diagnostic tools are limited to cultures and genomic analysis of infection-site aspirate, imaging, and general blood markers of infection. Some patients recover with antibiotics, but others suffer chronic infection leading to revision surgery, sepsis, or death. The transition between acute and chronic infection is mediated by *S. aureus* protein expression, biofilm formation, and modulation of a protective or pathogenic immune response. The immune response can be characterized by anti-*S. aureus* antibody and cytokine levels. Most antibodies are protective and help clear bacteria by neutralizing antigens or tagging them for opsonization. Others, such as anti-IsdB, have pathogenic functions leading to an increased risk of sepsis. Combinations and ratios of antibody response have been used as diagnostic and prognostic biomarkers of *S. aureus* infection but have not yet been translated to a clinical tool. TNFα and IL-6 are inflammatory cytokines that enable neutrophils to reach the infection site. IL-17A, IL-17F, IL-27, and IL-10 have been found to modulate T cell response between proinflammatory IL-17-producing helper T cells (Th17) and immunosuppressive regulatory T cells (Treg), a balance that drives the protective vs. pathogenic phenotype. Thus, we hypothesize that simultaneous quantification of cytokines and anti-*S. aureus* antibodies will provide insight into the human immune response against *S. aureus*, and patterns in the antibody and cytokine levels can be used to diagnose infection and prognose outcome.
Methods: A dual scale cytokine and antibody biosensor has been developed using Arrayed Imaging Reflectometry (AIR), a label-free reflectometric biosensor. This novel assay combines label-free antibody detection with mass-based enhancement of cytokines. It can detect proteins with a billion times difference in abundance (pg/mL to mg/mL) in a single dilution of sample. The newest StaphAIR array measures antibody response against 18 *S. aureus* antigens and toxins plus 6 cytokines, procalcitonin, and C-reactive protein.
Results: Multivariate Receiver Operating Characteristic (ROC) analysis of a subset of antibody responses produced an Area Under the Curve (AUC) of 0.85, which indicates excellent discrimination between groups of healthy controls and those with orthopedic *S. aureus* infections. A Principal Component Analysis (PCA) of antibody response on an expanded StaphAIR panel clustered *S. aureus* related diseases such as Atopic Dermatitis differently from orthopedic infections. Cytokine detection on the dual-scale array has lower limits of detection <10 pg/mL for recombinant IL-17A, IL-6, and IL-10 and <50 pg/mL for TNFα, IL-17F and IL-27. These LLODs are significantly lower than average values measured by Luminex in 194 samples from infected patients, except for TNFα. Incubation of the dual-scale array in a single dilution of human serum demonstrates functionality of cytokine and antibody detection. Responses titrated out as expected when tested with a pooled positive sample.
Discussion: Results to date suggest this approach enables the study of immune response patterns in *S. aureus* related disease and infection in a new and useful manner. ROC/AUC and PCA analysis demonstrate diagnostic and predictive potential of StaphAIR. The addition of cytokines to the array is satisfactory except for TNFα. Improving the LLOD of TNFα detection has so far been unsuccessful, but it may still have value identifying high titer samples.
Significance: This dual-scale StaphAIR assay advances the study of orthopedic infections by measuring multiple aspects of the human immune response to *S. aureus* with a new level of detail using a single dilution of sample. This work can be applied to study the immune response to infection in other anatomical locations and related diseases.

14th Annual Center for Musculoskeletal Research Symposium
October 17, 2024

Title: Validating Anti-S. aureus Immunotherapies via Time-Lapse Fluorescent Confocal Microscopy of Neutrophil Survival, Swarming, and Opsonophagocytosis of Bacteria on Metal Implants

Presenting Author: Sashank Lekkala

Co-Author(s): Youliang Ren, Edward M. Schwarz, Chao Xie

Lab PI / Mentor: Edward M. Schwarz, Chao Xie

ABSTRACT

Introduction: Implant-associated osteomyelitis remains a major orthopedic challenge and Staphylococcus aureus is the most common causative pathogen. Even with improved surgical care, infection rates for elective surgery cannot be reduced below 1% indicating deficits in host immunity in these patients. We previously showed that patients undergoing surgery for bone infection had low and undetectable levels of protective antibodies, suggesting that they could benefit from passive immunization with antibodies against S. aureus. As S. aureus vaccine failures have made it clear that targeting multiple functional antigens are required, we aimed to develop an in vitro screening approach that could quantify immunotherapy efficacy in terms of increasing neutrophil survival, swarming, and opsonophagocytosis of bacteria on metal implants. To this end, we utilized time-lapse fluorescent confocal microscopy to evaluate two anti-S. aureus monoclonal antibodies (mAb): 1) anti-glucosaminidase (Gmd) that neutralizes an autolysin subunit required for binary fission; and 2) anti-pore-forming toxins (PFT) that neutralizes two different S. aureus toxins (a-hemolysin (HLA) and LukED).

Methods: We developed an in vitro co-culture system of fluorescent neutrophils and S. aureus. Briefly, etched titanium K-wires were incubated in overnight cultures of EGFP+ USA300 methicillin-resistant Staphylococcus aureus (MRSA). These implants were cocultured with tdTomato+ neutrophils isolated from the long bones of Catchup mice. The antibodies were added to the system at 50μg/ml at the beginning of the co-culture. We performed longitudinal time-lapse fluorescent microscopy at 1-, 3-, and 6- hours using a laser scanning confocal microscope. At 6 hours, SYTOX Blue, a non-vital DNA dye, was added to visualize neutrophil extracellular traps (NETs) and dead cells. Volumetric quantification of the neutrophils, S. aureus, and their co-localization was performed in Imaris, and 2-way ANOVA tests were used for statistical analyses.

Results: S. aureus nidus formation in the etches of the titanium pins were readily detected in all samples and used as the fixed region of interest for longitudinal imaging. Both anti-Gmd and anti-PFT mAb treatment resulted in increased neutrophil volume compared to the untreated controls, indicating increased neutrophil survival. This result was also confirmed by reduced SYTOX staining in the mAb treatment groups at 6 hours. The co-localized fluorescent volume (yellow) of neutrophils (red) and S. aureus (green), a surrogate for phagocytosis, was 13-fold greater in the anti-PFT treated group compared to the untreated control ($p<0.05$). In addition, the size of the co-localized clusters was 1.15-fold greater in the anti-Gmd mAb treatment group compared to the anti-PFT mAb treated ($p<0.05$) and 1.21-fold greater than the untreated control group ($p<0.05$) at 6 hours. Surprisingly, we did not see a difference in the S. aureus volume with either mAb treatment compared to the untreated control. This discrepancy might be explained by residual EGFP signal from dead bacteria. In the future, we plan to perform CFU assays at the end of imaging to quantify viable bacteria.

Discussion: Critical for the development of a polyvalent immunotherapy is the development of a rapid screen to assess the efficacy of different mAb cocktails in real time. Here we demonstrated the feasibility of our system by confirming the activity of anti-PFT and anti-Gmd mAb on increasing neutrophil survival, swarming, and opsonophagocytosis. Of note, although both mAb treatments resulted in increased neutrophil survival, their effects differ: anti-Gmd treatment resulted in reduced dissemination of S. aureus with megacluster formation, whereas anti-PFT treatment resulted in increased phagocytosis. Based on this in vitro efficacy, in vivo studies to assess the efficacy of combination anti-Gmd + anti-PFT immunotherapy to prevent and treat implant-associated osteomyelitis are warranted.

14th Annual Center for Musculoskeletal Research Symposium
October 17, 2024

Title: Fluid Flow Impacts Endothelial-Monocyte Interactions in a Model of Vascular Inflammatory Fibrosis

Presenting Author: Isabelle Linares

Co-Author(s): Raquel Ajalik, Kaihua Chen

Lab PI / Mentor: James McGrath, Ph.D., Hani Awad Ph.D.

ABSTRACT

Introduction: In contrast to healthy tendons which are hypovascular, injured tendons are characterized by vascularized fibrotic scar tissue. The increase in vasculature following tendon injury promotes chronic inflammation and the infiltration of leukocytes. Yet, the role of vascular crosstalk in the dysregulated tendon healing response remains unclear. To address this question and enable studies of cellular and molecular crosstalk, our laboratory developed a human tendon-on-a-chip (hToC) featuring a 3D tendon matrix that interfaces with a vascular compartment. The current hToC model is missing the important physiological influences of fluid flow and shear stress at the vascular wall. Thus, we hypothesize that fluid flow will alter the vascular inflammatory response in the hToC by impacting endothelial barrier function, surface adhesion protein expression, and the rate of immune cell infiltration.

Methods: We developed a plug-and-play flow insert that converts the static hToC into a fluidic hToC enabling improved mechanistic studies of the tendon vascular response. Human umbilical vein endothelial cells (ECs) were cultured in the flow channel for 24 hours statically or with physiological fluid shear stress of 1.5 and 10 dynes/cm^2. ECs were characterized via immunofluorescence staining (F-actin, VE-cadherin, PECAM-1, ICAM-1). We assessed monocyte transmigration in response to prominent cytokines in the tendon inflammatory milieu (TNF-α, TGF-β1, MCP-1) via live-phase imaging and confocal microscopy. Monocytes isolated from healthy donors (200 cells/µl) were circulated at a flow rate of 50 µl/min. We next implemented vascular flow in the hToC quad culture, which includes a tenocyte-laden tissue compartment with monocyte-derived macrophages. All data were analyzed using a one-way ANOVA with Tukey's post hoc test (n=4 biological replicates per condition).

Results: We first examined the impact of fluid flow on EC responses in the hToC and found improved barrier properties with flow as quantified by decreased VE-cadherin junctional gap width and improved PECAM-1 continuity. To investigate ICAM-1 expression, which mediates monocyte infiltration, we stimulated ECs with TNF-α and applied low (1.5 dynes/cm^2) or high (10 dynes/cm^2) shear stress. Interestingly, under low shear stress conditions, we found that a greater proportion of ECs had high levels of ICAM-1 expression (31.5 ±6.2%) when compared to static cultures (12.3±4.1%). We then live-labeled the circulating monocytes and quantified adhesion and transmigration in response to MCP-1 via confocal microscopy. With circulating flow, we observed a five-fold increase ($p<0.05$) in the number of adhered and transmigrated monocytes compared to static conditions. To further dissect the monocyte response to cytokines in the fibrotic secretome, we leveraged real-time phase microscopy. While TGF-β1 resulted in minimal monocyte transmigration, TNF-α and MCP-1 induced over 50% transmigration. These results indicate that monocyte infiltration may be less dependent on TGF-β1. With these studies in place, we applied vascular flow in the hToC quad culture model with or without tissue macrophages and found that the inclusion of tissue macrophages significantly increased ($p<0.01$) circulating monocyte infiltration.

Discussion: Collectively, our results underscore the importance of physiological fluid flow in modeling the vascular inflammatory response associated with tendon fibrosis. The fluidic hToC provides a reductionist approach to elucidate critical endothelial-monocyte interactions and their crosstalk with tendon cell types. Future work will extend vascular flow studies in the complete hToC model to investigate myofibroblast differentiation, matrix deposition, and secretome profiles in the tissue. The inclusion of circulating flow in the hToC will also enable us to model systemically administered therapeutics and evaluate drugs targeted against immune cell infiltration.

14th Annual Center for Musculoskeletal Research Symposium
October 17, 2024

Title: Optimizing tissue engineered periosteum biochemical cues to hasten allograft healing

Presenting Author: Alyson March

Co-Author(s): Regine Choe, Danielle Benoit

Lab PI / Mentor: Regine Choe and Danielle Benoit

ABSTRACT

Though allografts remain the gold standard for treating critical-size bone defects, ~60% fail within ten years post-implantation. To emulate periosteum-mediated healing of live autografts, we have developed a tissue-engineered periosteum (TEP) to improve allograft healing. The TEP comprises cell degradable poly(ethylene glycol) hydrogels encapsulating mouse mesenchymal stem cells and osteoprogenitor cells to mimic the periosteal cell population. Our studies have shown that the extracellular matrix (ECM) that supports cell transplantation and soft tissue infiltration to initiate healing in vivo is critical. Here, we evaluated adhesive peptide identity and potential synergies between multiple peptide epitopes to investigate the role of TEP hydrogel biochemical cues that coordinate healing. We hypothesize that vascularization, as a surrogate measure for host tissue infiltration within the TEP, can be optimized via unique combinations of adhesive peptides, leading to improved allograft healing.

Endothelial cell (EC) and pericyte-like mesenchymal stem cell (MSC)-based spheroids were encapsulated in hydrogels with 1 mM RGD, GFOGER, and/or YIGSR, which mimic the ECM proteins fibronectin, collagen, and laminin, respectively. A design-of-experiments (DOE) approach was utilized to identify the effects of hydrogel functionalization on sprouting over time.

In vitro total network length and average branches per sprout increased with time for all groups. Hydrogels functionalized with RGD, RGD and YIGSR, or all three adhesive peptides produced the greatest total network length at day 5. A DOE model was developed using day 1 sprout number and day 5 total network length and branches, as we hypothesize that hydrogels that support continued vascular development in vitro would correspond to superior bone healing in vivo. Only RGD significantly promoted all three responses, while GFOGER promoted network formation and early sprout number and YIGSR did not significantly impact sprouting responses. No synergies between peptide epitopes were observed, as hydrogels with multiple adhesive peptides had less positive impact on sprouting outcomes than hydrogels with RGD or GFOGER individually. Therefore, hydrogels with RGD or GFOGER were chosen to evaluate as TEP in vivo. To assess bone graft healing, 4-mm defects were created in femurs of 10-12 week-old female C57Bl6 mice. Defects were filled with RGD or GFOGER-functionalized TEP-modified allografts, unmodified allografts, or autografts, with intact periosteum. At 3-weeks, RGD TEP and GFOGER TEP increased allograft vascular volume over unmodified allografts by 5.9-fold and 3.4-fold, respectively. However, both TEPs had comparable vascular volume to allografts at 9-weeks post-implantation. At 3-weeks, both TEPs improved bone callus volume, with RGD TEP- (3.3 ± 1.5 mm3) and GFOGER TEP-allograft bone callus volume (3.2 ± 1.5 mm3) greater than allografts (1.7 ± 0.7 mm3). At 6 and 9-weeks, RGD TEP allografts and GFOGER TEP trended toward increased bone callus volume compared to allografts. Analysis of TEP-mediated bone healing via histomorphometry and biomechanics is in progress.

In summary, RGD-functionalized hydrogels enhance vascular cell parameters to a greater extent than GFOGER or YIGSR. In vivo, RGD and GFOGER TEP orchestrate improved healing over unmodified allografts. However, RGD TEP mediated higher levels of bone callus. This study demonstrates adhesive peptide identity's effect on bone healing in vivo. The periostea's vascular network is enriched during healing, with ECs upregulating the RGD-binding αvβ3 integrin. The periosteum also recruits MSCs that differentiate into cartilage and deposit GFOGER-containing collagen. Results indicate that RGD functionalization improves bone healing, which could be attributed to the importance of RGD in the early stages of bone healing via neovascularization, while GFOGER may aid in later stages, such as cartilage callus formation.

Rosier Award Finalists 3MT Posters

Disclaimer

14th Annual Center for Musculoskeletal Research Symposium
October 17, 2024

Title: Loss of Nr4a1 expression protects cartilage during post-traumatic Osteoarthritis

Presenting Author: Katherine Escalera-Rivera

Co-Author(s):

Lab PI / Mentor: Jennifer H. Jonason and Jennifer H. Anolik

ABSTRACT

INTRODUCTION: Osteoarthritis (OA) is a complex disease that involves pathological processes in joint tissues such as cartilage and synovium. Macrophages are the most abundant immune cells in the OA-inflamed synovium and modulate inflammation by secreting both pro- and anti-inflammatory signals. Chondrocytes, the main cells in the cartilage, respond to inflammation by secreting matrix metalloproteinases (MMPs), which degrade cartilage. Prior studies found that Nr4a1-expressing macrophages play a role in resolving synovial inflammation by secreting anti-inflammatory factors and pro-resolving molecules. Data from the Accelerating Medicines Partnership (AMP) RA Phase I study revealed that as the degree of synovial inflammation increases, cell populations in the OA synovium, including monocytes/macrophages, upregulate expression of the transcription factor Nr4a1. However, the role of Nr4a1 in cells within joint tissues during OA is not fully understood. We propose that Nr4a1 acts by dampening inflammation during OA and hypothesize that its loss will lead to chronic inflammation of the synovium and accelerated cartilage degradation. METHODS: Meniscal ligamentous injury (MLI) was used to induce OA in the right knee joint of male mice. A sham surgery was performed on the left knee joint. To explore immune cell heterogeneity in the joint, the synovium of C57BL6/J wild-type (WT) mice was disaggregated one week after MLI, and flow cytometry was conducted (n=5). This experiment was also performed with Nr4a1-GFP reporter mice to assess Nr4a1 expression (n=5). Comparisons between MLI and SHAM groups were made using Unpaired t-tests. To understand the role of Nr4a1 in OA joint tissues, MLI was performed on Nr4a1 WT, Heterozygous (Het), and Knockout (KO) littermates (WT n=3, Het n=4, KO n=6). Hindlimbs were harvested 4 weeks later for histology. Comparisons were made using one-way ANOVA, Tukey's post-hoc test. To assess the impact of Nr4a1 loss in chondrocytes during OA-like conditions, ATDC5 chondrogenic cells were transfected with non-targeting and siRNA targeting Nr4a1. After 48 hours, cells were treated with IL-1β for 4 hours followed by RNA extraction. Once confluent, primary Nr4a1 KO and WT chondrocytes were also treated with IL-1β. Expression levels of genes related to cartilage catabolism and anabolism were measured by qPCR. Comparisons were made using Two-way ANOVA, Tukey's post-hoc test. P values <0.05 indicate significant differences between groups. RESULTS: We observed a higher percentage of macrophages in the synovium of WT mice after MLI compared to sham joints ($p<0.05$). Nr4a1-GFP reporter mice exhibited a higher percentage of macrophages expressing Nr4a1 in the synovium after MLI compared to sham joints ($p<0.05$). Histomorphometry analysis revealed a significant loss of total tibial cartilage area in Nr4a1 WT knee joints compared to Het and KO joints ($p<0.01$ and $p<0.05$, respectively). Furthermore, loss of Nr4a1 in both ATDC5 chondrogenic cells transfected with Nr4a1 siRNA and primary Nr4a1 KO chondrocytes led to a significant decrease in MMPs gene expression after IL-1β treatment compared to controls. There were no significant changes in cartilage anabolism-related genes after IL-1β treatment. DISCUSSION: Unexpectedly, KO of Nr4a1 led to the preservation of cartilage integrity in our OA mouse model. Our findings suggest that Nr4a1 is expressed in macrophages and chondrocytes during OA-related inflammation, and its downregulation reduces the expression of MMP genes in chondrocytes. Targeting Nr4a1 during OA could be a new approach to reduce MMP secretion and preserve cartilage integrity. Undergoing experiments will assess synovial cell composition and MMP cartilage expression in Nr4a1 KO mice after OA induction. Future studies will focus on conditional deletion of Nr4a1 in macrophages and chondrocytes to understand its role in these cell populations during OA, addressing a current limitation of our mouse model.

14th Annual Center for Musculoskeletal Research Symposium
October 17, 2024

Title: Taurine Transporter Mediated Regulation of Mesenchymal Stromal Cells

Presenting Author: Christina M. Kaszuba

Co-Author(s): Benjamin J. Rodems, Sonali Sharma, Edgardo I. Franco, Takashi Ito, Emily R

Lab PI / Mentor: Dr. Jeevisha Bajaj (primary) & Dr. Hani Awad (co-advisor)

ABSTRACT

Background & Hypothesis: Mesenchymal stromal cells (MSCs) are type of multipotent cells that reside in the bone marrow microenvironment and have the ability to differentiate into various cell types including osteoblasts, adipocytes, fibroblasts, and chondrocytes. Our analysis of publicly available single cell RNA sequencing datasets of the murine bone marrow microenvironment indicates that MSCs have the highest expression of the Slc6a6 gene relative to other non-hematopoietic stromal populations. This gene encodes for the taurine transporter (TauT) where the majority of taurine, a non-essential amino acid, is transported into cells via this transporter. These data indicate that TauT may play a functional role in MSCs. Recent work has identified that taurine may mitigate the onset of bone defects in aged populations. However, it is not known if deficiencies in taurine uptake can alter MSC populations that give rise to these osteolineage cells, and whether this can contribute to defects in bone formation in young populations.

Experiments, Methods, & Results: Our data show that both male and female TauT murine femurs have significantly lower number of MSCs (n=14). Consistent with this, in vitro fibroblastic and osteogenic colony forming unit (CFU) assays show that TauT-/- MSCs have a decreased rate of proliferation and differentiation, indicating functional defects in TauT-/- MSC function. To determine the effects of TauT loss on in vivo bone properties, we carried out dual-energy X-ray absorptiometry (n=6), micro-computed tomography (n=15), and grip strength testing on young-adult (16 week) TauT+/+ and TauT-/- mice. Our data suggests that while the loss of TauT decreases both cortical and trabecular bone mineral density and thickness, there is no impact on muscle strength. Further, our bone biomechanical torsion and compression analysis suggests there is a bone strength defect associated with TauT loss (n=5). Power analysis was used to determine sample size ($\beta = 0.80$) for each experiment. Quantifiable outcomes were compared using ANOVA or statistical student's unpaired T-tests with the assumption of parametric or non-parametric distribution. Furthermore, data was blinded for analysis. Mechanistically, our RNA-Seq analysis indicate a striking upregulation of hypoxia associated gene sets in MSCs lacking TauT expression, indicating that taurine mediated regulation of hypoxia may be essential for maintaining MSC function.

Discussion & Conclusion: Collectively, our data indicate that TauT loss decreases the number of functional MSCs and thus leads to weaker bone formation in young mice. We thus identify the taurine transporter on MSCs as a key regulator of bone formation and maintenance.

14th Annual Center for Musculoskeletal Research Symposium
October 17, 2024

Title: Compartmentalized Niche and Spatially Heterogenous Inflammatory Landscape Regulate Tet2+/- Mediated Clonal Hematopoiesis

Presenting Author: Kevin Lee

Co-Author(s): Cih-Li Hong, Gulzada Kulzhanova, Wimeth Dissanayake, Senthil Sivakumar, Lauren Benoodt, Zi Yin, Jeevisha Bajaj, Chia-Lung Wu, Laura Calvi, and Shu-Chi A. Yeh

Lab PI / Mentor: Shu-Chi A. Yeh

ABSTRACT

Background: Clonal hematopoiesis (CH) is diagnosed when greater than 2% of blood cells contain mutations associated with hematological cancer. Tet2 loss-of-function in hematopoietic stem cells (HSCs) is a prevalent driver in CH and widely affects myeloid neoplasms. It is understood that both the mutation-associated mechanisms and cell-extrinsic factors, such as inflammation, lead to selective expansion of mutant cells within the bone marrow (J. Exp Med. 218:e20201544, 2021). Despite the presence of these systemic factors, our prior work showed that clonal expansion of leukemia cells is compartmentalized by bone marrow cavities with bone remodeling (resorption) activities, whereas cells remain solitary at sites predominated by bone modeling (formation) (Nature 578:278, 2020). Guided by these findings, we ask whether local bone remodeling controls pathogenesis and progression of CH and hypothesize that resident cells in the bone-forming cavities express anti-CH factor(s) that are lost in the setting of bone remodeling. Elucidating the niche factors around Tet2 +/- cells will potentially uncover a targetable mechanism shared across hematopoietic clonal disorders.

Methods: We recently reported that ultralow-dose irradiation enables engraftment and intravital tracking of disease initiating niches in CH (Sci. Reports 14:20486, 2024). In brief, we transplanted 2.5x106 Tet2+/-/GFP+ whole bone marrow cells into 0.5 Gy-irradiated C57/BL6 adult mice and performed intravital imaging to track CH clones in the calvarial bone marrow. To identify the niche, bone front staining (Calcein blue and Alizarin Red, 30mg/kg) were administered 2 days apart to demarcate bone forming and resorbing cavities along niche cell specific antibodies. To further assess niche factors, we harvested cells from hot spots (dense Tet2+/- cells) and cold spots (solitary Tet2+/- cells) under image guidance and performed characterization using single cell transcriptomics (10x Genomics) and Seurat. The effects of anti-resorptive therapy on CH progression were further evaluated through flow cytometry analyses of peripheral blood and bone marrow. Two-sided Mann Whitney tests were used to determine statistical significance ($p < 0.05$).

Results: Our results showed that Tet2+/- cell expansion remained restricted within the marrow cavities undergoing bone remodeling (N=5) and revealed host CD206+ tissue resident macrophages (TRMs) association to Tet2+/- cells throughout disease progression (N=12). Via spatial single cell transcriptomics, we further showed that TRMs exhibited significantly downregulated antigen presentation (MHCII) within the cold spots (N=3). In accordance, macrophages from the bone forming cavities had significantly downregulated immune response (FDR value=0.044), exhibited anti-inflammatory phenotypes (CD206+) and reduced MHCII positivity when compared to the bone resorption site. Notably, anti-resorptive Zoledronic Acid (1224 ng/mouse total accumulated dose) led to a reduction of Tet2+/- stem and progenitor cells (Kit+Lin-Sca1+) 1-week after treatment while the healthy counterpart remained unchanged. While Tet2+/- cells in the marrow remained significantly reduced 5 months after treatment, peripheral blood analysis demonstrated a rebounding trend after 3-months, suggesting potential contributions from non-skeletal hematopoietic niches, such as the spleen.

Discussion: This work revealed a previously unrecognized heterogeneity of inflammatory landscape in the bone marrow, defined by bone remodeling and associated with Tet2+/- clonal hematopoiesis. Future work will focus on validating the anti-CH factors via loss- and gain-of-function of antigen presentation. We realize that promoting the anti-inflammatory niche may lead to immune escape and rebound effects. To address this potential limitation, we will harvest the cell population from bone marrow and spleen before the rebound of disease burden to further navigate protective mechanisms for the residual cells.

14th Annual Center for Musculoskeletal Research Symposium
October 17, 2024

Title: Microfluidic-Based Synthesis of Amorphous Calcium Phosphate Nanoparticles Enables Precise Control of Nanoparticle Characteristics and Enhance Osteogenesis

Presenting Author: Bei Liu

Co-Author(s):

Lab PI / Mentor: Hani Awad

ABSTRACT

INTRODUCTION: Non-healing bone defects present significant challenges. Globally, 2.2 million bone grafts are performed annually, costing $2.5 billion. While autografts are the gold standard due to their osteogenic properties, they are limited by availability and donor site morbidity. Allografts and xenografts, though more available, carry risks of immunological rejection and disease transmission.To overcome these limitations, this study focuses on synthesizing carboxymethyl chitosan (CMC) and amorphous calcium phosphate (ACP) nanoparticles (NPs) to enhance bone healing. CMC serves as an analog for non-collagenous proteins, stabilizing and transporting ACP to mimic natural bone mineralization.3 However, traditional bulk synthesis methods suffer from batch-to-batch variability. To address this, we utilize a microfluidic system for nanoparticle synthesis, offering precise control over particle size, enhanced mixing, and greater reproducibility. We hypothesize that ACP nanoparticles synthesized via this microfluidic approach will promote accelerated mineralization and bone healing.

METHODS: CMC/ACP NPs were synthesized using the microfluidic mixing chip “Fluidic 187” with syringe-pump flow contr ol. CMC was dissolved in a 4 mM potassium phosphate solution to achieve a final concentration of 0.67 mg/mL, while calcium chloride was dissolved in DI water to reach final concentration of 6 mM. The CMC and calcium chl oride solutions were injected into separate channels under varying flow rates. The resulting NP suspension was purified using a dialysis cassette with a 20k molecular weight cutoff. NPs were characterized by dynamic light scattering (DLS), Fourier-transform infrared spectroscopy (FTIR), X-ray scattering, and scanning electron micr oscopy (SEM). The effect of varying CMC/ACP NP concentrations on cell viability and proliferation was evaluated using the Cell Counting Kit-8 (CCK-8) assay on the ST2 cell line. Osteogenesis was assessed by treating ST2 cells with oste ogenic medium and CMC/ACP NPs at concentrations of 0, 50, 250, and 500 µg/mL for up to 14 day s, with mineralization quantified by Alizarin Red staining.

RESULTS: DLS indicated that the flow rate did not significantly impact NP characteristics. The highest flow rate of 300 µL/min produced NPs with an average size of 182.5 nm, a PDI of 0.17, and a surface charge of -14.9 mV. Dialysis purification reduced NP size to 120.9 nm and increased the negative charge to -19.9 mV. SEM images showed unif orm NP size distribution. Storage stability analysis confirmed consistent NP characteristics over 3 months. FTIR and XRD analyses verified the preservation of ACP's amorphous nature in the NPs. Cell viability assays dem onstrated that CMC/ACP NPs at concentrations up to 1000 µg/mL did not negatively affect ST2 cell viability and pr oliferation. Treatment with a high concentration of NPs (500 µg/mL) significantly enhanced mineralization at Day 14, corrob orating a dose-dependent effect on osteogenesis.

DISCUSSION: The microfluidic mixer chip provides a controlled and efficient platform for synthesizing monodisperse CMC/ACP NPs with consistent and reproducible characteristics. Dialysis purification enhances nanoparticle production by selectively removing unbound precursors and surface contaminants, thereby reducing nanoparticle size and increasing surface charge, leading to a more homogeneous and stable nanoparticle suspension. Importantly, our results indicate that CMC/ACP nanoparticles are cytocompatible and significantly enhance osteoprogenit or cell mineralization at high concentrations. This highlights the osteo-regenerative potential of these nanoparticles. Future research will optimize this microfluidic system to produce nanoparticles tailored for antibiotic delivery in b one-targeted therapies.

14th Annual Center for Musculoskeletal Research Symposium
October 17, 2024

Title: Senescent cells impair fracture repair by promoting ubiquitination and proteasomal degradation of PDGFRb in mesenchymal progenitor cells of aged mice

Presenting Author: Yiwei Lu

Co-Author(s): Jiongnan Xu, Jun Zhang, Brendan Boyce, Lianping Xing, Hengwei Zhang

Lab PI / Mentor: Hengwei Zhang

ABSTRACT

Introduction: Senescent cells (SCs) inhibit the growth of callus-derived mesenchymal progenitor cells (CaMPCs) and impair fracture repair in aged mice. However, intrinsic molecular mechanisms underlying the regulatory influence of SCs on CaMPCs, particularly via senescence-associated secretory phenotype (SASP), remain inadequately understood. Numerous studies indicate that aged individuals have increased protein ubiquitination and degradation due to higher levels of inflammatory cytokines. We reported that the proteasome inhibitor, bortezomib (Btz) enhanced MPC growth and fracture repair in aged mice. Thus, we hypothesize that SCs impair fracture repair in aging by increasing protein ubiquitination and proteasomal degradation via SASPs.

Methods: 1. 4-m- (young) and 20-m-old (aged) C57BL/6J male mice received open tibial fracture surgery and were treated with the following agents or combinations at day 1, 3, and 5 post-fracture: 1) FACS sorted p16tdTomato+ SCs (10e5/local injection) 2) Senolytic drugs, dasatinib (D, 5 mg/kg) and quercetin (Q, 50 mg/kg); 3) Proteasome inhibitor, bortezomib (Btz, 0.6mg/kg, i.p.); 4) PDGF (1.5μg/callus injection); 5) PDGFRb selective inhibitor, su16f (10mg/kg by gavage); 6) Solvent control. n=8-10/group. Only male mice will be used to avoid any misleading by estrogen in aged female mice.
2. Callus-derived MPCs (CaMPCs) were treated with SC conditioned medium (CM) to examine the inhibition of cell growth.
3. Total protein from the callus of young and aged mice was used for the expression of PDGFRb and Ub-PDGFRb.
4. All results are given as mean ± SD. Comparisons between 2 groups were analyzed using a 2-tailed unpaired Student's t test. One-way ANOVA and Tukey post-hoc multiple comparisons were used for comparisons among 3 or more groups. Two-way ANOVA and Tukey post-hoc multiple comparisons were used for analysis with two variables. p values <0.05 were considered statistically significant.

Results: To test our hypothesis, we generated SC conditioned medium (CM) by culturing callus pieces from fractured mice. CM from 18m-old mice (aged CM), but not CM from 18m-old mice treated with senolytic drug Dasatinib+Quercetin (D+Q), inhibited cell growth and increased expression levels of total ubiquitinated (Ub)-proteins in CaMPCs. The increased protein degradation caused by aged CM was prevented by Btz, but not the lysosome inhibitor. Injection of FACS sorted p16 tdTomato+ SCs to the callus of young mice (3m-old) reduced the bone strength, which was blocked by Btz (biomechanics: 40.5±3.4 Ctl vs. 28.6±4.2 SCs vs. 41.4±2.2 Btz+SCs N.mm, $p<0.05$). Using Ub-proteomics we detected PDGFRb as a major targeted protein of Btz in MPCs. TGFb1 is known as the most highly expressed SASP in callus of aged mice. We found that TGFb1 dose-dependently increased Ub-PDGFRb and decreased PDGFRb protein levels in CaMPCs, which was majorly blocked by Btz. Aged CM decreased CaMPC growth and PDGFRb expression were blocked by TGFb neutralizing antibody, which was further abrogated by PDGFRb inhibitor su16f. Because PDGF expression decreased in callus of aged mice, we further examined whether PDGF and D+Q synergistically enhance fracture repair in aged mice. Data showed that D+Q, but not PDGF, increased bone strength in aged mice, which was boosted by the combination of D+Q and PDGF (biomechanics: 22.1±3.5 Ctl vs. 21.6±5.6 PDGF vs. 31.6±5.2 D+Q vs. 40.9±4.9 D+Q+PDGF N.mm, $p<0.05$).

Discussion: Our results indicate that SASP factor, TGFb1 regulates ubiquitination and proteasomal degradation of PDGFRb thereby CaMPC function, representing a new molecular interaction between SCs and CaMPCs, and senolytics in combination of PDGF is an effective therapy to promote fracture repair in aging.

14th Annual Center for Musculoskeletal Research Symposium
October 17, 2024

Title: Phsiological loading via voluntary wheel running promotes stronger murine Achilles tendons

Presenting Author: Samantha Muscat

Co-Author(s): Elsa Lecaj, Nolan Sparks, Mark Buckley

Lab PI / Mentor: Anne Nichols

ABSTRACT

Introduction: Tendons act as a mechanosensitive bridge that transmits muscle forces to bone to enable successful locomotion. While mechanical loading is critical to maintain tendon homeostasis, tendons also have a paradoxical response to load in which both over- and under- loading can lead to tendon degeneration. Numerous models of under- and over-loading have failed to identify the cellular mechanisms underpinning this paradoxical response and how the subsequent tissue-level adaptive or maladaptive mechanoresponse is mediated remains unknown. The goal of the present study was to evaluate voluntary wheel running (VWR) as a model of physiological loading that could be used to identify possible candidates regulating tendon homeostasis in response to mechanical load. Methods: Individually housed mice were allowed to freely run on the open surface of a slanted plastic saucer shaped wheel inside the mouse cage for 8 or 12 weeks. Sedentary control mice were placed in cages with a locked wheel. After 8 and 12 weeks (n=7 per timepoint/group), total RNA was isolated for bulk-RNA sequencing and gene ontology analysis. Biomechanical properties were assessed by preloading with 10 cycles at 6% strain, followed by stress relaxation at 8% and 16% strain, each with 500 second relaxation and finally, single ramp-to-failure. Paraffin sections were stained for Collagen Hybridizing peptide (CHP)-Cy3 and DAPI. Results: Compared to sedentary controls, peak stress increased by 54.5% (p=0.006) while elastic modulus increased by 43.8% (p=0.03). No significant differences were seen after 12 weeks of VWR. GO analysis of DEGs at 8 weeks (22 genes upregulated, 22 genes downregulated compared to locked control) revealed that after 8 weeks of running, VWR Achilles tendons upregulate pathways relating to morphogenesis, embryogenesis, and cell adhesion processes, suggesting a developmentally directed adaptation process. No significantly enriched downregulated pathways were observed. At 12 weeks, GO analysis of DEGs (97 genes upregulated, 129 downregulated compared to locked controls) demonstrated a shift in the Achilles tendon transcriptional response to loading with a downregulation of developmental pathways and upregulation of GO terms associated with heat generation and metabolic processes related to fatty acid beta oxidation. Relative to sedentary controls, 8- and 12-week VWR tendons exhibited significantly increased CHP-cy3 staining by 823.26% (p=0.006) and 1057.54% (p=0.04), respectively, within the insertional region of the Achilles tendon. Together, these results suggest that after 12 weeks of running VWR Achilles tendons have dampened the growth promoting adaptation state observed at 8 weeks and shifted towards an adaptive homeostasis and altered metabolic state.
Discussion: The results of our study show that Achilles tendons demonstrate increased mechanical properties, suggesting that tendons are stronger than sedentary controls. This is consistent with our transcriptomic findings that developmentally guided processes after 8 weeks of VWR are upregulated, suggesting an anabolic growth adaptation response. Interestingly, similar developmental pathways are downregulated after 12 weeks, indicating that the VWR tendons have adjusted to loading and reached adaptive homeostasis. The transcriptomic analysis and the improvement in mechanical properties demonstrate a positive adaptation response, suggesting that the CHP-cy3 staining is indicative of collagen remodeling rather than damage. Taken together, these data support that VWR is sufficient model of physiological loading that promotes an adaptive response in mouse Achilles tendon. Significance: Establishing a model of physiological loading in Achilles tendon will allow for future characterization of the complex tendon mechanotransduction network.

14th Annual Center for Musculoskeletal Research Symposium
October 17, 2024

Title: Identification of Telocytes in the Synovial Lymphatic System and their Roles in Lymphatic Vessel Homeostasis and Function

Presenting Author: Yue Peng

Co-Author(s): H. Mark Kenney, Karen L de Mesy Bentley, Lianping Xing, Benjamin D. Korman, Christopher T. Ritchlin, Edward M. Schwarz

Lab PI / Mentor: Edward M. Schwarz

ABSTRACT

Introduction: Rheumatoid arthritis (RA) patients and TNF-transgenic mice have lymphatic dysfunction (Bouta, Bell et al. 2018). Recently, we showed mast cell involvement, as genetic ablation and drug inhibition decreased lymphatic drainage and exacerbated arthritis in TNF-Tg mice (Peng, Kenney et al. 2023). Single-cell RNA sequencing studies identified genes (i.e., Efhd1) selectively expressed in mouse popliteal lymphatic vessels (PLVs) (Kenney, Wu et al. 2022). However, the identity and function of the Efhd1-expressing cells and their relationship with mast cells on PLV biology are not known. Here we aimed to characterize a novel Efhd1-CreERT2 mouse model as a tool for PLV gain and loss-of-function studies and elucidate the mechanisms of peri-lymphatic mast cell regulation of lymphatic vessels.

Methods: Efhd1-CreERT2 mice were crossed to Ai9-tdTomato (tdT) reporter mice. The heterozygous offspring were treated with tamoxifen as neonates or adults for lineage tracing studies in the popliteal vasculature and adjacent adipose tissue via immunofluorescent microscopy (IFM) and subsequent transmission electron microscopy (TEM). The Efhd1-CreERT2 mice were also crossed to ROSA-diphtheria toxin A (DTA) mice to determine in vivo cell depletion efficiency and lymphatic clearance by IFM and near-infrared imaging of indocyanine green (NIR-ICG) injected into the footpad, respectively. Ex vivo response to hyperosmotic stress was assessed in primary PLV-cell cultures supplemented with 10 mM Ca^{2+} and various concentrations of sucrose or ionomycin, followed by Fluo-4 imaging. Results: Developmental and adult lineage tracing demonstrated Efhd1-tdT+ peri-vascular telocytes based on their fibroblastic morphology and characteristic telopods. Telocyte identity was confirmed by CD31-/CD34+/Vimentin+/Efhd1+ IFM (Rosa, Faussone-Pellegrini et al. 2021). Histomorphometry revealed decreased telocytes in TNF-Tg synovium compared to WT synovium (84.15%±7.99% vs. 26.04%±7.38%; $p<0.001$). Decreased telocytes in TNF-Tg synovium was partial prevented with anti-TNF therapy (43.93%±4.48%; $p<0.05$). Parallel TEM and IFM revealed tdT+ telopods integrated along the PLV, and within mast cells. Functionally, telocytes exhibited increased calcium influx in response to osmotic stress in vitro. DTA-induced depletion of telocytes resulted a 25.11% reduction in lymphatic clearance ($p>0.05$), suggesting that telocytes are able to sense osmotic pressure changes and regulate lymphatic function by mediating mast cell and PLV communication.

Discussion: We developed and validated a novel Efhd1-CreERT2 transgenic mouse for inducible gain and loss-of-function studies in telocytes, whose function in joint homeostasis and arthritis is unknown. Two distinct subtypes of peri-PLV telocytes exist: one with telopods longitudinally attached along PLVs, and the other with telopods integrated within the plasma membrane of peri-PLV mast cells. Based on these findings, we hypothesize that: 1) PLV telocytes sense and modulate the extracellular matrix (ECM) stiffness of PLVs, potentially through the secretion of myocilin, TIMPs and MMPs for ECM remodeling (3), and 2) interstitial telocytes that may sense osmotic pressure and regulate PLV contractility indirectly by interacting with mast cells to induce the release of factors (e.g. histamine) that modulate PLV contractions. Our findings are also consistent with the loss of telocytes in RA synovium (Rosa, Faussone-Pellegrini et al. 2021), phenotypic changes to a yet to be defined population of fibroblastic cells in RA synovium (Zhang, Jonsson et al. 2023) that may be telocytes, and lymphatic dysfunction during disease progression (Bouta, Bell et al. 2018). Future directions will focus on investigating whether synovial telocytes differentiate into pro-fibrotic synovial fibroblasts during inflammatory-erosive arthritis, and if depletion of these telocytes exacerbate TNF and collagen antibody-induce arthritis in mice.

14th Annual Center for Musculoskeletal Research Symposium
October 17, 2024

Title: Ablation of Tumor-Derived IGFBP-3 Attenuates TGFβ-Associated Muscle Catabolism in Two Independent Murine Models of Pancreatic Ductal Adenocarcinoma

Presenting Author: Zachary R. Sechrist

Co-Author(s): Edward M. Schwarz, Calvin L. Cole

Lab PI / Mentor: Calvin L. Cole

ABSTRACT

INTRODUCTION: Pancreatic ductal adenocarcinoma (PDAC) is the fourth leading cause of cancer-related deaths and is highly associated with skeletal muscle wasting (SMW). Our lab previously identified tumor secreted insulin-like growth factor binding protein 3 (IGFBP-3) as a potential driver of PDAC-induced SMW in a pre-clinical murine model. Furthermore, the roles of TGF-b signaling, and the ubiquitin proteasome pathway (UPP) activation have been duly noted in SMW (Cole 2021). Recent literature supports an interaction between IGFBP-3 and TGF-b signaling in muscle. Here we tested the hypothesis that genetic depletion of tumor-derived IGFBP-3 in non-metastatic KCKO and metastatic KP2 PDAC tumor cells is sufficient to attenuate SMW in syngeneic-orthotopic murine models of PDAC via the downregulation TGF-b signaling in skeletal muscle. METHODS: Before tumor inoculation, C57BL/6J female mice (6-8 weeks old) were scanned using dual energy X-ray absorptiometry (DEXA) to acquire baseline lean mass measurements of the lower hindlimbs. Mice were randomized into four experimental tumor-bearing groups: 1) parental KCKO-Luc (n=14), 2) KCKO-Luc IGFBP-3-/- (n=14), 3) parental KP2-Luc (n=10), and KP2-Luc IGFBP-3-/- (n=10). Tumor-bearing mice were compared to non-tumor controls (NTC) (n=10). Mice were injected orthotopically with 1E5 KCKO or 5E4 KP2 tumor cells. Weekly DEXA scans monitored changes in lean mass and tumor growth. Mice were sacrificed based on previously established failure to thrive criteria or at the predetermined endpoint (100 days KCKO, 90 days KP2 model). Serum and lower limbs were harvested following euthanasia. Quadriceps muscles were preserved for transcriptional analysis and proteomics. ELISA was performed on serum for the quantification of IGFBP-3. RNA was extracted from quadriceps muscles for RT-qPCR gene expression analysis of igfbp3, tgfβr1, and UPP-associated, muscle specific genes: fbxo32 and trim63. Western blots assessed markers of protein synthesis (AKT and S6), and markers of autophagy (FOXO1, ULK1 and LC3b). Statistical analyses were performed using GraphPad Prism software. One-way ANOVA was used to analyze within and between group changes in IGFBP-3 concentrations, lean mass, gene, and protein expression. Kaplan–Meier estimator of survival was used to quantify survival of experimental mice. $p<0.05$ was considered significant. RESULTS: Mice inoculated with parental tumor cells, in both models, experienced significantly reduced survival compared to mice inoculated with IGFBP-3-/- tumor cells which correlate with elevated serum expression of IGFBP-3. Furthermore, tumor bearing mice lost significantly more lean mass as measured by DEXA compared to NTC mice and IGFBP-3-/- animals ($p<0.5$). Western blot analysis displayed an increase in FOXO1, and autophagic markers ULK1, and LC3b in parental tumor bearing animals compared to NTC and IGFBP-3-/- animals in both models ($p<0.05$). Additionally, IGFBP-3-/- animals in the KCKO cohort experienced a recovery in AKT and S6 signaling ($p<0.05$), while KP2 IGFBP-3-/- animals only recover AKT signaling. RT-qPCR analysis on quadricep muscles indicated that tumor bearing animals in both models display significantly increased expression of igfbp3, tgfβr1, and UPP associated genes fbxo32 and trim63 compared to NTC and IGFBP-3-/- mice, while no difference was seen between NTC and IGFBP-3-/- mice. DISCUSSION: In this study, we demonstrated a relationship among upregulation of IGFBP-3, increased TGF-b signaling, autophagy, the UPP, and SMW. Tumor-specific ablation of IGFBP-3 significantly attenuates the loss of lean mass measured via DEXA and improves survival in two independent models of PDAC. Further work will validate IGFBP-3 dependent effects on SMW using AAV-IGFBP-3 overexpression models and investigate therapeutic neutralization of IGFBP-3 as a treatment for PDAC-induced SMW.
ACKNOWLEDGEMENTS: This research is supported by NIH grants (K01 CA240533, P30AR69655, and P50CA257911).

14th Annual Center for Musculoskeletal Research Symposium
October 17, 2024

Title: PRDM16 is required for normal nasal septal cartilage and bone development in mice

Presenting Author: Eliya Tazreena Tashbib

Co-Author(s): Victoria Hansen, Eloise Fadial, Alexis Klee, Maeve O'Brien, Kathryn Lambright

Lab PI / Mentor: Chia-Lung Wu

ABSTRACT

INTRODUCTION: Abnormal epigenetic regulations may lead to craniofacial anomalies, affecting approximately 35% of the birth defects. A recent GWAS study suggests that abnormal craniofacial developments in humans are associated with PRDM16, a histone methyltransferase and zinc finger transcriptional factor. Previous studies have shown that Prdm16 global knockout mice (gKO) exhibit underdeveloped Meckel's cartilage, shortened mandible, and ventricular hypoplasia. However, Prdm16 gKO mice are not only unable to decipher the role of PRDM16 in a tissue-specific manner but also neonatal lethal. Thus, the goal of the current work is to unravel the function of PRDM16 in craniofacial cartilage and bone development, using an osteochondral lineage-specific Prdm16 conditional knockout mouse model (Col2a1Cre;Prdm16fl/fl, cKO). We hypothesize that PRDM16 is a positive regulator for proper craniofacial cartilage and bone formation.

METHODS: Mouse skulls were harvested from WT and Prdm16 cKO mice at E18.5, P5, 4wk, and 12wk of age according to IACUC approved protocol. Cre-negative littermates were used as controls (WT). PRDM16 knockout was confirmed via Western blot of costal cartilage. To assess craniofacial bone and cartilage development, E18.5 WT and cKO mice were stained with Alcian Blue and Alizarin Red. Skulls from P5, 4wk, and 12wk-old WT and cKO mice were submitted for μCT analysis. Histological analysis and IHC against CO10A1, RUNX2, MKI67, and CASP3 were performed to determine chondrocyte phenotypes in the nasal septum ($n \geq 3$ for all groups). Data were analyzed with Student's t-test or Two-way ANOVA, accordingly.

RESULTS & DISCUSSION: At E18.5, there is no significant difference in nasal length between WT and Prdm16 cKO mice, but a decreasing trend in cranial length in Prdm16 cKO vs. WT mice was observed. Both male and female Prdm16 cKO mice exhibited significantly shorter nasal and cranial lengths vs. WT mice at 4 and 12wk of age. At 4wk of age, nasal BV/TV was similar between WT and cKO mice. However, 12wk-old male, but not female, Prdm16 cKO mice had significantly higher nasal BV/TV than corresponding WT mice, suggesting a potential sex-dependent role of PRDM16 in nasal bone development. As female Prdm16 cKO and WT mice showed comparable nasal BV/TV, we focused on the male mice thereafter. Histological analysis revealed no nasal septal deviation in male Prdm16 cKO mice at P5, but severe deviation was observed at both at 4 and 12wk of age. Moreover, significantly increased RUNX2+ cells were observed near the deviation site in 4wk-old male cKO mice. These results imply that loss of PRDM16 may accelerate chondrocyte hypertrophy as well as increase BV/TV and osteogenesis of nasal bone in the cKO mice, leading to severe nasal septal deviation. Although %MKI67+ cells were comparable in the nasal cartilage between WT and cKO male mice at 4 and 12wk of age, significantly increased CASP3+ apoptotic chondrocytes were observed in nasal cartilage of the cKO mice at 12wk of age. Our observations suggest that PRDM16 is critical in maintaining the balance between chondrocyte proliferation and apoptosis, providing a possible explanation for decreased nasal cartilage length in the cKO mice. To further elucidate the gene regulatory networks and cell-cell interactions governing the homeostasis of nasal septal cartilage and bone, our next step is to perform scRNA-seq and spatial transcriptomics on nasal septal cartilage and bone cells of WT and cKO mice at P5 and 4wk of age.

CONCLUSION: We demonstrated that KO of PRDM16 in an osteochondral lineage-specific manner leads to severe nasal septal deviation in mice, potentially due to accelerated chondrocyte hypertrophy and enhanced osteogenesis as well as imbalanced chondrocyte proliferation/apoptosis. Our findings help elucidate the functionality of PRDM16 in craniofacial development and provide a potential therapeutic target for patients with congenital nasal bone and cartilage disorders.

14th Annual Center for Musculoskeletal Research Symposium
October 17, 2024

Title: Study of the role of neutrophil extracellular traps in age-related bone loss

Presenting Author: Cheng Xiang

Co-Author(s): Jun wu, Rong Duan, Zhenqiang Yao

Lab PI / Mentor: Brendan F Boyce

ABSTRACT

Background & Hypothesis: Osteoporosis is characterized by weakened bones and an increased risk of fractures. Various factors, including neutrophils, contribute to an inflammatory microenvironment in bone and can exacerbate bone loss during aging. We reported previously that TGFβ+CCR5+ neutrophil numbers increase in BM during aging and cause age-related osteoporosis by promoting bone resorption and inhibiting bone formation. Neutrophil extracellular traps (NETs), which are released by neutrophils in response to infections, can be released in non-infectious conditions and contribute to tissue damage and inflammation, but their role in bone loss during age-related osteoporosis is unknown. Triggering receptor expressed on myeloid cells 1 (TREM1) is an orphan immune receptor that amplifies Toll-like receptor-4 (TLR4) inflammatory responses, promotes NET release by human and murine neutrophils, and is a component of the NET structure. We hypothesize that NETosis increases in bone marrow (BM) during aging and contributes to age-related osteoporosis through TREM1 by promoting bone resorption and inhibiting bone formation.

Experiments & Methods: ELISA and immunofluorescence staining with recognized NETosis markers to assess expression of NETs in BM from young (3-mon-old) and aging (18-mon-old) mice and a cytokine array to identify factors in BM promoting NETosis during aging. A TREM1 inhibitor (nangibotide) was used to examine the effect on NETs released in BM from young and aging mice by comparing dsDNA generation and visualizing NETs (using Sytox Green). The NETosis inducer, PMA (Phorbol 12-myristate 13-acetate), was used as a positive control. Established procedures were used to generate NETs and examine their effects on osteoblast (bone marrow mesenchyme stromal cell (BMSC,) and bone-derived mesenchyme progenitor cell (BdMPC)) and osteoclast (bone marrow macrophages (BMMS)) precursor differentiation in vitro.

Results: Levels of biomarkers of NETs, including dsDNA, DNA- myeloperoxidase (MPO) complex, and neutrophil elastase, were all increased in the BM of aging mice. Immunostaining showed that NETs colocalized with citrullinated histone 3 (CitH3), MPO, and Ly6G in samples from aging mice, while they were observed rarely in young mice. TREM1 expression was significantly increased in a BM supernatant from aging mice in the cytokine array, and treatment with the TREM1 inhibitor indicated that TREM1 was positively associated with NETs release. NETs promoted osteoclast formation and inhibited osteoblast differentiation in vitro.

Discussion & Conclusions: NETs levels increased in BM in aging mice, in part through TREM1 signaling and could contribute to age-related osteoporosis by promoting bone resorption and inhibiting bone formation. Further studies are required to determine if TREM1 inhibition can prevent age-related bone loss and if NETs released by TGFβ +CCR5+ neutrophils contribute to this bone loss. Prevention of NET release could be a novel mechanism to prevent age-related osteoporosis.

Keywords: Age-related osteoporosis, neutrophil extracellular traps, TREM1, inflammaging

14th Annual Center for Musculoskeletal Research Symposium
October 17, 2024

Title: Type III collagen supports self-assembly of hiPSC-Endothelial Cells in a vascularized Human Tendon-on-a-Chip

Presenting Author: Victor Zhang

Co-Author(s):

Lab PI / Mentor: Hani Awad and James McGrath

ABSTRACT

INTRODUCTION: The Human Tendon-on-a-Chip (hToC) is a microphysiological system (MPS) of the myofibroblast microenvironment in peritendinous fibrosis including cellular signaling and extracellular matrix (ECM) interactions. Early versions of the hToC use tenocytes and macrophages suspended in a type I collagen hydrogel to mimic tendon scar tissue. This lacks the neovascularization seen in fibrotic tendon. We aim to incorporate microvascular structures within the hToC hydrogel to model the spatial cellular interactions of fibrosis. Other MPS models use endothelial cells (ECs) to form self-assembled microvascular structures, however this is typically achieved using fibrin gels. Type I collagen gels do not support very robust microvasculature. Our prior work has shown that adding type III collagen may better mimic the fibrotic microenvironment in the hToC. Importantly, type III collagen supported more angiogenic sprouting from EC spheroids. Therefore, we hypothesized that type III collagen would facilitate the formation of robust microvascular networks in the hToC.

METHODS: Human induced pluripotent stem cells (hiPSCs) reprogrammed from primary tenocytes (TC) were differentiated into endothelial cells (iECs) using an endothelial cell differentiation kit (StemCell Technologies). iECs and TCs were cultured in collagen hydrogels to test iEC self-assembly. Two hydrogel mixtures were used for this study, a commercially available type I collagen hydrogel (95% type I and 5% type III) and a mixture supplemented with type III collagen (80% type I and 20% type III). Cells were passaged as single cells and suspended in neutralized collagen solutions at a density of 2 million iECs/mL and 500 thousand TC/mL. Two hToC hydrogel devices were prepared for each collagen ratio. After 6 days of culture, samples were fixed and stained for PECAM1 to visualize iECs and F-actin to visualize all cells. Three volumetric images were taken from each device using confocal microscopy. Microvascular structures were segmented using PECAM1 immunofluorescent signal and analyzed to quantify mean segment length, mean segment radius, and total vessel volume fraction. Statistics: Data was compared using unpaired t-test between low and high type III collagen hydrogels.

RESULTS: iEC microvascular structures cultured in high type III collagen hydrogels had significantly longer mean segment length (65 um vs 43 um), larger vessel radii (7.9 um vs 6.8 um), and lower vessel volume fraction (2.1% vs 3.4%). Additionally, microvascular structures cultured in high type III collagen hydrogels had what appeared to be open lumens when imaged with high magnification confocal microscopy.

DISCUSSION: The results in this study demonstrate that adding type III collagen to the hToC hydrogel supported more robust microvascular self-assembly by iECs. This suggests that the MPS vascularization that is facilitated by the use of fibrin gels may also be achieved through the use of type III collagen. The ability to support microvascular networks further reinforces the use of type III collagen to create the fibrotic microenvironment in the hToC. As these microvascular structures appear to have open lumens, immediate next steps will interrogate the patency and function of these microvessels by perfusing them with fluid flow. Future work will also incorporate the use of hiPSC-derived monocytes and macrophages to create a fully patient-specific hToC model of the vascular myofibroblast microenvironment for the testing and discovery of novel anti-fibrotic medications.

Posters

Disclaimer

14th Annual Center for Musculoskeletal Research Symposium
October 17, 2024

Title: Outcomes of Distal Radius Fractures in Geriatric Patients Following Volar Locked Versus

Presenting Author: Thomas Carroll

Co-Author(s): Akhil Dondapati, Urvi Patel, Warren Hammert, Ronald Gonzalez

Lab PI / Mentor: Constantinos Ketonis

ABSTRACT

Hypothesis: Our primary hypothesis was that geriatric patients undergoing volar locked plating (VLP) for distal radius fractures, compared to dorsal bridge plating (DBP), would demonstrate significantly improved post-operative range of motion (ROM), radiographic outcomes, and patient-reported outcome scores. Our secondary hypothesis was that the improvements in ROM and radiographic outcomes would not be clinically significant.

Methods: In total, 2181 patients at least 65 years old with closed distal radius fractures were retrospectively analyzed. Wrist ROM and radiographic outcome data were calculated at 6-month follow-up. Patient Reported Outcomes Measurement Information System (PROMIS) Upper Extremity (UE), Physical Function (PF), and Pain Interference (PI) were calculated at each follow-up visit. Injury characteristics, surgical complications, and patient demographic data were also analyzed. A combination of propensity-score matching, multivariate analysis, T-test, and Chi-Square tests were used to conduct the statistical analysis.

Results: After propensity matching, a total of 1375 patients underwent VLP while 275 patients underwent DBP. Within the univariate analysis, the DBP demonstrated a higher proportion of AO/OTA 23-C fracture patterns, with fewer AO/OTA 23-A compared to VLP ($p<0.05$)(Table 1). Multivariate analysis demonstrated greater wrist flexion and extension, radial and ulnar deviation, supination, pronation, and grip strength, and higher PROMIS PF and PI among the VLP group ($p<0.05$)(Table 2). At 6-month follow-up, VLP patients demonstrated greater radial inclination (21.2 degrees vs. 20.3 degrees; $p<0.05$), lower articular step-off (0.76mm vs. 0.86mm; $p<0.05$), with similar volar tilt and radial height ($p>0.05$). DBP patients had higher rates of malunion (17/275 vs. 41/1375; $p<0.05$), nonunion (11/275 vs. 27/1375; $p<0.05$), and tendon rupture (7/275 vs. 13/1375; $p<0.05$) but similar rates of revision surgery and infection ($p>0.05$).

Conclusions: VLP was associated with greater wrist flexion, extension, radial deviation, ulnar deviation, supination, pronation, grip strength, and PROMIS PF and PI compared to DBP. There were significantly higher complication rates with DBP, however there was a similar rate of revision surgery. While the VLP group showed significantly greater ROM and radiographic outcomes, this likely did not represent a clinically significant difference in this population.

14th Annual Center for Musculoskeletal Research Symposium
October 17, 2024

Title: Volar Locked Plating Versus Dorsal Bridge Plating for Complete Articular (AO/OTA Type 23C) Distal Radius Fractures

Presenting Author: Thomas Carroll

Co-Author(s): Akhil Dondapati, Urvi Patel, Warren Hammert, Ronald Gonzalez

Lab PI / Mentor: Constantinos Ketonis

ABSTRACT

Objectives: Complete articular (AO/OTA 23C) distal radius fractures (DRFs) can be particularly challenging to treat with volar locked plating (VLP). The advent of dorsal bridge plating (DBP) has provided an alternative for adequate stability for these fractures. The purpose of this study was to compare functional, radiographic, and patient-reported outcomes, as well as complication rates, for AO/OTA 23C fractures of the distal radius treated with VLP versus DBP.

Patient Selection Criteria: Patients aged 18-90 years old who underwent VLP or DBP fixation for AO/OTA 23C DRFs from October 1, 2015 to October 1, 2023 were included. Patients not in this age range, polytraumatized patients, and those undergoing revision surgery were excluded.

Outcome Measures and Comparisons: Wrist range of motion (ROM) and radiographic outcomes data were calculated at 6-month follow-up. PROMIS Upper Extremity (UE), Physical Function (PF), and Pain Interference (PI) were calculated at each follow-up visit. Surgical complications, and patient demographic data were also recorded.

Results: A total of 1426 patients underwent VLP while 239 patients underwent DBP. After 5:1 propensity matching, 1069 VLP patients were matched to 214 DBP individuals. DBP patients had higher rates of nonunion (2.0% vs. 4.2%; $p<0.05$) and tendon rupture (0.5% vs. 3.3%; $p<0.05$), but similar rates of revision surgery, malunion, and infection ($p>0.05$) at 6 months. Univariate and multivariate analysis demonstrated greater wrist flexion, extension, radial deviation, ulnar deviation, supination, pronation, grip strength, PROMIS UE, and PROMIS PF among the VLP group compared to DBP ($p<0.05$). PROMIS PI was similar between the two groups ($p>0.05$). At 6-month follow-up, VLP patients demonstrated greater radial height (11.7mm vs. 11.4 mm; $p<0.05$) and radial inclination (21.3° vs. 19.8°; $p<0.05$), lower articular step-off (0.73mm vs. 0.83mm; $p<0.05$), and decreased volar tilt (6.7° vs. 7.1°; $p<0.05$).

Conclusions: For patients with complete articular (AO/OTA type 23C) DRFs, VLP was associated with greater ROM, grip strength, PROMIS UE, and PROMIS PF compared to DBP. DBP patients demonstrated higher rates of nonunion and tendon rupture but similar rates of revision surgery, malunion, and infection. VLP patients overall demonstrated improved radial height and radial inclination, and lower articular step-off, with decreased volar tilt compared to DBP

14th Annual Center for Musculoskeletal Research Symposium
October 17, 2024

Title: Neutrophil Attraction and Efferocytosis by Mesenchymal Stromal Cells

Presenting Author: Sandra Castillo

Co-Author(s): Ethan Kaiser, Emily Quarato, Laura Calvi, Roman Eliseev

Lab PI / Mentor: Dr. Roman Eliseev

ABSTRACT

Introduction: Senescence of bone marrow stromal cells (BMSCs), precursors of bone-forming osteoblasts, contribute to age-related bone loss. Despite their critical role in bone microenviron-ment, the mechanism underlying age-dependent BMSC dysfunction remains elusive. E erocyto-sis, the clearance of apoptotic cells by macrophages, is a vital process that declines with age within the bone marrow due to macrophages dysfunction, leading to a reduced clearance of end-stage apoptotic neutrophils (aPMNs). A recent study has shown that excessive e erocytosis by BMSCs impairs osteogenic di erentiation and promotes senescence. This suggests that ef-ferocytosis contributes to, and could be a novel mechanism of, BMSC dysfunction. We have ob-served that following neutrophil e erocytosis, mitochondria in BMSCs become less functional, produce more ROS, and are more fragmented. The mechanism of e erocytosis is not well un-derstood. Therefore, our goal is to understand the mechanism(s) of neutrophil attraction by BMSCs and post-e erocytic mitochondrial dysfunction in BMSCs.

Methods: To achieve our goal, we are using a microdevice (μSiM) mimicking the bone marrow environment. This device features a dual-scale silicon nitride membrane with nanopores and mi-cropores, which separates the top (vessel) and bottom (bone marrow stroma) compartments. HUVECs are seeded on the membrane to mimic the "vessels", while BMSCs are seeded in the bottom compartment to mimic the "bone marrow stroma". To investigate aPMNs attraction to-wards BMSCs, a high dose of aPMNs (10:1) is added to the top compartment, and the devices are incubated in either a static culture environment lacking physiological flow or with the flow to better mimic physiological conditions. To elucidate the role of mitochondrial fragmentation in post-e erocytic BMSC dysfunction, we are manipulating the mitochondrial fission/fusion machinery by deleting either Drp1 in Drp1f/f mouse cells or Mfn1/2 in Mfn1/2 f/f mouse cells, respectively. Re-combination is induced via viral transduction with Ad-Cre, using EV as a control. Cells are then exposed to varying aPMN doses (3:1 and 10:1) before flow cytometry analysis.

Results: Initial findings show aPMNs migration across the membrane in a static culture, con-sistent with our hypothesis. This transendothelial migration of neutrophils to the hMSC monolayer aligns with previous RNAseq data, which shows upregulation of CXCL12, chemokine that induc-es neutrophil migration, in e erocytic cells. Furthermore, our initial comparisons of static versus fluidic setups using our positive control, 40 ng/mL CXCL12 in bottom compartment, show higher percentage of transmigrated aPMNs in the flow setup, with 22.07% compared to 0.231% in static conditions. Additionally, preliminary studies show an increase in e erocytic BMSCs from 9.7% to 17.6% for the 10:1 ratio for the Cre- cells. However, in the absence of Drp1, there is a decrease in e erocytic BMSCs from 0.6% to 0.46%, indicating that deletion of Drp1 greatly diminishes the e erocytic ability of BMSCs.

Discussions: Our in vitro data suggests that BMSCs attract aPMNs via CXCL12 and, further-more, flow appears to increase the transmigration of neutrophils across the membrane. We will further test this under different conditions (e.g., no CXCL12, BMSCs and HUVECs, only BMSCs, only HUVECs, and with no cells). Additionally, deletion of Drp1 reduces efferocytosis by BMSCs. Preliminary flow cytometry analysis provided compelling evidence indicating that manipulating BMSC mitochondrial fission machinery directly impacts aPMNs efferocytosis. Ongoing in vitro and in vivo studies will further elucidate the mechanism of post-efferocytic BMSC senescence using BMSC-specific Prx1Cre mice crossed with Drp1f/f and Mfn1/2f/f mice.

14th Annual Center for Musculoskeletal Research Symposium
October 17, 2024

Title: Energy metabolism in osteoprogenitors and osteoblasts: prevalence of the pentose phosphate pathway

Presenting Author: Sarah E. Catheline

Co-Author(s): Charles O. Smith, Matthew McArthur, Chen Yu, Paul S. Brookes, Roman A. Eliseev

Lab PI / Mentor: Roman Eliseev

ABSTRACT

Introduction: Cells produce energy to fuel their bioenergetic needs using the cytosolic process of glycolysis that metabolizes glucose into pyruvate. Glycolysis is indelibly linked to another cytosolic pathway known as the pentose phosphate pathway (PPP), which produces NADPH required for redox reactions and fuels biosynthesis by making nucleotide precursors. While much is known about osteoblast differentiation, little is settled about their bioenergetic needs. In this study, we aim to answer lingering questions regarding metabolic flux during differentiation of bone marrow stromal (a.k.a. mesenchymal stem) cells (BMSC) down the osteogenic lineage using 13-C6-glucose or 13-C5-glutamine. We also begin to test the hypothesis that the PPP essentially contributes to bone homeostasis by maintaining production of NADPH and allowing for biosynthesis of proline that facilitates bone extracellular matrix (ECM) protein production.

Methods: Human BMSCs (hBMSCs) were osteogenically induced with ascorbate and B-glycerophosphate for 0. 5, 10, and 14 or 15 days. For metabolic flux experiments, cells were labeled following differentiation with either 5 mM 13-C6-glucose or 1 mM 13-C5-glutamine for 90 minutes, and metabolites extracted using methanol for liquid chromatography mass spectrometry. 13C labeling was determined as 'fractional saturation' (Fsat), i.e. 13C-labeled/total. Osteoblast differentiation was assessed by alkaline phosphatase (ALP) and alizarin red staining, as well as real time RT-qPCR. To measure cell growth and proliferation, cells were stained with Hoechst and analyzed using Celigo imaging cytometer. For all experiments, data are mean ± SD (n = 3-4); p value is determined via either unpaired t test or one-way ANOVA with post-hoc Tukey multiple comparisons test. To inhibit the PPP cells were treated with G6PDi at 20 mM.

Results: 13-C6-glucose tracing of glycolytic intermediates reveals that throughout osteoblast differentiation, glucose-derived labels are seen abundantly in early glycolytic metabolites such as glucose-6-phosphate (G6P) but are minimally present in later glycolytic (i.e. pyruvate) and all TCA cycle intermediates. In contrast, early metabolites from the PPP (i.e. ribose-5-phosphate) show high levels of glucose-derived labels which persists in later PPP metabolites with Fsat at >50% at all time points. Glutamine tracing of glycolytic metabolites shows low labeling of metabolites until midway through the glycolytic pathway, but nearly 100% Fsat at the late steps of the glycolysis and all TCA cycle metabolites. Given this data highlighting high flux of glucose through the PPP, we tested the effects of pharmacological inhibition of the PPP on osteogenic differentiation. hBMSCs at 14 days of osteogenic differentiation showed a significant reduction in both ALP and alizarin red staining relative to control cells when cultured with G6PDi, an inhibitor of key PPP enzyme G6PDH. In addition, proliferation appears to be impacted, as cell number increased at a significantly slower rate over 48 hours in the G6PDi treated group.

Discussion: Collectively, metabolic-tracing experiments show that glucose primarily contributes to early glycolytic intermediates, but then preferentially shunts towards entry into the PPP rather than continuing through the later stages of glycolysis and TCA cycle. Glutamine supplies the whole TCA cycle and the later steps of glycolysis, likely via the malate-aspartate shuttle (MAS). This PPP preference allows for production of NADPH to maintain the reducing environment within the cytosol needed to allow for redox reactions, biosynthesis of nucleotide precursors to power proliferation, and production of ECM proteins. In summary, we report a novel, unusual metabolic setup in osteolineage cells that may be beneficial as they have high capacity for rapid proliferation and robust matrix biosynthesis, e.g. during bone fracture.

14th Annual Center for Musculoskeletal Research Symposium
October 17, 2024

Title: Analyzing the Association of the Area Deprivation Index on Patient-Reported Outcomes after Hip Arthroscopy

Presenting Author: Jordan Cruse

Co-Author(s): Hashim Shaikh, James Brodell Jr., Mina Botros, Terrence Daley-Lindo, Raymond Kenney

Lab PI / Mentor: Brian Giordano

ABSTRACT

Introduction:
Hip arthroscopy is a valuable tool, through which intra- and extra-articular hip pathologies may be addressed, with the goal of improving pain and function while preventing osteoarthritis progression. Little data are available regarding the association of social determinants of health on hip arthroscopy outcomes. The Area Deprivation Index (ADI) is a metric of relative socioeconomic disadvantage and has been shown to be associated with worse post-operative outcomes for several procedures. This study aimed to analyze the association of the ADI with patient-reported outcomes following hip arthroscopy for patients with femoroacetabular impingement syndrome.

Methods:
Patients undergoing hip arthroscopy between 1/1/2015–6/30/2022 at our institution were identified using Current Procedural Terminology codes. Patients' ZIP-codes were utilized to identify ADI measures. Patients were divided into quartiles of ADI, and the most deprived (ADIHigh) and least deprived (ADILow) quartiles were compared. Pre- and post-operative patient-reported outcomes measurement information system (PROMIS) scores along the pain interference (PI), physical function (PF), and depression (D) domains were obtained. For the PF and PI domains, the minimal clinically important difference (MCID) was defined using an anchor-based approach using previously established cutoffs. For the D domain, the MCID was defined using a distribution-based approach and calculated as one-half of the standard deviation of the pre-operative PROMIS score. Multivariable logistic regression models were estimated to characterize the association of the ADI with MCID attainment along PROMIS domains.

Results:
A total of 172 patients were included in the analysis of the ADIHigh and ADILow cohorts. Age, BMI, smoking status, and race did not significantly vary between groups. No significant differences in MCID attainment were observed at any timepoint in the PF, PI, or D domains. However, the ADIHigh cohort had higher average PI (worse) scores compared to the ADILow cohort at the pre-operative, 1 year, and final follow-up (mean = 2.50 years) time points. In multivariable logistic regression analyses, ADI was not associated with the odds of MCID attainment.

Discussion:
For patients undergoing hip arthroscopy for femoroacetabular impingement, increased social disadvantage measured by the ADI was not associated with the odds of MCID attainment in any PROMIS domain. This information provides guidance for care providers, researchers, and policymakers to seek and identify other mechanisms that may impact outcomes following hip arthroscopy.

14th Annual Center for Musculoskeletal Research Symposium
October 17, 2024

Title: Defining Provider Electronic Health Record Use Profiles for Outpatient Orthopaedic Surgery Encounters

Presenting Author: Eric Davis, MBA

Co-Author(s): Andrew Rodenhouse, MD; Gregg Nicandri, MD

Lab PI / Mentor: Gregg Nicandri, MD

ABSTRACT

Introduction:

For each patient encounter, there is an incredible burden imposed on physicians by electronic health record (EHR) related expectations including notes, in basket communications, clinical review, and orders. With a high volume of patients and limited time, completing EHR related tasks in a timely and efficient manner is challenging, and most often these activities are completed after hours interfering with physician personal time. This study categorizes total EHR usage patterns amongst orthopaedic surgeons to define and determine "Provider EHR Use Profiles." By examining provider time allocation both within and outside of scheduled hours, this analysis provides insight into the daily life of orthopaedic surgeons, highlighting specialty specific variations. Leveraging the results from this categorization approach can influence targeted interventions to improve workflow efficiency and work-life balance.

Methods:

A retrospective, quality improvement study of outpatient EHR data from faculty within the Department of Orthopaedics at an urban, academic medical center and satellite facilities over a one-month period was conducted. Epic Signal data, which provides detailed provider-level information were used to classify providers based on EHR use patterns into the following Provider EHR Use Profiles: 1) "best practice" (takes a break mid-day and finishes during standard work hours), 2) "long haul" (works in the EHR over lunch hour despite no patients scheduled, but finishes during standard work hours), 3) "I'm starving, but will be late for dinner" (works in the EHR over lunch hour despite no patients scheduled and prolongs work-day), 4) "classic pajama time" (ends the day as scheduled, but returns to the her later in evening), 5) "long day pajama time" (ends the day late and returns to the EHR later in evening), and 6) "code red" (starts early in the morning, works in the EHR over the lunch hour despite no patients scheduled, and continues to work late in the evening). Two reviewers independently categorized work patterns and time allocation.

Results:

49 providers from 9 orthopaedic specialties were included: 2 (4%) were categorized as "best practice," 13 (27%) "long haul," 10 (20%) "I'm starving, but will be late for dinner," 9 (18%) "long day pajama time," 8 (16%) "classic pajama time," and 7 (14%) "code red." 15 (31%), 18 (37%), and 16 (32%) of physicians were doing well, had room for improvement, or need to be considered for intervention, respectively. Inter-rater reliability between the two reviewers was assessed using Cohen's kappa coefficient and was determined to be acceptable (0.47). One "best practice" physician practices in Foot/Ankle, while the other specializes in Hand/Upper Extremity. Sports/Shoulder (42%) and Hand/Upper Extremity (50%) have the greatest number of physicians doing well. Specialties that have the most physicians with room for improvement include General (100%) and Foot/Ankle (86%). Interventions should be considered for physicians in the following specialties: Joints (57%), Sports/Shoulder (17%), Tumor (50%),
Hand/Upper Extremity (38%), Trauma (67%), and Spine (60%).

Conclusion:

This novel approach to define Provider EHR Use Profiles serves as an innovative and unique insight into the daily life of orthopaedic surgeons. These findings underscore the burden placed on physicians by the EHR and documentation requirements, which should be addressed in order to develop sustainable practice environments that allow for less burnout, increased efficiency, and improved work-life balance. This technique could be used in the future to better understand provider working styles, evaluate provider wellness, and assess the efficacy of strategies aimed at improving physician efficiency in performing EHR related tasks.

14th Annual Center for Musculoskeletal Research Symposium
October 17, 2024

Title: Quantifying the Burden of Documentation in the Electronic Health Record in Outpatient Orthopaedic Surgery Encounters

Presenting Author: Eric Davis, MBA

Co-Author(s): Andrew Rodenhouse, MD; Gregg Nicandri, MD

Lab PI / Mentor: Gregg Nicandri, MD

ABSTRACT

Introduction:

Documentation within the electronic health record (EHR) is a time-consuming, onerous task that contributes to physician burnout and interferes with both clinical and personal responsibilities. There is a paucity of literature on the burden of the EHR, most specifically the documentation process, in the field of orthopaedic surgery.

Methods:

A retrospective, quality improvement study of outpatient EHR data from faculty within the Department of Orthopaedics at an urban, academic medical center and satellite facilities over a 1-year period was conducted. Epic Signal data, which provides detailed provider-level information were used to quantify the burden of EHR-related tasks including documentation. Metrics included the number of appointments per day, average time in notes per day, pajama time, progress note length, and percent of appointments closed per day. Pajama time is defined as the average number of minutes a provider spends on charting activities on weekdays outside the hours of 7:00 AM - 5:30 PM or outside scheduled hours on weekends or non-scheduled holidays. Physicians were categorized based on orthopaedic subspecialty and experience (years in practice).

Results:

52 providers from 9 orthopaedic subspecialties were included. The average number of appointments per day were 23.4 and the average progress note length was 3,427 characters. The average time in notes and pajama time were 21.4 and 27.1 minutes per day, respectively. The average percentage of appointments closed the same day was 65.6%. Sports/ Shoulder had the highest average number of appointments per day (32.0) compared to Spine, which had the fewest (11.3). Joints had the longest average progress note length at 5,459 characters and largest average time in notes per day (30.2 minutes). However, Tumor and Trauma demonstrated the greatest average pajama times (56.9 and 71.2 minutes, respectively). General orthopaedists had the highest percentage of appointments closed the same day at 97.4%. Physicians with 5 years or less experience had the highest percentage appointments closed the same day (74.8%) while having the largest pajama time (40.3 minutes). Interestingly, providers with >20 years close a similar percentage of appointments the same day (73.5%), but with only 20.4 minutes of pajama time. Additionally, those between 15 and 20 years of experience had a markedly reduced percent of appointments closed the same day (24.4%).

Conclusion:

Quantification of EHR metrics provides a baseline understanding of the orthopaedist's experience with the EHR, including the documentation process, and its resultant burden on both clinical and personal obligations. Analysis of EHR metrics using Epic Signal data is a novel method to identify groups of individuals for targeted efficiency improvement and to evaluate the utility of workflow interventions in the future.

14th Annual Center for Musculoskeletal Research Symposium
October 17, 2024

Title: Clinical and Radiographic Outcomes of Distal Radius Fractures Following Dorsal Bridge Fixation to the Second Versus Third Metacarpal

Presenting Author: Akhil Dondapati MD

Co-Author(s): Thomas J. Carroll MD, Warren Hammert MD, Ronald Gonzalez DO

Lab PI / Mentor: Constantinos Ketonis MD PhD

ABSTRACT

Purpose: Dorsal bridge plating (DBP) can effectively treat complex distal radius fractures (DRFs), however, techniques vary for metacarpal fixation. There remains a paucity of literature directly comparing clinical outcomes and complication rates between second and third metacarpal fixation with DBP. The purpose of our study was to compare range of motion (ROM), grip strength, patient-reported outcomes, radiographic parameters, and complication rates between patients undergoing DBP with fixation to the second versus third metacarpal for DRFs.

Methods: We retrospectively analyzed 432 patients aged 18 to 90 years with DRFs. Wrist ROM and radiographic data were calculated at 6-month follow-up. Exclusion criteria comprised revision surgery, patients outside the specified age range, those with polytrauma, prior wrist surgery, and individuals lacking at least 6 months of follow-up. We calculated PROMIS Upper Extremity, Physical Function, and Pain Interference at each visit. Additional data collected included surgical complications, and demographic data. Statistical analysis was conducted via multivariate analysis, T-test, and Chi-Square tests.

Results: A total of 329 patients underwent DBP to the second metacarpal, while 103 patients underwent DBP to the third. Demographics, comorbidities, and AO/OTA fracture classification were similar between the groups ($p>0.05$). Tendon rupture was more common in the third metacarpal group (3.9% vs. 0.9%; $p<0.05$), with two EPL and one EIP ruptures in each group and an additional, unspecified tendon in the third metacarpal cohort. All other complication rates were similar. The second metacarpal group demonstrated greater wrist flexion (57.8° vs. 56.2°; $p<0.05$), ulnar deviation (23.9° vs. 20.7°; $p<0.05$), and grip strength (62.3% vs. 57.8%; $p<0.05$). All other ROM measurements were similar. There was no difference in any PROMIS metric at 6-month follow-up. The second metacarpal group demonstrated greater radial inclination (21.3° vs. 19.5°; $p<0.05$) and less volar tilt (6.8° vs. 7.1°; $p<0.05$) with similar radial height and articular step-off.

Discussion/Conclusions: DBP to the second metacarpal for treatment of DRFs, is associated with lower rates of extensor tendon rupture and improved clinical and radiographic outcomes compared to third metacarpal fixation. However, some differences in these outcomes may not be clinically relevant. Both techniques lead to acceptable results and can be considered depending on fracture pattern and preference. Future randomized or prospective studies may seek to further characterize any differences in metacarpal fixation technique.

14th Annual Center for Musculoskeletal Research Symposium
October 17, 2024

Title: Machine Learning Utilization to Predict Osteoporosis Status from Plain Hand Radiographs

Presenting Author: Akhil Dondapati MD

Co-Author(s): Andrew Rodenhouse MD, Thomas Carroll MD, Gilbert Smolyak BS, Jeffrey Lillie PhD, Ajay Anand PhD, Lisa Pink MS, David Mitten MD

Lab PI / Mentor: Constantinos Ketonis MD PhD

ABSTRACT

Introduction: It has previously been demonstrated that the second metacarpal cortical percentage (2MCP) correlates with osteoporosis status. We hypothesize that a machine learning algorithm can predict osteoporosis status from plain hand radiographs. We propose a novel, end-to-end pipeline that takes raw hand radiographs, identifies and segments the second metacarpal, and uses its features, specifically the 2MCP, to predict osteoporosis status.

Methods: A large, multi-institutional dataset of patients having undergone x-ray(s) of the hand within one year of a dual x-ray absorptiometry (DEXA) scan was generated. A series of preprocessing steps removed extraneous information and a convolutional neural network was trained on 61488 AP hand x-rays (image augmentation from 427) to detect and automatically segment the second metacarpal. Images were augmented by rotation in increments of 5 degrees and flipping to make the classifier robust and independent of rotation. A total of 1660 hand x-rays were passed through the trained algorithm to extract the second metacarpal. Post-segmentation steps included edge detection, truncation, and visualization of the middle third on a line profile through the center of the metacarpal. A computer vision-based approach was implemented to automatically compute the average 2MCP and compared with measurements performed by two, independent measurers.

Results: Automatic second metacarpal detection accuracy was 100% in a testing set of 1660 radiographs that were used in the subsequent steps. The machine learning algorithm was able to perform independent of rotation of the presented image. The middle third of the metacarpal was then isolated. Interobserver reliability between two independent human experts was high, with a correlation coefficient of 0.67. The automated 2MCP measurement was in good agreement with manual measurements (correlation coefficient 0.74). Even though this automatically generated metric can be used as a proxy for osteoporosis status, next steps will include direct correlation between 2MCP and T-scores from the DEXA scans at the forearm and hip.

Discussion/Conclusions: We present a novel, machine learning algorithm, trained on a large, multi-institutional dataset, that can accurately measure the 2MCP, a metric previously shown to predict osteoporosis status. The algorithm output will further be directly correlated with T-scores from DEXA scans (ground truth) to refine osteoporosis prediction. With this large, multi-institutional dataset, we aim to generate a complete end-to-end pipeline that will produce consistent, generalizable results. Future iterations of this machine learning algorithm could serve as a serendipitous screening tool to diagnose osteoporosis earlier to prevent osteoporotic fractures.

14th Annual Center for Musculoskeletal Research Symposium
October 17, 2024

Title: Role of Mitochondrial Genetics in the Response of Bone Marrow Stromal Cells to Mechanical Stimulation

Presenting Author: Renae Duncan

Co-Author(s): Sarah Catheline, Chen Yu, Sandra Castillo

Lab PI / Mentor: Roman Eliseev

ABSTRACT

Background & Hypothesis: Previous work shows that mitochondrial oxidative function affects osteoblast (OB) differentiation and age-related bone loss, highlighting the significance of mitochondria in bone health. Mitochondrial genome (mtDNA) variations, represented by haplogroups formed by inherited SNPs, impact mitochondrial oxidative efficiency. More efficient original African haplogroup L is associated with stronger bones than more recent Eurasian haplogroups. Mouse strains C3H/HeJ (C3H) and C57BL/6 (C57) mimic these human haplogroups, with C3H mice exhibiting more efficient mitochondria and stronger bones. Importantly, recently developed mitochondrio-nuclear exchange (MNX) technology allows dissection of contribution of nuclear genome vs mtDNA to the phenotype. In this regard, C3H MNX cells (C3H nucleus with C57 mitochondria) show less efficient while C57 MNX cells (C57 nucleus with C3H mitochondria) show more efficient oxidative function when compared to their wild-type (WT) counterparts. Mechanical stimulation has been shown to activate mitochondria in bone marrow stromal cells (BMSCs), regulating bone metabolism. This study aims to examine how mtDNA haplotypes affect BMSC response to mechanical stimulation from exercise. The hypothesis for this project is exercise will enhance mitochondrial oxidative phosphorylation, osteogenicity in BMSCs, and bone formation in OBs, and thus improve bone phenotype, with mice having more efficient mitochondria showing a stronger response.
Experiments & Methods: Mice used will be: C57 WT, C57 MNX, C3H WT, and C3H MNX, including both young (3-6 mths) and aged (18 mths) males and females. Mice will undergo treadmill training for two weeks at 10 m/min, and 10^0 incline for 30 minutes per day after a 3-day acclimation period. Post-training, both trained and untrained mice will be euthanized, and tibias will be isolated for micro-CT imaging. Serum will be collected for ELISA analysis of bone formation marker P1NP and bone resorption marker CTX1. BMSCs from femurs will be used for colony-forming (CFU) assays, and mitochondrial oxidative function assays via flow cytometry. Data will be analyzed using GraphPad Prism 10, with statistical tests including Student's t-test and ANOVA for two- and multi-variable comparisons respectively, using a significance level of 0.05.
Results: During exercise female C3H MNX mice took significantly more rest than C3H WT mice. Exercise significantly boosted CFUs in both young and aged male and female C57 and C3H strains, with C3H mice displaying higher CFUs consistent with its more robust bone phenotype. Micro-CT of tibias showed that introducing less efficient C57 mitochondria into C3H bone significantly reduced bone parameters, while the reverse had no effect. Flow cytometry analysis of mitochondrial function showed that BMSCs from male and female aged C57 mice have significantly increased mitochondrial membrane potential and mitochondrial mass.

Discussion & Conclusions: Female C3H MNX mice took more rest when compared to C3H WT mice. This suggests that having less efficient C57 mitochondria may lead to lower endurance in female mice. Mechanical stimulation increases the number of BMSC CFUs in both strains which implies that mechanical stimulation induces colony formation which suggests a potential bone anabolic effect. C3H WT BMSCs more efficiently form colonies than C57 WT BMSCs consistent with its more robust bone phenotype. Replacing C3H mitochondria with C57 ones reduces trabecular and cortical bone parameters in C3H mice as the C57 mitochondria are less efficient and result in weaker bones. Increases in both mitochondrial mass and function and CFUs in aged BMSCs post-exercise suggest that mechanical stimulation is beneficial for BMSCs, highlighting the importance of mitochondria in BMSC and bone response to mechanical stimuli. Ongoing studies are exploring molecular mechanisms connecting mechanical stimulation and mitochondrial response in osteoprogenitors.

14th Annual Center for Musculoskeletal Research Symposium
October 17, 2024

Title: CUT&Tag applied to zebrafish adult tail fins reveals a return of embryonic H3K4me3 patterns during regeneration

Presenting Author: Phu Duong

Co-Author(s): Anjelica Rodriguez-Parks, Junsu Kang, and Patrick J. Murphy

Lab PI / Mentor: Patrick J. Murphy

ABSTRACT

Regenerative potential is governed by a complex process of transcriptional reprogramming, involving chromatin reorganization and dynamics in transcription factor binding patterns throughout the genome. The degree to which chromatin and epigenetic changes contribute to this process remains only partially understood. In particular, the chromatin-level understanding of zebrafish's caudal fin regeneration remains relatively unexplored. Here we provide a modified CUT&Tag protocol suitable for improved characterization and interrogation of changes in chromatin modifications during adult fin regeneration in zebrafish. Our protocol generates data that recapitulates results from previously published ChIP-Seq methods, requires far fewer cells as input (2 or 3 caudal fins per replicate instead of 40 fins in prior studies), and significantly improves signal to noise ratios. With three pooled replicates, we deliver high-resolution enrichment maps for H3K4me3 of uninjured and regenerating fin tissues. During regeneration, we find that H3K4me3 levels increase over gene promoters which become transcriptionally active and genes which lose H3K4me3 become silenced. Interestingly, these reprogramming events recapitulate the H3K4me3 patterns observed in developing fin folds of 24-h old zebrafish embryos which were also pooled into at least three replicates. Our results indicate that changes in genomic H3K4me3 patterns during fin regeneration occur in a manner consistent with reactivation of developmental programs, lending the support to the ideas that developmental program is a part of regeneration and that such process is conserved among the organisms with high regenerative potentials. Additionally, our work also demonstrates CUT&Tag to be an effective tool for profiling chromatin landscapes in regenerating tissues. Despite the past technical challenges, Cut&Tag allows for the new types of insights because it provides potentially clearer, more easily obtainable data, enabling the detection of rare cell types, analysis of exotic animal tissues, and the formulation of new hypotheses and models.

14th Annual Center for Musculoskeletal Research Symposium
October 17, 2024

Title: Patient-Specific Factors Impact Outcomes Following Flexor Tendon Repair

Presenting Author: Christopher Dussik, MD

Co-Author(s): Andrew J. Rodenhouse, MD, Akhil Dondapati, MD, Gilbert Smolyak, BS, Thomas J. Carroll, MD, Giap Vu, MD, Gabriel Ramirez, MS, Constantinos Ketonis, MD, PhD

Lab PI / Mentor: Constantinos Ketonis, MD, PhD

ABSTRACT

Introduction: This study sought to evaluate patient-specific factors that may impact outcomes after flexor tendon repair. We hypothesized that age, gender, comorbidities, insurance-type, and area of deprivation index (ADI) would all affect postoperative outcomes.

Methods: This is a retrospective study of patients who underwent primary flexor tendon repair between 2015-2023 at an academic institution. Electronic medical records were reviewed. Thumb and Zone 1 FDP avulsion injuries were excluded. Mixed effects linear regression with a random intercept at the digit level, logistic, linear, and negative binomial regression models were constructed to identify factors associated with ASSH Total Active Motion (TAM), return to operating room (RTOR), compliance, time until return to work and discharge from hand therapy, and Patient Reported Outcomes Management Information System (PROMIS) T-scores. Significance was defined as p-values < 0.05.

Results: In total, 397 patients met inclusion criteria. Advanced age resulted in significantly greater odds of RTOR with individuals ≥30 and <50 having 3.7 higher odds (p-value 0.002) whereas those ≥50 had 6.4 higher odds (p-value 0.000). Interestingly, age ≥50 had 2.7 higher odds of postoperative compliance with rehabilitation expectations (p-value 0.02). Patients ≥30 and <50 had significantly poorer PROMIS scores including lower physical function at 12 weeks (p-value 0.016), higher pain interference at 6 weeks (p-value 0.004) and 12 weeks (p-value 0.001), and higher depression at 6 weeks (p-value 0.018) and 12 weeks (p-value 0.001). Patients ≥50 also had significantly higher pain interference at 12 weeks (p-value 0.001). Men had significantly lower odds of compliance postoperatively relative to women (p-value 0.036). Black / African American patients had significantly impaired functional outcomes at 6 weeks with 20.0 degrees less TAM on average (p-value 0.047). Likewise, they experienced inferior PROMIS scores with significantly higher pain inference (p-value 0.037) and depression (p-value 0.006) scores at 6 weeks. Overweight BMI (≥25, <30) resulted in significantly reduced time until return to work (p-value 0.045). Surprisingly, patients with workers' compensation had 7.07 greater odds of postoperative compliance (p-value 0.013), however, they also had longer time until discharge from hand therapy (p-value 0.000). Lastly, one unit increase in ADI was associated with significantly lower odds of compliance by 23% (p-value 0.037) and with 8% longer length of hand therapy (p-value 0.008).

Discussion: Patient-specific factors including age, gender, BMI, insurance, and ADI are associated with flexor tendon repair outcomes including PROMIS, TAM, RTOR, compliance, complications, time to therapy discharge and return to work.

14th Annual Center for Musculoskeletal Research Symposium
October 17, 2024

Title: Endothelial Cell Remodeling in an Idh2 Mutant Murine Model

Presenting Author: Edgardo I Franco

Co-Author(s): Christina M. Kaszuba, Benjamin J. Rodems, Sonali Sharma, Omar Abdel-Wahab, and Jeevisha Bajaj

Lab PI / Mentor: Jeevisha Bajaj

ABSTRACT

Hematopoiesis is the process of self-renewal and differentiation of hematopoietic stem and progenitor cells (HSPCs) within the bone marrow microenvironment (BMME). Various cell types reside within the BMME including mesenchymal stromal cells, osteoblasts and endothelial cells. A disruption in the differentiation and functionality of HSPCs may lead to disorders such as myelodysplastic syndromes (MDS) and acute myeloid leukemia (AML). MDS occurs when HSPCs become abnormal or have mutations that lead to a block in differentiation, resulting in progressive bone marrow failure. One such mutation is the Isocitrate dehydrogenase 2 (IDH2) mutation, where 70% of MDS patients with this mutation are classified with high-risk MDS. Further, it is recognized that alterations to the endothelial niche within the bone marrow, specifically in the vessel structure and density, are associated with human MDS. To model this disease, we transplanted HSPCs from Idh2R140Q/+ mice into healthy wildtype recipient controls. After confirming the onset of pre-MDS in the recipient mice, we analyzed endothelial cell quantity through flow cytometry. Our data suggests a change in distinct endothelial subsets, where there is an increase in arteriolar endothelial cells and a decrease in sinusoidal endothelial cells, which in turn may also indicate functional changes. To determine functional mechanisms that can promote MDS development, we used tube formation assays to quantify angiogenesis of endothelial cells. Likewise, diffusion of fluorescently labelled dextran was used to analyze the diffusion and permeability of the endothelial cells. These functional assays suggest that exposure HSPCs with Idh2R140Q mutations may induce pro-angiogenetic properties such as increased tube formation and endothelial cell permeability. We are currently working on identifying mechanisms by which the IDH2 mutations lead to these changes in the endothelial populations, and their role in disease progression. These studies indicate that altered endothelial cell growth and function may support disease progression, and blocking these changes in endothelial cells may be of therapeutic relevance in MDS.

14th Annual Center for Musculoskeletal Research Symposium
October 17, 2024

Title: Rotator Cuff Tear Adversely Induces Articular Cartilage Thickening and Subchondral Bone Remodeling in Mice in a Sex-Dependent Manner

Presenting Author: Dylan N. Greif*

Co-Author(s): Paromita Kundu*; Farah A. Al-Omari*; Yaxin Zhang; Yufei Jiang; Do-Gyoon Kim

Lab PI / Mentor: Sandeep Mannava, Whasil Lee

ABSTRACT

Introduction: Rotator cuff tears (RCT) remain a common orthopaedic injury causing substantial pain and disability, with tears involving two or more tendons causing significant instability to the glenohumeral joint. On a biomechanical level, this process can lead to rotator cuff tear arthropathy (CTA), where articular cartilage is worn over time leading to abnormal destruction of the glenohumeral (GH) joint due to alterations in mechanical stimuli causing chondrocyte remodeling. However, there remains a significant lack of knowledge addressing how cartilage degeneration occurs after RCTs. Furthermore, while women are known to have a higher risk of clinically suffering from osteoarthritis compared to men, there is limited work addressing if the same bears out with CTA specifically, what differences occur immediately after injury, or what exact mechanisms may cause this progression over time. Therefore, the objective of this study is to present an expanded murine based model that assesses the immediate articular response to injury within the GH joint and whether female sex potentiates this injury response.

Methods: After obtaining IRB approval, a total of fifty 12 week old mice (30 female, 20 male), were subjected to surgical ligation of the supraspinatus and infraspinatus tendons to induce rotator cuff injury. Mice were divided into two groups: sham and bilateral RCT. Bilateral RCT was chosen in order to prevent mice from purposely favoring the uninjured limb, thus promoting more weight-bearing and thus theoretically accelerating CTA development. Associated bone volume and tissue mineral density (TMD) of the subchondral bone were assessed in response to RCT injury through in-vivo micro-CT analysis 8 weeks after surgery, with the glenoid cavity defined as the GH joint articulating region. Mice were subjected to grip and gait testing (front tracking width) 20 weeks after surgery in order to assess behavioral response to RCT injury. Mice were sacrificed 24 weeks after surgery, and humeral explants were harvested and stained with fast green to visualize intact joint morphology and Safranin-O (SafO) to selectively visualize cartilage. OARSI grading was used to measure histological OA development.

Results: SafO staining demonstrated no significant differences in OARSI grading between male and female mice. Hyaline cartilage was notably thicker in the bilateral RCT group for female and male mice respectively, suggesting adverse response to injury. Bilateral RCT notably altered gait in both male and female mice, with females showing a significantly greater decrease in stride width following the injury. After undergoing micro CT, frequency plotting of total mineral density (TMD) for male and female mice showed decreased mineralized bone in female versus male mice. RCT surgery further stimulated active bone remodeling after injury, though RCT led to decreased mineralization of newly formed subchondral bone, particularly in female mice.

Discussion: Our findings show that after inducing bilateral RCT injury, mice begin to quickly develop adverse responses to altered mechanical stimuli. In particular, female mice were more prone to increased HC thickness at both the humeral head and glenoid, which for the shoulder specifically is an adverse response to injury as the shoulder is not a weight-bearing joint (thus there is reduced compressive loading) and thus does not show thinning typically seen in the knee or hip. This may also be explained by the more significantly altered gait female mice demonstrated compared to male mice. RCT stimulated active bone modeling in response to injury, however subchondral bone produced was notably less mineralized compared to the sham group, particularly in females. Overall, while RCT induces early articular cartilage thickening and adverse subchondral bone remodeling in general (suggesting GH changes occur soon after injury), female sex is at risk for more exaggerated changes from onset of injury.

14th Annual Center for Musculoskeletal Research Symposium
October 17, 2024

Title: Efficacy of Transcatheter Arterial Embolization in Traumatic Pelvic Fractures: A Systematic Review and Meta-Analysis

Presenting Author: Paul G. Guirguis

Co-Author(s): Ankit Punreddy, Mina Botros, James D. Brodell Jr., Michael T. Gorczyca, Noah M. Joseph, John P. Ketz, Catherine Humphrey, John T. Gorczyca

Lab PI / Mentor: John T. Gorczyca

ABSTRACT

Introduction: Pelvic ring injuries are high-energy traumatic disruptions of the osseo-ligamentous structures of the pelvis which can result in significant hemorrhage. Arterial embolization is one method employed to reduce ongoing hemorrhage; however large studies regarding the efficacy of embolization in the management of pelvic fractures are scarce. The purpose of the present study is to compare (1) mortality, systolic blood pressure, and transfusion requirements among pelvic fracture patients who underwent angiography without embolization versus with embolization, (2) mortality after embolization versus after open pelvic packing, and (3) mortality after embolization within 120 minutes of arrival versus after 120 minutes.

Methods: Online databases (PubMed; MEDLINE; EMBASE; CINAHL; ClinicalTrials.gov) were queried for studies regarding pelvic fractures and embolization. Original studies written in English were included and screened. Case reports, reviews, animal studies, and cadaveric studies were excluded. Screening and data extraction was conducted by two independent reviewers. Discordance was settled by a third adjudicator. Meta-Analyses were conducted with random effects model to determine pooled risk ratio (RR), effect size, and odds ratio (OR).

Results: Twenty-two studies reported clear outcomes of embolization. A total of 1473 pelvic fracture patients underwent angiography and 1053 (71.5%) of these were embolized. Mean time from hospital arrival to angiography was 271.7 minutes (60–840; n=1150). Injury Severity Score (ISS) of embolized patients was significantly higher than those who underwent angiography without embolization (M-H=10.44; 95%CI: [0.67, 20.20]; p=0.04). Systolic blood pressure (SBP) was significantly lower in those embolized compared to those who underwent angiography without embolization (M-H=-9.60; 95%CI: [-19.30, 0.10]; p=0.04). Transfusion requirements (units of packed red blood cells) in the first 24 hours after arrival to emergency department was significantly higher in those embolized versus those who underwent angiography without embolization (M-H=4.19; 95%CI: [2.19, 6.19]; p<0.0001). Patients who underwent angiography within two hours of arrival had mortality rate of 18% (95%CI: [0.13, 0.25]), while patients who underwent angiography more than two hours after arrival had mortality of 24% (95%CI: [0.16, 0.33]). There was no significant difference in mortality rate between embolized and packing patients (OR=2.44: 95%CI: [0.81, 7.36]; p=0.11).

Conclusions: Overall, there seems to be a benefit to expedited evaluation and treatment of these patients. Embolized pelvic fracture patients presented with higher ISS and lower SBP and had higher transfusion requirements compared to those who underwent angiography without embolization. Embolized pelvic fracture patients who underwent angiography within two hours had reduced mortality compared to those who underwent angiography later. Mortality was not different between embolized patients and those treated with packing.

14th Annual Center for Musculoskeletal Research Symposium
October 17, 2024

Title: Stiffness and Topography Modulates TRPV4 Activation in AF Mechanotransduction

Presenting Author: Johannes Hasler

Co-Author(s): Mikkael Lamoca, Gabbie Wagner, Karin Wuertz-Kozak

Lab PI / Mentor: Karin Wuertz-Kozak

ABSTRACT

Low back pain (LBP), a major cause of disability, often results from intervertebral disc (IVD) degeneration. IVD degeneration, commonly associated with disc herniation, significantly compromises the structural integrity of the outer region known as the annulus fibrosus (AF). This results in increased substrate stiffening and disorganization of the collagen I fiber architecture. Transient receptor potential (TRP) channels, specifically TRPV4, facilitate pivotal cell regulatory responses by sensing mechanical stimuli and are implicated in inflammation and pain, but their role in IVD degeneration remains underexplored. The hypothesis of the study is that TRPV4 modulates essential cellular responses to changes in substrate stiffness, topography, and mechanical loading via enhanced intracellular Ca2+ levels, thereby modulating downstream targets associated with degeneration and inflammation. Experiments were conducted in bovine AF cells. (1) The downstream effects of TRPV4 activation were analyzed via RT-qPCR after an 18-hour GSK101790A (=TRPV4 activator) treatment (n=3). (2) Substrate stiffness was varied using polydimethylsiloxane (PDMS) substrates with different ratios of Sylgard 184 and 527 (0, 14, and 24 wt%), incorporated into cell stretching chambers using aluminum molds and cured for 24h at 65°C. Young's Modulus was obtained using a uniaxial tensile tester at a strain rate of 10 mm/s until rupture (n=5). TRPV4-mediated Ca2+ flux was measured using a Fura-2 QBT assay with GSK101790A on different substrate stiffnesses (n=5) or inhibited on tissue culture plastic (TCP) with GSK2193874 (n=3). (3) Mechanically induced Ca2+ flux was assessed using Calbryte 520AM via fluorescent microscopy in PDMS cell stretching chambers subjected to cyclic stretching (10%, 0.167 Hz, 15 min). Shapiro-Wilk test for normality assessment and one-way ANOVA was performed in GraphPad Prism. (1) Preliminary results show that TRPV4 activation increases inflammatory (IL8, COX2) and catabolic (MMP3) markers. PDMS substrates (2), with 9, 63, and 240 kPa stiffness, effectively mimic healthy to degenerated AF conditions. TRPV4 activation induces stiffness-dependent Ca2+ influx, with the lowest intracellular Ca2+ levels at 9 kPa compared to the higher substrate stiffness (63, 240k Pa). Ca2+ influx is inhibited in a dose-dependent manner by the TRPV4 inhibitor, with complete inhibition at 5 µM. (3) Additionally, cyclic stretching triggers Ca2+ flux, which is also suppressed by 5 µM TRPV4 antagonist. The in vitro biocompatible cell-substrate interaction model replicates the increased stiffness during degeneration, which resulted in TRPV4 activation evidenced by enhanced Ca2+ flux, indicating a possible correlation between TRPV4 activation and stiffness-associated degradation. Preliminary gene expression indicates that TRPV4-driven Ca2+ modulates cell behavior, promoting catabolism and upregulation of inflammatory genes. The inhibitory effect of GSK2193874 further supports the specificity of TRPV4 activation. Our data indicates the central role of TRPV4 in IVD metabolism by sensing stiffness and mechanical cues, resulting in changes in inflammatory and catabolic markers that further progress AF degeneration. Ongoing experiments aim to link enhanced TRPV4-dependent Ca2+ flux due to different stiffnesses with relevant extracellular matrix, inflammatory, and degeneration-associated downstream targets using RNA-seq. To further enhance the cell-substrate interaction model for studying AF degeneration, we fabricate topographies with PDMS fibers to mimic healthy (aligned) and degenerated (random) collagen fibers. By incorporating topographical cues into our stretching chambers, we can explore stiffness and topography in combination with mechanical activation of TRPV4 through cyclic stretching in the future.

14th Annual Center for Musculoskeletal Research Symposium
October 17, 2024

Title: The Bone Marrow Stromal Network Communicates Through Intercellular Calcium Waves and is Disrupted via Gap Junction Inhibition and Single-cell Deactivation of the "Hub" Cells

Presenting Author: Cih-Li Hong

Co-Author(s): Montgomery L. Whalen, Juwell Wu, Charles P. Lin, Shu-Chi A. Yeh

Lab PI / Mentor: Shu-Chi A. Yeh

ABSTRACT

Introduction: Intercellular communication through calcium signaling orchestrates coordinated cell functions across diverse tissues, including neuronal signal transduction [Kuga, et. Al., 2011], myocyte contraction [Sridhar, et. Al., 2020], and endocrine secretion [Beekers, et. Al., 2020]. Bone marrow stromal cells (BMSCs) form a pervasive 3D network in the marrow. It has been shown that BMSCs in culture utilize intercellular calcium waves (ICWs) through gap junctions to enable synchronized transcriptional reprograming and release of CXCL12, a key cytokine regulating healthy/malignant hematopoiesis and inflammatory responses [Schajnovitz, et. Al., 2020]. However, whether the same mechanism is involved in vivo remain poorly understood. We hypothesize that BMSCs utilize ICWs to achieve long-range communications in vivo and can be abolished by gap junction inhibitors. In addition, as ICW require a "hub cell" to initiate calcium propagation cascades, we also hypothesize that hub cells exist within the BMSC network; de-activating or stimulating the hub cells will modulate ICWs and cytokine secretion.

Methods: To visualize the network activity, we developed intravital calcium imaging and analysis pipelines to study BMSCs in the calvarial bone marrow of live mice under steady state or acute inflammation (1 hour after lipopolysaccharide (LPS), IV, 20 μg/mouse). Adult female and male LepRcre; Salsa6f mice were used, where genetically encoded calcium indicator GcaMP6f are expressed within BMSC lineages. To manipulate ICWs, gap junction inhibitor Carbenoxolone (CBX) were topically administered to the skull surface (1.5 mg/mouse, 1 hour) to avoid systemic disruption of calcium signaling. We also employed laser-assisted single-cell ablation [Hill, et. Al., 2017; Schmalz, et. Al., 2023] to specifically deactivate the hub cells. Calcium signals in steady state, LPS, LPS/CBX, and LPS/hub ablation groups were quantified based on the frequency of calcium spikes per pixel over time and the rate of spatial propagation of ICWs (activated pixel area/unit time). Moreover, to quantify coordinated calcium activities, we adapted previously published methodologies [Smedler, et. Al., 2014; Rubinov, et. Al., 2010; Ho, et. Al., 2023] to retrieve the landscape of cell pairs that exhibit high cross-correlation of calcium transients. Two-sided Mann Whitney test was used to determine statistical significance.

Results: We demonstrated that only a subset of BMSCs communicate through ICWs and LPS treatment significantly increased both the frequency of calcium spikes and wave propagation. Network analysis identified a subset of BMSCs as "hub" cells, responsible for initiating long-range (> 100 microns) correlations within the stromal network (N= 8). Notably, gap junction inhibition using CBX abolished the dynamic syncytium triggered by LPS, as evidenced by a reduction in the cross-correlation of calcium transients (N=3). Preliminary data also suggested that ablation of hub cells alone was able to disrupt ICWs, whereas deactivating non-hub cells did not alter calcium activities (N=2), suggesting that ICW disruption was not a result of ablation-induced damage response.

Discussion and Conclusion: Our results suggested that BMSCs are heterogenous. Communicative network forms within a subset of cells upon acute inflammation and can be disrupted by gap junction inhibitor or focal ablation of hub cells. It further suggested that cytokine secretion are likely spatially heterogenous, and the findings provide a novel approach for identifying and manipulating functional subsets of stromal network function in vivo. One limitation in this study is that CBX is not specific to connexins, thus future investigations will include genetic deletion and gain of function studies of connexin 43 to better delineate the mechanisms of ICWs. Functional significance will be further established via cytokine secretion and maintenance of healthy and leukemic stem cells.

14th Annual Center for Musculoskeletal Research Symposium
October 17, 2024

Title: Young and Aged Quiescent Joint Tissues Fail to Repair DNA Efficiently, Implications for Chronic Knee Pain After Irradiation

Presenting Author: Nick James

Co-Author(s): Alexander Matthewson, Katherine Escalera-Rivera, Danielle Benoit, Jennifer Jonason

Lab PI / Mentor: Jennifer Jonason

ABSTRACT

INTRODUCTION: Osteoarthritis (OA) is the most common form of arthritis and is characterized by progressive loss of articular cartilage which can cause chronic joint pain and loss of mobility. Recently studies have shown that aged or OA human knee cartilage contains more DNA-damaged chondrocytes than young or healthy cartilage. Furthermore, proinflammatory pathways are activated in response to DNA double-strand breaks (DSBs) including the NF-κB pathway. We previously identified increased NF-κB activity in aged chondrocytes and demonstrated early OA onset in young mice in a model of chondrocyte-specific NF-κB induction. However, whether DNA damage causes proinflammatory signaling in chondrocytes remains unknown. Here, a combination of in vitro DNA DSB induction and highly localized X-irradiation to induce DNA damage in young and aged mouse knee joints in vivo was used to examine the role of DNA damage in chronic inflammation, pain-related behaviors, and OA onset. METHODS: Chondrocyte-like ATDC5 cells were placed in maturation media for 1 or 2 weeks before treatment with 25 μM etoposide for 48 hours to induce DNA DSBs. Protein and RNA were collected for analysis. Male C57BL6/J mice, 4 or 20 months old, were irradiated using the small animal radiation research platform (SARRP). Irradiated mice received either a single 8.2 Gy dose (n=6) or a more clinically relevant 3x8.2 Gy fractionated dose (n=8) to the right knee joint. Non-irradiated mice and/or non-irradiated contralateral limbs acted as controls. Mouse mobility and pain-related behaviors were assessed 6- and 9-months post-irradiation by locomotor, gait, rotarod, and knee pressure application measurement (PAM). Mouse hind limbs were collected 2 hours, 48 hours, or 1 week, after single or 9 months after 3x8.2 Gy irradiation for paraffin histology. γH2AX IHC was used to evaluate DNA DSB repair in vivo. All animal studies were approved by UCAR. RESULTS: Maturation of chondrocyte-like cells decreased their proinflammatory response to DNA DSBs. Undifferentiated ATDC5 responded to DNA DSBs with phosphorylation of p65 (P-p65, S536), indicating activation of NF-κB signaling, and induction of proinflammatory genes (Ccl20, Ccl2, Il6, and Isg15). Following 1 week in maturation media, P-p65 was still induced by DNA DSBs, but not at 2 weeks, when the cells are hypertrophic. Following a single 8.2 Gy X-ray dose, most articular chondrocytes were γH2AX+, with slower repair in mineralized versus unmineralized regions. Notably, synovium and marrow cells completely repaired from a single dose within 48 hours while cartilage, growth plate, and subchondral bone repaired slowly over a week. After 3x8.2 Gy irradiation, DNA DSBs were significantly more abundant at 1 week, but had nearly repaired by 9 months. Mice showed no joint functional differences by gait, locomotor, or rotarod tests, but PAM thresholds were lower in irradiated limbs at 6 and 9 months. Student's t-test and ANOVA with post-hoc Tukey's were used for statistical analysis. DISCUSSION: Localized irradiation of mouse knee joints induced persistent DNA DSBs and knee hyperalgesia. These results along with our in vitro work demonstrating hypertrophy reduces proinflammatory signaling highlight the importance of chondrocyte DNA damage response to our understanding of the pathogenesis of OA in aging. Surprisingly, DNA DSBs persisted in post-mitotic tissues at least a week after irradiation while proliferative tissues completely repaired within 48 hours likely due to availability of DNA repair pathways. Although we observed little effect on mouse mobility by locomotor and rotarod behavioral tests, we recorded consistently lower pain thresholds by PAM. These data suggest that chondrocytes and other post-mitotic joint tissues are relatively resistant to irradiation, but further investigation is needed to determine which DNA repair pathways are utilized by these cell types and how they survive with persistent DNA DSBs.

14th Annual Center for Musculoskeletal Research Symposium
October 17, 2024

Title: Raman Spectroscopy of Femoral Neck samples can predict Bone Mineral Density and preliminarily classify patients as Osteoporotic

Presenting Author: Kyle Jerreld

Co-Author(s): Anthony Yosick, Sashank Lekkala, Christine Massie, Andrew Rodenhouse, Andrew Berger, Constantinos Ketonis, Hani Awad

Lab PI / Mentor: Hani Awad

ABSTRACT

Introduction: Osteoporosis (OP) screening rates remain startlingly low despite a third of women and a fifth experiencing fragility fractures in their lifetimes. The gold standard for OP screening is the use of dual X-ray absorptiometry (DXA) scans that provide metrics on a patient's bone mineral density (BMD). However, BMD only explains 21% of all non-vertebral fractures in men and 44% in women. Raman spectroscopy, a chemical fingerprinting method, can be leveraged to gain information such as the bone's hydroxyapatite (mineral) and collagen (matrix) makeup. In this analysis, we aim to use Raman compositional parameters to create a model for classifying patients as normal or OP and to determine preliminary sensitivity and specificity of our model.

Methods: Femoral necks were obtained from patients undergoing total hip arthroplasty (THA). The samples were wrapped in PBS-soaked gauze and stored at -80°C. Each sample was divided into quadrants: Inferior, superior, anterior, and posterior. We identified the quadrant with the thickest cortex as the inferior quadrant. We used DXA to measure the BMD. The samples were thawed before testing. To measure the Raman signal, the samples were excited using an 830nm, 150mW laser, and the scattered light was collected. Each spectrum was an average of 5 spectra with an integration time of 60 seconds. A custom MATLAB code was used to calculate the Raman outcomes. The 10-year risk of major OP fracture and hip fracture were calculated using the FRAX® online tool. Values from patient chart information were inputted into the tool and values were calculated. Individual Raman compositional parameters were analyzed using linear regression and descriptive statistics to illustrate the correlation of population demographics and between single Raman variables as well as BMD. Multivariate regression with principal components were used to test both the relationship between Raman variables against BMD values or world health organization (WHO) classification using descriptive statistics (R-squared) or a receiver-operating characteristic curve (ROC) and area under the ROC curve (AUC), respectively. The ROC curve was further analyzed through the sensitivity, specificity, odds ratio, and accuracy for each WHO classification.

Results: Femoral neck specimens were obtained from 32 male and 28 female THA patients. All analysis described are based on measurements in the inferior quadrant due to greater reliability. BMD showed weak correlation with age and BMI, even when stratified by sex. Individual Raman parameters also showed weak correlations with BMD, crystallinity being the exception showing modest correlation. BMD correlations with Raman principal components were modest but improved when compared to individual parameters. R-squared values were 0.27 and 0.29 for female and male patients, respectively. Using ROC curves for females, there was an AUC of 0.8827 and 0.8295 for normal, and OP, respectively. For males, there was an AUC of 0.7632 and 0.8762 for normal and OP, respectively. The sensitivity for OP classification was 0.82 for females and 0.70 for males. The specificity for OP classification was 0.68 for females and 0.81 for males.

Discussion: By linear regression, Raman parameters are only able to achieve modest correlations. However, when using the ROC curves, the AUCs indicate a promising ability to characterize the samples to being normal, or OP. Despite this small cohort the sensitivity and specificity for OP classification showed promise for potential use as a means of assessing OP risk. Future work with cadaveric samples and biomechanical fracture assessment could lead to further improvement of the model. Successful development of a classification model could lead to the use of
Raman spectroscopy as a pre-screening tool for OP used in the clinic to facilitate patients receiving the gold-standard DXA scans.

14th Annual Center for Musculoskeletal Research Symposium
October 17, 2024

Title: The Lower Extremity Impacts a Spine Patient's Balance and Cone of Economy

Presenting Author: Kade Kaufmann

Co-Author(s): Haseeb Goheer, Gabriel Ramirez, Andrew Megas, Ashley Rogerson, Varun Puvanesarajah, Ram Haddas

Lab PI / Mentor: Ram Haddas

ABSTRACT

INTRODUCTION: Balance changes are common in individuals with spinal disorders and may cause falls. Patients with anatomical deformities of the spine and the lower extremities, such as scoliosis, kyphosis, and lordosis, may experience changes in their balance. Specifically, balance is impacted by the unique and complex relationship between spinal alignment and lower extremity biomechanics. Patients with spinal deformities usually maintain their spinal alignment through the compensatory mechanism in which the body has the least energetic consumption possible. Balance efficiency, often referred to as the Cone of Economy (CoE), is the ability of a person to maintain their center of gravity with minimal neuromuscular expenditure. This study aims to explore differences in lower extremity involvement in patients with spinal disorders compared to healthy controls. No previous work has investigated the role of lower extremity with patients' CoE, nor its potential in a clinical scenario.

METHODS: This study was a retrospective, single-institution, cohort study comprised of adult patients with symptomatic lumbar degenerative (LD) disease and healthy volunteers who received disability and functional evaluations between 2023 and 2024. Participants with an elevated body mass index (>40.00 kg/m2), a history of neurological disorders, and/or prior surgeries were excluded. Participants underwent three-dimensional (3D) balance analysis using a full-body reflective marker set. 60-second Romberg and a 60-second seated balance on a force plate to assess balance metrics were completed by all participants. Data were collected at 100 Hz with a 10-camera system. Sagittal and coronal range of sway (RoS) for Center of mass (CoM) and head movements were calculated using a custom algorithm. Participants also completed the Oswestry Disability Index, PROMIS, and Tampa Scale of Kinesio phobia. Linear mixed-effects regression models were estimated with a random intercept at the subject level and only the group as a categorical independent variable. Groups were then compared using post-estimation comparisons using Stata 16.1, StataCorp, College Station TX. Statistical significance was set at $p < 0.05$. Institutional review board approval was obtained.

RESULTS: Coronal head sway was found to be much larger in standing (LD:34.8 vs C: 28.7 cm, $p<0.001$) in comparison to sitting (LD: 2.35 vs H: 1.7, $p=0.005$). Moreover, total head sway was found to be larger in standing (LD: 65.2 vs H: 38.1, $p<0.001$) when compared to sitting (34.8 vs H: 28.3 $p>0.050$). When comparing the differences between standing and sitting balance, LD patients presented with significantly reduced head (LD: 30.4 vs H: 9.9 cm, $p<0.001$) and CoM (LD: 19.1 vs H: 4.5 cm, $p<0.001$) total sway in sitting in comparison to standing (Table 1). A similar trend was observed with CoE dimensions in the head (Sagittal: LD: 2.6 vs H: 0.8 cm, $p=0.009$). DISCUSSION: Patients with spinal disorders presented with large seated CoE and high neuromuscular activities in contrast to healthy volunteers. Our results suggest the lower extremity is significantly involved in a spine patient's balance and CoE. While standing CoE assessments are standard, seated CoE measures have been under-captured. This approach quantifies seated CoE and permits a better understanding of a patient's balance and disability. Further prospective investigations are warranted to characterize the involvement of the lower extremity in the assessment of CoE associated with improved spinal alignment and clinical outcomes.

SIGNIFICANCE/CLINICAL RELEVANCE: This novel study quantified and compared differences in lower extremity involvement in standing balance between patients with LSR and healthy controls. No previous work to our knowledge has investigated the role of the lower extremity with a patient's CoE, nor its potential clinical significance.

14th Annual Center for Musculoskeletal Research Symposium
October 17, 2024

Title: Anti-diabetic drugs and risk of tendinopathy---A TriNetX analytic network-based study

Presenting Author: Elizabeth Kogan

Co-Author(s): Haiyin Li, David Ciufo

Lab PI / Mentor: Chike Cao

ABSTRACT

Introduction: Tendinopathy is a painful and disabling musculoskeletal condition, a ecting millions of people in both the athletic and general population and causing great socio-economic impact. The standard treatment of tendinopathy typically involves rest, physical therapy, and NSAIDs, which often provide short-term or partial pain relief but no long-term benefits. Thus, there remains an unmet clinical need for non-operative pharmacological intervention which requires the understanding of the disease pathogenesis. The exact etiology and natural history of tendinopathy are currently unknown. Both intrinsic and extrinsic risk factors contribute to the development of tendinopathy, such as age, metabolic disorders, family history, joint mobility, muscle weaknesses, overuse, improper training, and medications. Metabolic diseases, such as diabetes mellitus, are frequently associated with the development and poor prognosis of chronic tendinopathy. But it remains unclear whether treatment with anti-diabetic agents decreases or increases the risk of tendinopathy. To this end, we performed a case-control study using the TriNetX Network to investigate whether the 6 types of anti-diabetic drugs were associate with an altered risk of tendinopathy.

Method: Using the TriNetX clinical database, we performed a case-control analysis to investigate the association between each type of Type 2 diabetes mellitus (T2DM) medication and tendinopathy. All participants were 18-90 years old, without Type I diabetes Mellitus. The case subjects were defined as those with diagnosed tendinopathy based on the ICD-10-CM codes, with prior history of T2DM (ICD-10-code: E11), and took monotherapy of anti-diabetic medications including insulin, SGLT-2 inhibitors, GLP-1 receptor agonists/DPP-4 inhibitors, sulfonylureas, thiazolidinediones, and metformin (based on RxNorm codes). The control group enrolled subjects who had no diagnosed tendinopathy, but with T2DM and on anti-diabetic drug monotherapy. Both the case and control groups were retrospectively followed up for a history of each type of anti-diabetic medications. We set metformin as the reference drug. Chi-squared tests were used to analyze the associations, and odds ratios (ORs) with 95% confidence intervals (CIs) were calculated. A p-value of <0.05 was considered statistically significant.

Result: Among 103,507 tendinopathy participants, the patients had previously diagnosed T2DM and took monotherapy insulin, SGLT-2 inhibitors, GLP-1 receptor agonists/DPP-4 inhibitors, sulfonylureas, thiazolidinediones, and metformin are 40893, 952, 3611, 4888, 763, and 52563, irrespectively. While among 2,025,918 non-tendinopathy participants, the patients had previously diagnosed T2DM and took monotherapy insulin, SGLT-2 inhibitors, GLP-1 receptor agonists/DPP-4 inhibitors, sulfonylureas, thiazolidinediones, and metformin are 1174691, 33469, 76039, 73269, 10326, and 658124, irrespectively. We found that the T2DM patients taking insulin had 56% reduction (OR=0.44, 95% CI: 0.43, 0.44, $p<0.001$), on GLP-1 receptor agonists/DPP-4 inhibitors with 40% reduction (OR=0.0.60, 95% CI: 0.58, 0.62, $p<0.001$), on SGLT-2 inhibitors with 64% reduction (OR=0.36, 95%CI: 0.33,0.38, $p<0.001$) and on sulfonylurea with 16% reduction (OR=0.84, 95% CI: 0.81, 0.86, $p<0.001$) in the odds of tendinopathy compared with the T2DM subjects who took metformin. But no significant e ect of thiazolidinedione on risk of tendinopathy was detected compared with metformin (OR=0.93, 95% CI: 0.86, 1.00, $p=0.046$). Conclusion & Discussion: In summary, we found anti-diabetic drugs including insulin, GLP-1 receptor agonists/DPP-4 inhibitors, SGLT-2 inhibitors, and sulfonylurea, but not thiazolidinedione had beneficial e ect to reduce the risk of tendinopathy compared with metformin.

14th Annual Center for Musculoskeletal Research Symposium
October 17, 2024

Title: Injury-Specific Factors Impact Outcomes Following Flexor Tendon Repair

Presenting Author: Richard Lander MD

Co-Author(s): Andrew J. Rodenhouse MD, Gilbert Smolyak BS, Thomas J. Carroll MD, Giap Vu MD, Gabriel Ramirez MS

Lab PI / Mentor: Constantinos Ketonis MD PhD

ABSTRACT

Introduction: Many advancements in flexor tendon repair techniques and rehabilitation protocols have been developed over time, however, the risk of post-operative complications after flexor tendon repair remains high. Our study sought to investigate injury-specific risk factors that impact outcomes following flexor tendon repair.

Methods: This was a retrospective study of patients that underwent primary flexor tendon repair at a single, large academic institution between 2015-2023. Review of medical records was performed by one medical student and four physicians. Demographic information, injury-specific factors, patient-reported outcomes, and complication rates were collected. Patient-Reported Outcomes Measurement Information System (PROMIS) scores were also collected. Thumb injuries were excluded due to insufficient sample size. Mixed-effects linear regression, logistic regression, and negative binomial regression were performed. Statistical significance was defined with a p-value < 0.05.

Results: 397 patients were included in this study. Relative to the index finger, the ring and small fingers had significantly lower TAM by 18.3° and 22.1°, respectively. Digits with Zone 1 injuries had improved American Society for Surgery of the Hand (ASSH) total active motion (TAM) relative to Zone 2 injuries at both 6 and 12 weeks post-operatively. The improvement was noted to be 46.7° and 31.1° degrees, respectively. Those with concurrent digital nerve injuries had impaired functional outcomes, with TAM decreased by 13.6° and 20.6° at 6 and 12 weeks post-operatively. Similarly, TAM in patients with concurrent fractures was worsened by 35.7° at 6 weeks. Patients with sawblade injuries had an increased odds of compliance with hand therapy (OR 2.79). Additionally, they had 83% more days until return to work and 25% more days until discharge from hand therapy relative to those with lacerations. These patients also had significantly worse PROMIS physical function and pain interference at 12 weeks and PROMIS depression at 6 weeks. Patients with multiple injured digits had 32% more days until discharge from hand therapy relative to those with single digit injuries.

Discussion/Conclusions: After flexor tendon repair, the ring and small fingers, injuries in Zone 2, and patients with concurrent digital nerve injuries and fractures have decreased TAM. Patients with multiple injured digits have increased days to discharge from therapy. Patients with sawblade injuries have greater odds of therapy compliance, but worse PROMIS scores and increased days to return to work and discharge from therapy. These results can provide insight as to post-operative expectations after flexor tendon repair.

14th Annual Center for Musculoskeletal Research Symposium
October 17, 2024

Title: Dose-dependent association between hypertensive drugs and the risk of tendinopathy in a US population-based study

Presenting Author: Haiyin Li

Co-Author(s): David Ciufo

Lab PI / Mentor: Chike Cao

ABSTRACT

Introduction: Achilles tendinopathy is a painful and disabling musculoskeletal condition with significant socio-economic impact. Currently, there is no definitive treatment for Achilles tendinopathy other than surgery, which can lead to lengthy recovery and potential complications. Our previous analysis using the TriNetX platform suggested a protective e ect of beta-blockers (BBs) and calcium channel blockers (CCBs) against Achilles tendinopathy, but not angiotensin-converting enzyme inhibitors (ACEIs)/angiotensin II receptor blockers (ARBs) or diuretics (DIUs). However, the built-in analysis tool in TriNetX platform did not provide the dose information. Therefore, we requested the electronic medical records (EMRs) of patients who were on anti-hypertensives and examined the dose-response relationship between antihypertensive drugs and the risk of Achilles tendinopathy.

Method: We requested from TriNetX the EMRs (up to 2022) of patients who had antihypertensive prescription between 01/01/2011 and 12/31/2015. Eligible patients were aged 18-90, diagnosed with primary hypertension, but no infectious musculoskeletal diseases or auto-immune diseases, no tendinopathy at entry between 01/01/2011 and 12/31/2015. The included patients were then stratified into four groups based on the type of antihypertensives at entry: BBs, CCBs, ARBs/ACEIs and DIUs. The initial analysis was performed without considering dose to validate our previous findings, with DIUs as the control group. A 7-year follow-up was performed for the Achilles tendinopathy. Next, to evaluate the dose-dependent e ect of each type of antihypertensives on Achilles tendinopathy, we performed a cohort study within each type of antihypertensives. Thus, hypertensive patients with prescription of one type of antihypertensives between 01/01/2011 and 12/31/2015 were further stratified into four subgroups based on the duration of drug prescription: < 3-month prescription (the control cohort) vs 3~6-month, 6~9-month and > 9-month prescription (the exposure cohorts). A 7-year follow-up was carried out for the Achilles tendinopathy. The potential confounders were adjusted by multivariate survival analysis using Cox regression. Hazard ratio (HR) and 95% confidence intervals (CIs) were calculated for the outcome over the 7-year follow-up. P-trend tests were performed to detect the trend of antihypertensive prescription duration on Achilles tendinopathy. Statistical significance was set at two-sided $p < 0.05$.

Results: A total of 295,373 eligible hypertensive patients were exposed to an antihypertensive drug during 01/01/2011 to 12/31/2015. After confounding factor adjustment, we found significantly decreased risks of Achilles tendinopathy in patients with BBs (HR: 0.75; 95% CI: 0.66,0.85, $p <0.001$) or CCBs (HR: 0.85; 95% CI: 0.73,0.99, $p = 0.036$) compared with those on DIUs. In contrast, ARB/ACEI had no e ect on the risk of Achilles tendinopathy. Furthermore, higher dose of BBs or CCBs with longer prescription duration was associated with a decreased risk of Achilles tendinopathy vs lowest prescription duration of BBs (> 9 months vs < 3 months, HR: 0.67; 95% CI: 0.45,0.99, PTrend = 0.048), CCBs (> 9 months vs < 3 months, HR: 0.58; 95% CI: 0.35,0.94, PTrend = 0.029) or ACEI/ARBs (> 9 months vs < 3 months, HR: 0.64; 95% CI: 0.51,0.80, PTrend < 0.001), irrespectively. Interestingly, higher dose of DIUs displayed no association with the new-onset Achilles tendinopathy (> 9 months vs < 3 months, HR: 0.87; 95%CI: 0.74,1.04, PTrend =0.1235).

Discussion & Conclusion: Our study proved that BB or CCB prescription in HTN patients was associated with decreased risk of Achilles tendinopathy and this decreased risk displays a dose-dependent pattern. A limitation of the study is the lack of information regarding medication nonadherence which may obscure the true impact of anti-hypertensive drugs on the incidence of tendinopathy, potentially underestimating the actual drug e ect.

14th Annual Center for Musculoskeletal Research Symposium
October 17, 2024

Title: The Effect of CCL3 on T Cell Populations in Acute Myeloid Leukemia Bone Marrow Microenvironment

Presenting Author: Kevin Li

Co-Author(s):

Lab PI / Mentor: Benjamin Frisch, PhD

ABSTRACT

Background & Hypothesis

Acute myeloid leukemia (AML) is a highly heterogeneous hematologic malignancy. Studies in human patients and mouse models have shown that C-chemokine (C-C motif) ligand 3 (CCL3) is overexpressed in leukemic cells in the AML bone marrow microenvironment (BMME). CCL3 can promote the expansion of leukemic cells, regulate hematopoietic stem cell differentiation, and disrupt the regulation of bone remodeling. In addition, CCL3 was shown to recruit specific T cell types such as Type I helper T (Th1), CD8 T, and regulatory (Treg) cells through interaction with receptors CCR1, CCR4, and CCR5 expressed on the T cell surface in infectious and solid tumor disease models. Previous studies showed that blocking CCR1/5 can lead to less accumulation of Treg cells in the BMME and lower the AML burden, thus making it a potential target for therapy. However, the mechanism of how CCL3 overexpression leads to the accumulation of T cells in the BMME is still unclear. Here, we hypothesize that CCL3 overexpression recruits more T cells from the circulation into the BMME or retains more T cells in the BMME, preventing them from reentering the circulation through interaction with CCR1, 4, and 5.

Experiment & Methods

Murine AML model with MLL-AF9 (MA9) genetic alteration induced in 6- to 8-week-old male C57BL/6 and CCL3 knockout (KO) mice were used to investigate the shift of T cell populations when having either overexpression or absence of CCL3 signaling pathway. In this study, wild-type (WT) healthy B6 mice were used as the control group. The size of each control and sample group is n=3. T cell populations from the femur, tibia, and pelvis were analyzed using flow cytometry. A two-way ANOVA test was applied for statistical analysis and comparison across each group.

Results

We compared the percentage of T cells within the total bone marrow cells across WT healthy, WT AML, and CCL3 KO AML groups. Our results showed that the WT AML group has a significantly higher percentage of CD3+ T cells (3.55% ± 0.85%) compared to the control (1.95% ± 0.31%) and the CCL3 KO AML group (1.26% ± 0.23%), while no difference was discovered between the control and the CCL3 KO AML group. Specifically, we discovered that CD4 T cells were significantly increased in the WT AML group (control = 0.6% ± 0.09%, WT AML = 2.5% ± 0.74%, CCL3 KO AML = 0.67% ± 0.24%), and within the CD4 T cell population, Treg cells were significantly increased (control = 0.026% ± 0.004%, WT AML = 0.072% ± 0.065%, CCL3 KO AML = 0.038% ± 0.033%).

Conclusion and Discussion

Our preliminary data suggested that CCL3 overexpression leads to the accumulation of T cells in the BMME and specifically CD4 T cells. Within CD4 T cell populations, Treg cells were significantly increased in the WT AML group compared to the control. However, the Tregs subset was not the only CD4 T cell subset that was increased in the BMME. Future studies will include a thorough evaluation of other CD4 T cell subsets such as Th1, Th2, and Th17 in the leukemic bone marrow.

14th Annual Center for Musculoskeletal Research Symposium
October 17, 2024

Title: Characterizing bone marrow interstitial pH by two-photon ratiometric imaging

Presenting Author: Melissa MacLiesh

Co-Author(s):

Lab PI / Mentor: Shu-Chi Yeh

ABSTRACT

Introduction: Myelodysplastic syndrome (MDS) is a blood disorder characterized by ineffective hematopoiesis and a high risk of leukemic transformation, as the blood stem cells with leukemia-associated mutations expand and become a dominant clone in the bone marrow [1]. In both MDS and leukemia, despite a high remission rate, relapse is extremely common [2]. It has been suggested that relapse is initiated by a metabolic switch of the residual stem cells; in particular, these cells favored oxidative phosphorylation (OXPHOS) , compared to the more mature blast cells that primarily rely on glycolysis [3-5]. Of note, cell metabolism and environmental pH are closely linked [6]. Specifically, acidic interstitial pH (6.7-6.9) in the bone marrow has been shown to promote OXPHOS and consequently alter phenotypes of leukemic cells [7,8]. Interestingly, using intravital pH imaging, our prior work revealed focal acidic zones in the bone marrow [9]. This raised questions of whether the residual stem cells can be protected by those focal acidic zones. We hypothesize that low pH is found surrounding disease initiating cells and that alkalinization agents can modify interstitial pH and the metabolic profiles of the residual cells.

Methods: Using two-photon fluorescence microscopy (TPFM) and ratiometric pH probe, SNARF-1, we mapped interstitial pH in live bone marrow at single-cell resolution [9]. In brief, SNARF-1 was administered retro-orbitally and was subsequently sequestered to the interstitial space. The fluorescence emission spectrum of SNARF-1 undergoes a pH dependent shift from 580nm to 640nm, allowing quantification of the fluorescence ratio to determine relative pH. Interstitial pH in the bone marrow was then measured surrounding expanded and solitary MDS clones (Idh2R140/Q). To identify focal acidic zones in the bone marrow, pH distribution was characterized in steady-state, after treatment with hypomethylating agent (HMA, 200 mg/kg), a first line treatment for MDS, and after systemic administration of akalinization agent (sodium bicarbonate, 200 mmol/L). To determine the metabolic needs of mutated Idh2R140/Q vs healthy cells in the above conditions, the seahorse cell analyzer was used to track oxygen consumption and extracellular cell acidification over time.

Results: The methodology revealed a heterogenous pH microenvironment in the bone marrow (pH = 6.7 – 7.5). Local pH near mutated MDS cells did not appear significantly different from the pH surrounding native autofluorescent cells (n=2). Preliminary image data indicated that the interstitial pH increased after treatment. Additionally, the serum pH appeared to increase after introducing an akalinization agent, showing that it is possible to modify pH in vivo. In vitro data gathered using seahorse showed that MDS mutated cells have a different baseline oxygen consumption rate than healthy bone marrow cells.

Conclusion: Focal acidic zones was found in the bone marrow. In this study, we attempted to investigate localized pH near disease initiating cells and correlate with metabolic reprogramming. One of the limitations in this work is that pH and metabolic profiles will likely be altered when cells were removed from the in situ environment for downstream analyses. Therefore, we are optimizing transcriptomic profiling in situ under image guidance. We have established protocols to preserve RNA quality in formalin fixed paraffin embedded (FFPE) histology slides and co-register them with in vivo localization, thus allowing subsequent analyses using GeoMx Digital Spatial Profiling and mechanistic studies of healthy and leukemic microenvironments.

References. [1] Caponetti 2020, [2] M. de Lima 2021, [3] Kumar 2023, [4] E. Andreucci 2023, [5] Sriskanthadevan 2015, [6] Bajaj 2019, [7] Liao, M. 2023, [8] Chen, J. 2008, [9] Yeh S-C 2022.

14th Annual Center for Musculoskeletal Research Symposium
October 17, 2024

Title: PROMIS Scores Inferior in Patients Undergoing Arthroscopic Rotator Cuff Repair with C-Spine Conditions

Presenting Author: Michaela Malin

Co-Author(s): Hashim Shaikh MD, Andrew Jeong MD, Sandeep Mannava MD, PhD

Lab PI / Mentor: Sandeep Mannava MD, PhD

ABSTRACT

Introduction:
Rotator cuff pathology is the most common cause of disability in the shoulder. These conditions are often complicated by preexisting conditions such as cervical spine disease. Cervical myelopathy and radiculopathy are common pathologies in older adults presenting with pain, weakness, or numbness of the upper extremity, making them difficult to distinguish from shoulder conditions since both can cause pain in the neck and the shoulder. In this study, we hypothesized that patients with cervical spine disease undergoing arthroscopic rotator cuff repair would demonstrate lower absolute values in PROMIS scores compared to those without concomitant disease, but would experience a similar improvement and achievement of minimal clinically important difference (MCID).

Methods:
Retrospective chart review captured PROMIS, demographic, surgical data, and cervical spine pathologies. PROMIS questionnaires were administered on Apple iPads (Apple, Cupertino, CA) as part of routine clinical care at outpatient orthopedic clinics. Results were promptly accessible in the patient's electronic medical record and stored in a prospectively maintained research database. Assessments covered three PROMIS domains: physical function, pain interference, and depression. Bivariate student t-test analysis evaluated descriptive differences. Pearson chi-square analysis or Fisher's exact test were used to assess descriptive features and minimal clinically important difference between the two cohorts. Multiple variable logistic regression was conducted to analyze the role of preexisting C-spine conditions in achievement of MCID.

Results:
A total of 490 patients were included in the final analysis. Of these, 82 patients had concomitant cervical spine disease. Both cohorts demonstrated significant improvement at final follow-up compared to their preoperative PROMIS values for PF, PI, and Dep, however patients with preexisting cervical diagnoses had significantly worse (higher) preoperative PROMIS scores: PI (62.6 ± 6.8 vs 60.1 ± 6.6), Dep (50.4 ± 9.8 vs 47.6 ± 9.8) and PF scores (39.5 ± 7.3 vs 42.6 ± 8.4) which persisted at final follow-up: PI (53.9 ± 7.9 vs 50.5 ± 8.1), Dep (43.3 ±9.4 vs 41.1 ± 7.8), and PF (45.6 ± 7.6 vs 48.6 ± 7.9). Logistic Regression analysis found that preexisting cervical condition was a nonsignificant predictor for the achievement of MCID PI [p=0.91], D [p=0.92], or PF [p=0.11]. However, higher preoperative PF scores (greater preoperative function) were found to be associated with a significant decrease in the odds of reaching MCID PF [OR 0.85; 95 CI 0.83-0.88; p=0.001]

Discussion:
Despite observing comparable improvements in both groups, our study highlights the significant impact of preexisting cervical conditions on preoperative PROMIS scores, which remain considerably lower at the final follow-up compared to their counterparts without such conditions. This underscores the crucial need to emphasize and manage patient expectations before surgery, conveying that while they may experience improvement from the procedure, it might not reach the same magnitude as individuals without concurrent cervical issues. Clearly articulating these expectations before surgery becomes paramount in shaping patient satisfaction. Although our investigation did not delve into patient satisfaction assessments, future studies should prioritize evaluating the effectiveness of preoperative counseling regarding multiple conditions, including cervical issues, and its influence on satisfaction post-rotator cuff surgery. This study emphasizes the

complexity of managing shoulder pathology with concomitant conditions such as cervical spine disease and the importance of expectation-setting for patients depending on their preexisting conditions prior to surgery.

14th Annual Center for Musculoskeletal Research Symposium
October 17, 2024

Title: Involvement of S100a4 in post-operative abdominal adhesion formation

Presenting Author: Alexander Mathewson

Co-Author(s): Matthew Byrne MD, Miranda Chacon MD, Nicole Wilson MD PhD

Lab PI / Mentor: Alayna Loiselle PhD

ABSTRACT

Background: Fibrotic adhesions occur in over 50% of patients receiving abdominal surgery, are the primary cause of life-threatening bowel obstructions, and can also result in infertility, chronic pain, and surgical complications. Adhesions form between abdominal and visceral peritoneum following damage to the peritoneal cavity, constraining the movement of intra-abdominal organs . The molecular etiology of adhesion formation is complex, involving peritoneal macrophage aggregation, inflammation, fibrinolytic imbalance, and tissue hypoxia, resulting in a fibrin-rich mass of immune cells which bridges adjacent tissues. This is solidified by peritoneal fibroblasts, which migrate onto the fibrin bridge, depositing collagenous extracellular matrix to form a mature adhesion . Though the signaling mechanisms that initiate this reprogramming have not been identified, one potential mediator is the small calcium binding protein, S100a4, which is associated with fibrosis in the heart, lung, liver, kidney, and tendon. In fibrosis-associated proinflammatory environments, macrophages are capable of producing and secreting S100a4 to promote cell motility, invasion, and matrix deposition. In addition, recent work has demonstrated a robust population of S100a4+ fibroblasts in abdominal adhesions, making S100a4 a potential candidate as a mediator of adhesion formation .

Design: To determine if S100a4 plays an active role in adhesion formation, cecal abrasion surgery was performed on wildtype (WT) and S100a4+/- heterozygous mice. These mice were sacrificed at post-operative day 10 (POD10), and the extent of adhesion formation was scored clinically (n=5 WT, n=6 S100a4+/-) by 17 independent blinded observers. Tissues were then harvested for histological analyses and single cell RNA sequencing (scRNAseq) to assess S100a4 localization . Sections were stained with hematoxylin and eosin (H&E) to quantify adhesion area and immunofluorescence staining was performed on mouse (n=2 WT, n=2 S100a4+/-) and human (n=3) adhesive tissue to determine the localization of, and relationship between, S100a4+ cells, myofibroblasts (αSMA), and macrophages (F4/80).

Results: Clinical scoring between WT and S100a4+/- adhesions demonstrated a significant decline in adhesion formation in S100a4+/- mice ($p=0.033$). Qualitative analysis of the immunofluorescent staining revealed co-expression of S100a4 and F4/80 throughout adhesive tissue. Preliminary analysis of scRNAseq data from WT identify broad, but heterogeneous S100a4+ expression in fibroblasts.

Conclusions: The reduction in adhesion formation in S100a4+/- mice supports the therapeutic potential of modulating S100a4 to prevent adhesion formation. Based on our single cell dataset and immunofluorescent staining for macrophages, S100a4 expression persists in both fibroblast and macrophage populations in mature abdominal adhesions. Due to the lack of diverse cell types obtained in our single cell dataset, we are currently optimizing our tissue digestion protocol to preserve additional cell populations. We also plan on extending our study to earlier timepoints post-operation to establish how S100a4 signaling changes over time.

14th Annual Center for Musculoskeletal Research Symposium
October 17, 2024

Title: T cell dysfunction during Staphylococcus aureus osteomyelitis in humanized mice

Presenting Author: Katya McDonald

Co-Author(s): Motoo Saito, Himanshu Meghwani, Javier Rangel-Moreno, Edward Schwarz, Stephen Kates, and Gowrishankar Muthukrishnan

Lab PI / Mentor: Gowrishankar Muthukrishnan

ABSTRACT

INTRODUCTION: Staphylococcus aureus is the leading cause of implant-associated osteomyelitis. It has a high reoccurrence rate and a low post-operative cure rate and can lead to sepsis, multiorgan failure, and death. Surgical interventions have high failure rates and reinfection (10-50%), indicating a need for future innovation in therapeutics and vaccines. With our humanized mouse model, we have found enhanced susceptibility to S. aureus infection compared to conventional mice. Therefore, we wanted to investigate the human T cell response during infection, as T cells are critical for bacterial control during chronic infection. Previously, using single-cell RNA sequencing and immunohistochemistry, we have found preliminary evidence of T cell dysfunction in the bone marrow niche. Here, we use high-parameter spectral flow cytometry to characterize the human T cell response to S. aureus and show the occurrence of CD4 T cell dysfunction systemically (the spleen) and locally (the bone marrow).

METHODS: Humanized NSG-SGM3 BLT mice underwent transtibial implant-associated osteomyelitis using bioluminescent MRSA (USA300 LAC::lux). At fourteen days post-infection, splenocytes and bone marrow cells were isolated and subjected to flow cytometry analysis. Specifically, two panels were used to evaluate changes in CD4 T cell phenotypes and their functional capacity. Data analysis was completed using FloJo software.

RESULTS: In the spleen, we observed the increased frequency of T regulatory cells during infection, indicating a potentially more immunosuppressive systemic environment. In the bone, the local infection environment, we found an increase in immune checkpoint proteins, including LAG-3, PD-1, and TIM-3 on CD4 T cells. Interestingly, we also discovered that LAG-3 and TIM-3 positive cells had diminished Ki67 staining, a proliferation marker, indicating potentially impaired functional capacity. To investigate this further, we looked at the cytokine production (IFN-y, IL-2, IL-17A, and TNFa) of these cells and observed that LAG-3 and TIM-3 positive cells had diminished cytokine production.

DISCUSSION: At the bone marrow site, we have observed an increase in LAG-3+ and TIM-3+ cells during infection, and that these cells have diminished proliferation capacity and cytokine production, indicating they may be dysfunctional. Future experiments will look to explore the kinetics of this dysfunction by adding more timepoints during infection. Ultimately, this work will provide novel mechanistic insights into bacteria-T cell interactions during S. aureus bone infections.

14th Annual Center for Musculoskeletal Research Symposium
October 17, 2024

Title: IL-27 is Mediated by IL-17 to Elicit Sustained Protection Against Staphylococcus aureus Osteomyelitis

Presenting Author: Himanshu Meghwani

Co-Author(s): Chloe Kraft, Katya McDonald

Lab PI / Mentor: Gowrishankar Muthukrishnan

ABSTRACT

Background & Hypothesis: Interleukin (IL-27) is a heterodimeric cytokine produced largely by antigen-presenting cells that has functions in both immune suppression and activation in a context-dependent manner. Recently, the role of IL-27 in Staphylococcus aureus (S. aureus) osteomyelitis was elucidated, notably revealing that exogenous and prophylactic IL-27 treatment in mice led to reduced infection burden. Furthermore, this protective mechanism is associated with significant accumulation of RORγ(gamma)t+ neutrophils and production of IL17a, IL17f, and Rorc as depicted by RNA sequencing from infected tibias. It is well established that IL-17 is a proinflammatory cytokine that leads to increased neutrophil recruitment and activation, which would be beneficial to an early immune response against S. aureus infection. We therefore hypothesize that this IL-27 mediated protection against bone infection requires the IL-17/IL-17R axis.

Methods: We injected recombinant murine IL-27-expressing AAV into IL-17A/F double knockout (IL-17AF-/-) and WT mouse seven days prior to insertion of transtibial implants inoculated with S. aureus (USA300 LAC::Lux), serving as a model for implant associated osteomyelitis in humans. We measured bacterial burden via bioluminescent imaging (BLI), colony forming unit (CFU) quantifications, and histomorphometry as disease outcome measurements.

Results and Discussion: At fourteen days post infection, we observed that IL-27 pretreated WT mice had lower CFUs and bioluminescence as compared to untreated mice, as previously shown. The IL-17A/F-/- mice showed higher bacterial burden on BLI and higher CFU measurements in bone and soft tissue. These findings demonstrate that IL17A/F-/- results in higher bacterial load, indicating that IL-27 mediated protection against S. aureus is IL-17/IL-17R axis dependent. Further studies are required to understand the role of the IL-17 dependent IL-27 phenotype in S. aureus osteomyelitis, such as 1) identifying the cellular sources of IL-17A/F and 2) how disruption of this IL-17/IL-17R axis impacts neutrophil recruitment and function during infection. Overall, our preliminary studies indicate that the absence of IL17A/F impacts the ability of IL-27 to have sustained protective effects against S. aureus osteomyelitis.

14th Annual Center for Musculoskeletal Research Symposium
October 17, 2024

Title: StretchToC: a tendon-on-a-chip platform for investigating the role of mechanical stimulation in fibrotic tissues

Presenting Author: Hayley Miller

Co-Author(s):

Lab PI / Mentor: Hani Awad

ABSTRACT

INTRODUCTION: A common complication of zone II flexor tendon injuries is fibrotic adhesions, in which the tendon fuses to surrounding tissues due to the buildup of scar tissue. Prevalent in this process is the main regulator of fibrosis, Transforming Growth Factor-β1 (TGF-β1), and the downstream protein Plasminogen Activator Inhibitor-1 (PAI-1) [1]. It was previously found that PAI-1 knockout (KO) leads to reduced adhesion formation, but not when tendons were immobilized during the healing process. This suggests the importance of physical therapy in conjunction with biologic treatment [2]. This work aims to tailor our pre-existing hToC platform to include a stretching mechanic, allowing us to apply strain to embedded tissues. With such, we will be able to study the role of biomechanics in tendon adhesion. Few fabrication methods exist for such devices, with current options being costly and time-consuming. Therefore, we also aim to create a method by which millimeter-scale, stretchable layers with complex through-holes can be fabricated at a low cost of entry.

METHODS: The layer-by-layer StretchToC platform consisted of a membrane containing pillar-like protrusions for anchoring cells. Outside these pillars were vacuum chambers that, once activated, stretched both the membrane and attached anchors. 3D finite element analysis (FEA) was performed to determine if the proposed design was capable of achieving physiological strains of up to 4% [3]. Physical prototypes were produced through pseudo-injection molding. Pseudo-injection molds were created by 3D printing a separable mold. The extrusion roughness of the ABS was smoothed through exposure to acetone vapor. PDMS was poured into the injection molds at room temperature and left for 48 hours to fully cure. The system was hooked up to a Fluigent vacuum pump and videos were recorded while actuating under sinusoidal pressures with amplitudes up to -0.04 MPa. A custom MATLAB program was utilized to track the pillars and calculate their displacement at each frame, equating to the strain.

RESULTS: FEA yielded a device that stretched uniaxially when negative pressure was applied to the interior boundaries of the vacuum chambers. A simulated collagen matrix embedded around the pillars showcased strains of up to 30% when utilizing the maximum vacuum pressure attainable by the pump (-0.08 MPa). The proposed fabrication methods consistently produced intact devices with complex through-holes. Vacuum actuation of the physical prototype produced supraphysiological strains, similar to that of the FEA. However, the recorded pressure (~ -0.055 MPa) did not reach that of the set value (-0.08 MPa). MATLAB analysis reported strain values of roughly 8% using these settings.

DISCUSSION: Each stretchable hToc device maintains the same footprint as our pre-existing static systems, allowing for high throughput analysis of in vitro tendon structures with the novel incorporation of uniaxial strain. Finite element modeling confirms that the design is capable of producing strains within the physiological range. Stretch tests matched these conclusions, though further work needs to be done to reduce leaks in the system. Such leaks are likely due to tubing head loss and improper sealing at the vacuum inputs. Future incorporation of tenocytes into these systems will unveil the role of mechanical forces in a fibrosis model, including under potential pharmacologic conditions.

REFERENCES: [1] Farhat, Y., et al., J. Cell. Physiol., 2014. [2] Farhat, Y., PhD Dissertation, 2015. [3] Latash, M. & Zatskiorsky, V., Biomechanics and Motor Control, 2016.

14th Annual Center for Musculoskeletal Research Symposium
October 17, 2024

Title: Can Total Shoulder Arthroplasty Save More Than Just Your Shoulder?

Presenting Author: Jonathan Minto, MD

Co-Author(s): Patrick Castle, MD; Dylan Greif, MD; Gabriel Ramirez, MS, Andrew Jeong, M.D; Sandeep Mannava, M.D, PhD; Ilya Voloshin, M.D; Ram Haddas, PhD, MBA

Lab PI / Mentor: Ram Haddas, PhD, MBA

ABSTRACT

Introduction: Glenohumeral osteoarthritis (GA) leads to significant pain and disability, with patients reporting reduced strength and range of motion (ROM) leading to inability to perform activities of daily living (ADLs). Patients with GA suffer from pain and disability due to rotator cuff arthropathy, and therefore may be candidates for reverse total shoulder arthroplasty (rTSA) depending on rotator cuff function. RTSA success relies heavily on pre-operative deltoid function, as rTSA alters muscle recruitment and tension in order to overcome a defunct rotator cuff. Patients with GA often attempt to compensate to regain their lost motion and function with variable success. Therefore, the purpose of this study was to quantify trunk and pelvic compensation during common ADLs. We hypothesize that there are statistically significant deviations in cervical spine, lumbar spine, and pelvic motion in patients with end-stage glenohumeral arthritis when compared to healthy controls.

Methods: Seventy-five patients with GA, who were candidates for total shoulder arthroplasty, and 10 healthy controls (C) were enrolled for this study. Patients were asked to perform multiple overhead reach and hairbrush tasks with both surgical (S) and non surgical sides (NS). Shoulder, neck, trunk, and pelvis kinematics were measured using human motion capture (Vicon) system. Data was processed and analyzed using MTALAB. One-way ANOVA analyses was run using SPSS.

Results: Patients with GA presented with limited shoulder angle (Overhead reach: S:87.6° vs. NS: 106.1°, p=0.01, C: 121.8°, p=0.01; Hairbrush: S:59.2° vs. NS: 70.0°, p=0.14, C: 77.5°, p=0.03) and longer time to complete the tasks (Overhead reach: S:3.3s vs. NS: 2.2s, p=0.04, C: 1.6s , p=0.05; Hairbrush: S:1.7s vs. NS: 1.5s, p=0.33, C: 1.0s , p=0.01). These patients presented with compensation from their lumbar spine (S: -10.9° vs. NS: -5.3°, p=0.03, C: -2.5°, p=0.06) during overhead reach and cervical spine during hair brush (S:10.7° vs. NS: -4.1°, p=0.01, C: -3.8°, p=0.02) in comparison to H (Figure 1).

Discussion/Conclusion: Current metrics to assess pre-operative ROM and function include DASH and ASES, however self-reported metrics only provide a subjective overview while ADLs can still be executed with GA albeit more painful. 3D analysis utilizing human motion capture have recently become available with minimal literature addressing pre-operative range of motion (ROM) deficits in GA patients. Our findings demonstrate that there is statistically significant cervical and lumbar compensation during routine ADLs in patients with severe GA. We posit that these increased compensatory mechanisms may lead to further low back and neck pain if their GA is left untreated. Further research is needed to understand the specific risk and the degree of relief provided by arthroplasty.

14th Annual Center for Musculoskeletal Research Symposium
October 17, 2024

Title: Enhanced Efferocytosis by Bone Marrow Stromal Cells Decreases Support for the Hematopoietic Stem Cell Lineage

Presenting Author: Swachi H. Patel

Co-Author(s): Emily R. Quarato, Yuko Kawano, Noah A. Salama, Ronald Lakony

Lab PI / Mentor: Laura M. Calvi

ABSTRACT

Background: Bone marrow phagocytes are responsible for the non-inflammatory clearance of dead or dying cells, a process known as efferocytosis. Bone marrow-derived macrophages are the professional phagocytes of the bone marrow that perform efferocytosis. We previously demonstrated that with age, macrophages become deficient in their efferocytic function leading to increased apoptotic burden within the bone marrow microenvironment (BMME). Our lab also found that bone marrow-derived stromal cells (BMSC) can act as nonprofessional phagocytes within the BMME. We have previously shown that when BMSCs conduct efferocytosis, their ability to differentiate into bone is decreased. However, it is unknown whether enhanced BMSC efferocytosis impacts their ability to support hematopoietic stem cells (HSCs). Thus, we hypothesize that enhanced BMSC efferocytosis will reduce HSC support.

Methods: To test this in vitro, we introduced excess end-stage neutrophils to BMSCs and measured their ability to support hematopoietic stem and progenitor cells by measuring colony-forming unit cell (CFU-C) counts following efferocytosis. For in vivo studies, we developed a mouse model (PrxCreXBai1) that enhances efferocytosis by introducing a new efferocytic receptor specifically in BMSCs. The Bai1 receptor was selected for the gain of function model due to its direct binding to apoptotic cells without requiring a bridging molecule. The PrxCreXBai1 and control mice were aged to 12 months, with monthly blood collections via mandibular bleeds starting at 2 months of age for complete blood count (CBC) analysis. At 12 months of age, the bone marrow of both male and female PrxCreXBai1 and Bai1 wild-type mice was harvested and sorted for KLS transplantation into healthy 3 month old irradiation conditioned (4.75Gy 2x) CD45.1 mice. Monthly CBC and flow cytometry analysis were performed using peripheral blood obtained by mandibular bleeds to monitor engraftment and any alterations in their blood until 22 weeks post-transplant. Mice were analyzed by sex and genotype for differences.

Results: Our in vitro data showed that following efferocytic activity, BMSCs display a decreased CFU-C count compared to non-efferocytic controls suggesting decreased HSC support. Data from the PrxCreXBai1 mice showed significantly increased monocytes within the peripheral blood at 12 months of age via CBC analysis. Additionally, it was found that these mice also had increased myeloid progenitors (common myeloid progenitors and granulocyte-monocyte progenitors), and short-term HSCs compared to their wild-type controls within the bone marrow. Following successful transplantation of the KLS from PrxCreXBai1 and Bai1 controls into the CD45.1 mice, the peripheral blood analysis showed no significant differences in the terminally differentiated populations of the myeloid lineage while still maintaining high engraftment rates of 70-80%.

Discussion: Collectively, our in vitro and in vivo data suggest altered HSC support following efferocytosis which is reflected by the presence of myeloid skewing within the HSC lineage of the PrxCrexBai1 mice. However, upon removal of the HSCs from the BMME where enhanced efferocytic BMSCs are present, the myeloid skewing is not found. This suggests that the myeloid skewing is potentially the result of continuous but altered support from the BMSCs in the BMME. Therefore, increased efferocytosis may accelerate the development of myeloid malignancies. Future directions for this study involve investigating the bone marrow of the transplanted CD45.1 mice to measure myeloid progenitor levels and performing a cytokine multiplex assay to test for alterations in cytokine expression levels. Altogether, we have demonstrated that BMSC efferocytosis impacts immune support, suggesting that inhibiting BMSC efferocytosis may have novel clinical impacts in the treatment of diseases of aging such as Myeloid Dysplastic syndromes.

14th Annual Center for Musculoskeletal Research Symposium
October 17, 2024

Title: Surgery-Specific Factors Impact Outcomes Following Flexor Tendon Repair

Presenting Author: Amy Phan, MD

Co-Author(s): Andrew J. Rodenhouse, MD, Akhil Dondapati, MD, Gilbert Smolyak, BS, Thomas J. Carroll, MD, Giap Vu, MD, Gabriel Ramirez, MS, Constantinos Ketonis, MD, Ph

Lab PI / Mentor: Constantinos Ketonis, MD, PhD

ABSTRACT

Introduction: Despite advancements in surgical technique and rehabilitation protocols, the risk of complications following flexor tendon repairs remain relatively high. This study sought to evaluate the impact of surgery-specific factors on postoperative outcomes. We hypothesized that surgeon experience, surgeon training, and method of anesthesia used would have an effect on both objective and patient reported outcomes postoperatively.

Methods: This is a retrospective study of patients who underwent primary flexor tendon repair between 2015-2023 at a large academic institution. Electronic medical records were reviewed and demographics, outcomes and complications were tabulated. Thumb and Zone 1 FDP avulsion injuries were excluded. Mixed effects linear regression with a random intercept at the digit level, logistic, linear, and negative binomial regression models were constructed to identify factors associated with ASSH Total Active Motion (TAM), return to operating room (RTOR), compliance, time until return to work, discharge from hand therapy, and Patient Reported Outcomes Management Information System (PROMIS) T-scores. Significance was defined as a p-value < 0.05.

Results: There were 397 patients that met inclusion criteria. Patients whose surgeons had ≥ 15 years of experience had significantly fewer days until return to work (0.57; 95CI: [0.34, 0.94], p-value: 0.027) relative to surgeons with < 5 years of experience. However, surgeon years of experience was not associated with TAM, odds of RTOR, compliance, time until discharge from hand therapy, or PROMIS T-scores. Similarly, neither training in plastic versus orthopaedic surgery, nor completion of a hand fellowship were associated with any of the measured outcomes.

Discussion: Surgery-specific factors including surgeon years of experience and method of anesthesia influence postoperative outcomes after flexor tendon repair. Patients whose surgeons had ≥ 15 years of experience had significantly fewer days until return to work

14th Annual Center for Musculoskeletal Research Symposium
October 17, 2024

Title: Outcomes and Complications of Selected Intercarpal Fusions Using Various Fixation Devices

Presenting Author: Henna Purewal (MS2), BS

Co-Author(s): Ting Zhang, MD, Thomas Carroll, MD, Gabriel Ramirez, MS

Lab PI / Mentor: Constantinos Ketonis, MD PhD

ABSTRACT

Introduction

We evaluated outcomes of various fixation devices in intercarpal fusion for Scaphoid Nonunion Advanced Collapse (SNAC) wrist. We hypothesized that headless compression screw fixation is superior to staples or K-wire fixation in terms of faster operative time, higher union rates, fewer complications, lower reoperation rates, and Patient-Reported Outcomes Measurement Information System (PROMIS) scores.

Methods

This retrospective cohort study included patients over 18 treated with elective intercarpal fusion for SNAC wrist from 2014 to 2024, identified using CPT codes 25820 and 25825. Out of 90 patients, 29 were excluded for undergoing total wrist fusion or scaphoid-capitate fusion. We reviewed surgical procedures, implants used, discharge disposition, hardware failure, union rates, surgical revision needs, pain scores, infections, and other complications. Functional outcome scores, including PROMIS data, were analyzed preoperatively and postoperatively at 2 weeks, 6 weeks, 3 months, 6 months, 1 year, and 2 years. Confounding factors included age, hand dominance, gender, smoking status, diabetes, inflammatory conditions, and operation time. Chi-squared and Kruskal-Wallis tests compared categorical and continuous variables, respectively. Mixed effects linear regression models, with a random intercept at the patient level, examined associations between PROMIS T-scores and fixation techniques while adjusting for confounding variables. Analysis was conducted using State 16.1 (StataCorp, College Station, TX).

Results

The mean follow-up was 48.47 months (range 3 to 169 months). Screw fixation had the lowest complication rate (11%) and a 100% union rate. Staple fixation was used in 35 patients with a 91% union rate and a 23% complication rate. Fusion cup fixation was performed in 7 patients with an 86% union rate and a 57% complication rate. Plate and K-wire fixation had the highest complication rate (70%), despite a 0% reoperation rate, due to superficial pin site infections resolved by antibiotics. Regression analysis showed diabetes had a significant negative impact on all PROMIS domain T-scores, while smoking did not significantly affect outcomes

Discussion

We observed higher complication and reoperation rates with fusion cups due to hardware irritation, cartilage wear, and lunate fragmentation. Headless compression screws showed superior performance with higher union rates and lower complications. Diabetes and male gender significantly impacted PROMIS outcomes. Generally, patients fared well post-surgery with low non-union rates. Despite limitations like surgeon preference and heterogeneous data, this study provides valuable information comparing fixation devices in intercarpal fusions.

14th Annual Center for Musculoskeletal Research Symposium
October 17, 2024

Title: Regional Augmentation of PIEZO1 Expression in Human Humeral Head Cartilage

Presenting Author: Mumin Sabha, BA

Co-Author(s): Sukhee Lee, PhD

Lab PI / Mentor: Sandeep Mannava, MD/PhD; Whasil Lee, PhD

ABSTRACT

INTRODUCTION: Osteoarthritis (OA) is a joint disease characterized principally by progressive cartilage degeneration. Mechanical factors play a critical role in the health and maintenance of cartilage. Chondrocytes, the primary cell population in cartilage, express specialized membrane-bound mechanically activated ion channels, which provide the cells intrinsic mechano-sensitivity across a broad range of mechanical loading. PIEZO1 is a calcium-permeable cation channel highly expressed in chondrocytes. The upregulation of PIEZO1 under supraphysiological mechanical loading has been associated with chondrocyte senescence and apoptosis, promoting the development of knee OA in humans. Although PIEZO1 is a candidate therapeutic target for OA of the weightbearing joints, no study has examined the potential upregulation of PIEZO1 in OA of the shoulder, a non-weightbearing joint. The objective of this study is to investigate alterations in functional expression of PIEZO1 in human shoulder cartilage, which will provide insight into PIEZO1 as a potential target of a disease-modifying OA drug (DMOAD).

METHODS: This study was approved by the institutional Ethics Committee. Informed consents were obtained. Human humeral heads were collected from female patients (ages 62-83) undergoing anatomic total shoulder arthroplasty. Cartilage explants were harvested from superior and inferior regions of the humeral head. These categories were chosen due a demonstrated pattern of increased cartilage wear in the inferior region.

Ratiometric Ca2+ imaging was performed with isolated chondrocytes to quantify the intra-cellular Ca2+ response to Yoda1, a PIEZO1-specific agonist (n=3 pairs, inf vs sup). Cytosolic [Ca2+] of individual chondrocytes were calculated by 340nm/380nm fluorescence intensity using Incytim-2 software. At 1 min, the chondrocytes were treated with 20 μM Yoda1 and imaged for 6 min. Cytosolic basal [Ca2+] and maximal [Ca2+] influx were determined. Statistical analysis was performed by t-test using GraphPad Prism 10 ($p<0.05$). RNA isolation was performed and submitted for Bulk RNA Sequencing (RNAseq) to assess gene enrichment among inferior and superior regions of cartilage (n=5 pairs, inf vs sup).

Results: Ratiometric Ca2+ imaging was showed no significant difference in chondrocyte basal [Ca2+] between superior and inferior regions of the humeral head ($p=0.07$). However, upon Yoda1 treatment, there was a significant increase in the maximal [Ca2+] in the inferior region of the humeral head compared to the superior region ($p<0.01$). RNAseq analysis indicated that PIEZO1 expression was higher in the inferior region of the humeral head for each respective sample. In addition, TRPV4 expression was relatively higher in the inferior region compared to the superior region.

Discussion: The ratiometric Ca2+ imaging and RNAseq findings demonstrate higher PIEZO1 expression in the inferior region of the humeral head in each patient, which suggests augmented expression of PIEZO1 channels in osteoarthritic humeral head cartilage. This may be explained by the increased frequency of contact between the humeral head and the glenoid in the inferior region of the humeral head. The regional augmentation of PIEZO1 levels further suggest that the feedforward pathomechanism whereby increased PIEZO1 expression promotes OA development in the knee may also be present in the shoulder. Thus, the development of a DMOAD targeting PIEZO1 has potential in the shoulder as well. Surprisingly, there was co-modulation of PIEZO1 and T
RPV4, an anabolic pathway-associated mechanosensitive calcium channel, which were associated with low levels of collag
en 1-5. Limitations include sample size and variability between patients. Future work will investigate anabolic and catabolic biomarkers using pathway and WGCNA analysis.

14th Annual Center for Musculoskeletal Research Symposium
October 17, 2024

Title: Comparison of Kinematics between Markerless and Conventional Marker-Based Upper Extremity Analysis in Clinical Patients

Presenting Author: Emily Schillinger, MS

Co-Author(s): Ilya Voloshin, MD; Sandeep Manava, MD, PhD; Nicholas Morriss, MD; Gabriel Ramirez, MS; Ram Haddas, PhD, MBA

Lab PI / Mentor: Haddas

ABSTRACT

Introduction: A marker-based motion analysis is the current standard for disability and functional analysis (e.g. gait analysis). Recent advances have been made in markerless motion capture, primarily through the use of deep learning models for the estimation of pose based on standard video from multiple synchronized cameras. A markerless system may provide a more convenient and time-efficient method of performing motion analysis. By eliminating the need to place markers on the subject, setup time is reduced, and movement is not affected. Additionally, there is less need for extensive training in marker placement, although expert knowledge is still required for clinical examinations; inter-assessor variability of motion capture is also reduced. Therefore, this study aimed to examine the concurrent validity of a markerless system against a traditional marker-based system for assessing upper extremities.

Methods: Seventy-five glenohumeral osteoarthrosis candidate for a shoulder replacement surgery with 10 healthy controls underwent clinical upper extremity assessment with data being captured concurrently by a traditional marker-based motion capture (Vicon Nexus, Vicon Motion Systems Ltd, Oxford, UK) and a commercial markerless system (Theia3D, Theia Markerless Inc., Kingston, ON, Canada). Clinical assessment included overhead reaching, drinking, hair brush, and personal hygiene tasks. The marker-based system used 10 infrared cameras (Valkyrie-16) capturing at 100 Hz. Markers were placed on the subject by an experienced rehabilitation engineer following Southampton upper limb model and the data were processed in Vicon Nexus. The markerless system used 8 video cameras (FLIR) capturing at 100 Hz interfaced through the Vicon Nexus. Data were captured at the same time using both systems and synchronized to each other. To assess agreement in minimum, maximum, and range of motion in shoulder motion between markerless and marker-based measurements the Interclass Correlation Coefficient (ICC) estimates and their 95% confidence intervals were calculated using Stata 16.1, StataCorp, College Station TX, based on a mean-rating (k=3), absolute-agreement, two-way mixed effects model.

Results: Kinematics showed similar patterns between the marker-based and markerless systems. When analyzing shoulder motion, the ICC was ranging between moderate to excellent (Flexion/Extension: 0.576-0.955, $p<0.001$; Abduction/Adduction: 0.504-0.947, $p<0.001$) between moderate to excellent (Internal/External Rotation: 0.171-0.773, $p<0.001$) in different motions. Good to excellent correlation were found between the interpolated waveforms of the marker-based and markerless systems.

Discussion: The markerless system generally produced similar kinematics to the traditional marker-based system for the upper extremity. The main differences appeared to be in rotation movement and due to differences in segment definition rather than differences in tracking. Using markerless motion capture for upper extremity analysis offers several advantages, including faster patient setup and less intrusiveness since markers are not required. During the test, patients should not be exposed or wearing tight clothing, and anatomic landmarks such as the sternum and anterior/posterior superior iliac spines can be examined. As a result, patients may be able to move more comfortably and naturally, as well as reduce the time required for data collection, thereby increasing throughput and patient volume. The total time for processing is usually not longer than for traditional gait analysis and requires less active intervention by the operator; however, marker-based motion analysis allows for more efficient real-time quality control since only marker visibility needs to be verified.

14th Annual Center for Musculoskeletal Research Symposium
October 17, 2024

Title: Validating 3D Bone Marrow Microenvironment Models: Pivotal for Advancing In Vitro Models in Preclinical Acute Myeloid Leukemia Studies

Presenting Author: Azmeer Sharipol

Co-Author(s): Amal Khan, Celia Soto

Lab PI / Mentor: Benjamin J. Frish

ABSTRACT

Background & Hypothesis:
Dysregulation of the bone marrow microenvironment (BMME) driven by leukemia cells leads to the disruption of normal hematopoiesis. In acute myeloid leukemia (AML), leukemic cells functionally inhibit osteoblasts activity, disrupt mesenchymal stem/stromal cells (MSCs) differentiation, and alter the hematopoietic stem and progenitor cells (HSPCs) population. The current research paradigm focuses on understanding the role of the BMME, aiming to identify novel target pathways that could potentially improve the dismal 30% 5-year survival rate observed in AML patients. Several groups have developed in vitro BMME models to accelerate mechanistic and drug discovery studies. Still, their integration into preclinical research is hindered by insufficient validation of published in vivo and human cell experiments. Developers must demonstrate the superiority of 3D models over cost-effective 2D cultures.

Experiments & Methods:
We explored whether a 3D BMME-chip model could recapitulate the phenotypical alterations of the BMME components driven by AML cells. We developed a murine 3D model containing MSCs, mineralized osteoblastic, and flow-induced endothelial channel using Emulate Chip-S1™ that can maintain the long-term function of HSPCs.

Results:
We found that when blast cells from blast crisis chronic myelogenous leukemia mice (bcCML) were added to the BMME-chip, osteoblast activity was lost as seen by the reduction of mineralized calcium nodules via vonKossa staining (1293.33 ± 187.11 compared to 2759.67 ± 489.10 in healthy BMME-chip, N=3) and osteocalcin relative gene expression at Day 14 (0.17 ± 0.05, N=3). 10-fold overexpression of inducible nitric oxide synthase (iNOS) could indicate an immunosuppressive BMME. Flow cytometry data showed that at day 14 of culture, AML cells accounted for up to 29.00±2.35% of total live cells meanwhile HSPC populations are dysregulated as seen by increased lineage-, Sca1+, and cKIT+ cells (LSKs) and short-term repopulating hematopoietic stem cells (ST-HSC). In addition, we found that CCL3, a chemokine associated with inhibition of osteoblasts activity, in AML-BMME-chip is more than two-fold higher compared to healthy BMME-chip. To validate the findings of CCL3 receptor inhibition that partially restored BMME function, we developed BMME-chip with CCR1 and CCR5 (CCL3 receptors) double knockout MSCs and so far, found that the cells can differentiate into osteolineage cells indicated by positive alkaline phosphatase staining.

Discussions & Conclusions:
Currently, we are developing a human BMME-chip model and our preliminary findings show survival of primary AML cells in BMME-chip for at least 7 days in BMME-culture. We believe that validation of hallmark findings in vitro models will drive us closer to the adoption of complex 3D culture models in basic and translational studies.

14th Annual Center for Musculoskeletal Research Symposium
October 17, 2024

Title: Lysosomal Degradation of TRAF3 in T Cells Causes Immunosenescence, Associated with Age-Related Bone Loss

Presenting Author: Chutamath Sittplangkoon

Co-Author(s): Philip Milton, Xi Lin, Rong Duan, Jun Wu, Brendan F. Boyce, Zhenqiang Yao

Lab PI / Mentor: Zhenqiang Yao

ABSTRACT

Background & Hypothesis: Activated T cells not only cause bone destruction but also maintain bone homeostasis. Th17 is defined as the T cell subset that enhances osteoclastogenesis by producing RANKL to cause bone destruction in autoimmune diseases. Conversely, Th1, Th2 and regulatory T cell (Treg), produce a variety of cytokines, including IFN-γ, IL-4 and IL-10, to inhibit osteoclastogenesis. If dysfunctional T cells disrupt bone homeostasis during aging to cause age-related osteoporosis (AROP) remains unclear. Our aims are to characterize T cell dysfunction associated with AROP and demonstrate if this is caused by lysosomal degradation of TRAF3, a common mechanism that results in enhanced osteoclast and decreased osteoblast differentiation during aging, and TRAF3 also regulates T cell function.

Experiments & Methods: To avoid an effect of sex hormone on bone homeostasis, only male mice were used in all experiments. Bone marrow cells (BM) and fluid were harvested from young (3-mon-old) and aged (20-mon-old) C57BL/6 mice to examine the frequency of T cell subsets and their cytokine productions by flow cytometry and detect the levels of multiple cytokines and chemokines by antibody array. Paraffin-embedded vertebrae were performed spatial transcriptomic analysis to detect inflammatory factor expression in situ. CD4 T cells were isolated from bone marrow from young and aged mice to detect TRAF3 expression by Western blot and to test the effect of lysosomal inhibitor, hydroxychloroquine (HCQ), on T cell function and TRAF3 expression. Finally, aged mice were treated with vehicle or 16 mg/kg of bone targeted-hydroxychloroquine (BP-HCQ), 5 doses per week, for 5 weeks, L1 vertebrae was used to evaluate bone structural parameters by Micro-CT analysis, bone marrow cells were used to test T cell frequency and function by flow cytometry and bone marrow fluid was used to examine cytokines by antibody array.

Results: The aged mice have significantly increased % of CD3+ CD4+ T cells (7.99±2.13 vs 5.72±0.66), but significantly decreased % of CD44-CD62L+ naïve CD4+ T cell (0.69±0.25 vs 1.57±0.69), and CD3+ CD4+ CD25+ Tregs (41.75±9.62 vs 80.6±6.40) compared to young mice in BM. However, the % and MFI of CD3+CD4+ T cells expressing IFN-γ and IL-17 were unchanged, while those expressing IL-4 (67.4±23.10 vs 130±19.26) and TNF-α (631.5±91.88 vs 990±135.21) were significantly decreased and % of PD-1-expressing CD4+ T cells (3.25±0.83% vs 1.96±0.58 %), that attenuates T cell function, was markedly increased in aged compared to young mice. Antibody arrays show that IFN-γ, IL-4 and IL-10, were markedly reduced in the BM fluid from aged compared to young mice. Consistent with this, spatial transcriptomic analysis indicated that mRNA expression of these cytokines was also decreased, and particularly, inflammatory response related pathways were downregulated in vertebrae from aged mice. Interestingly, CD4+ T cells from aged mice have reduced TRAF3 protein level, which was blocked by HCQ. Treatment of aged mice with BP-HCQ significantly increased trabecular bone mass, reversed the increased % of CD3+CD4+ T cells and increased expressions of IL-4 and TNF-α and the % of the effector memory CD4+ T cells in BM of aged mice to the level in young mice and partly rescued the decrease in Tregs.

Discussion & Conclusions: AROP is associated immunosenescence characterized by reduced naïve T cells and accumulated impaired memory and helper T cells in BM associated with reduced production of inflammatory cytokines, mediated by lysosomal degradation of TRAF3, the shared mechanism involved in reduced osteoblastic bone formation and increased osteoclastic bone resorption. Particularly, reduction of the major T cell cytokines, such as IFN-γ, IL-4, IL-10, that inhibit osteoclast differentiation, could be a reason for the enhanced bone resorption in AROP. We conclude that targeted delivery of BP-HCQ to bone could treat both AROP and immunosenescence.

14th Annual Center for Musculoskeletal Research Symposium
October 17, 2024

Title: Analyzing the Predictive Capability of PROMIS for Management of Carpal Tunnel Syndrome

Presenting Author: Gilbert Smolyak

Co-Author(s): Jordan Cruse, Gabriel Ramirez

Lab PI / Mentor: Constatinos Ketonis

ABSTRACT

Introduction:
Carpal tunnel syndrome (CTS) is a common cause of pain and disability, affecting an estimated 3–4% of workers in the United States. Patient-reported outcome measurements, such as the Patient-Reported Outcomes Measurement Information System (PROMIS), are powerful tools in tracking clinical progression or improvement over time. PROMIS has been frequently used to evaluate post-procedural outcomes following intervention, but little is known on its pre-operative utility in the evaluation and management of patients with CTS. The aim of this study was to evaluate the association of pre-operative PROMIS scores with the likelihood that a patient undergoes operative intervention for CTS.

Methods:
Patients presenting to a tertiary academic medical center from 2018–2024 with a diagnosis of CTS were identified. Exclusion criteria included age <18 years old, patients who had another diagnosis at the first visit, and those with less than one year follow-up. Patients were separated by ultimate treatment: injections or surgery. Chi-square analysis was performed to identify confounding variables or demographic factors that affect treatment strategy. Patients were grouped by PROMIS score using predetermined cut-offs and a logistic regression was used to determine odds-ratio (OR) of surgical intervention based on age, sex, race, ethnicity, diabetic status, smoking status, BMI category, type of insurance (private, Medicare/Medicaid, or worker's compensation) and PROMIS score groups.

Results:
Of the 3,286 patients that met inclusion/exclusion criteria, the average age was 58 years old and 62% were female. By the end of the follow up period, 50% of patients received a corticosteroid injection, with 18% of those patients requiring ≥1 additional injection, and 83% eventually undergoing surgery. Patients who were older (OR 1.01, $p<0.001$), male (OR 1.37, $p<0.05$), or increased BMI (OR 1.02, $P<0.01$) had significantly increased odds of undergoing surgery. Surprisingly patients with moderate or severe physical impairment (OR .78, $p<0.05$) and moderate or severe pain interference (OR 0.77, $p<0.05$) at their initial visit had significantly decreased odds of undergoing surgery. Further, patient who identify as black (OR 0.66, $p<0.01$), also had a decreased odds of undergoing surgery.

Discussion:
PROMIS survey results could be used to identify patients that are more or less likely to undergo operative intervention for CTS. Other factors such as older age, male gender, and increased BMI were also found to be associated with increased odds of that patient choosing to undergo surgery. Future directions may include correlation of PROMIS with nerve conduction severity stratification at time of diagnosis and its influence on shared decision making in proceeding with surgery.

14th Annual Center for Musculoskeletal Research Symposium
October 17, 2024

Title: Optimization of an In Vitro Model of Staphylococcal Abscess Communities to Study Bactericidal Mechanisms

Presenting Author: Levy A. Sominsky

Co-Author(s): Gowrishankar Muthukrishnan, Chao Xie

Lab PI / Mentor: Edward M. Schwarz

ABSTRACT

Background: Staphylococcus aureus, the primary pathogen in bone infections, possesses unique abilities to evade antibiotics. For example, S. aureus forms abscesses within bone marrow or surrounding soft tissue, known as Staphylococcal abscess communities (SACs) (1), which protect the bacteria from antibiotics and host immunity via a fibrin pseudocapsule. Previous studies demonstrate that vancomycin, the standard of care (SOC) for MRSA bone infections, is ineffective against SACs in vivo; however, sitafloxacin, a fluoroquinolone clinically used in Japan, can kill bacteria within SACs while inducing degradation of the encasing fibrin ring via unknown mechanisms (2). Here, we used an in vitro SAC model (3) to define the dose-dependent kinetics of sitafloxacin killing and test the hypothesis that fibrin degradation is secondary to antibiotic-induced biofilm emigration.

Methods: In vitro SACs were grown using the MSSA JAR 06.01.31 strain as previously described (3) in collagen gel diluted with TSB or RPMI and overlaid with human plasma. After 24 hours, plasma overlying mature SACs was replaced with either PBS or antibiotic (sitafloxacin or vancomycin) at various concentrations. After 24 hours of treatment, collagen gels containing SACs were washed with PBS and then homogenized, sonicated, and enumerated for CFUs. Analysis was performed using two-way ANOVA with Tukey's multiple comparisons test ($p<0.05$ considered significant).

Results: Treatment of mature SACs for 24 hours with sitafloxacin resulted in a significant dose-dependent decrease in the percent survival of bacteria enumerated from collagen gels, with no CFUs at 10,000x MIC. Importantly, collagen gels overlaid with PBS did not display this decrease in CFUs, corroborating that the decreased survival seen with sitafloxacin treatment was due to bactericidal effects rather than nutritional insufficiency. In contrast, vancomycin treatment failed to decrease survival over the range of concentrations tested. Equivocal effects were seen in both TSB and RPMI-diluted collagen gels. Nonetheless, with TSB being the more nutritious media, TSB-diluted gels are ideal for testing antimicrobial efficacy to ensure decreased bacterial survival is solely due to the antibiotic. Mature SACs were then treated with sitafloxacin and enumerated longitudinally to determine if sitafloxacin's activity is time-dependent in our model. Mature SACs grown in TSB-diluted collagen gels were overlaid with either PBS or sitafloxacin at 1000x its MIC and enumerated at various time points over 6 hours, as stated above. Sitafloxacin killed over 90% of the bacteria after 30 minutes of treatment, which did not significantly change over other time points through 6 hours. Thus, sitafloxacin's potency is immediate.

Discussion: In this study, we demonstrated sitafloxacin's superior efficacy to vancomycin in vitro and defined its dose and time-dependent bactericidal activity in our model. Prior studies have revealed that sitafloxacin can uniquely disrupt the integrity of the fibrin ring of SACs. Since sitafloxacin cannot directly degrade the fibrin ring, we hypothesize that it must influence the structure by acting on the encased bacteria. By identifying the maximum dose at which CFUs are consistently recovered (1000x MIC) and the limited influence of the duration of treatment on the percent survival, we can now leverage our model to perform bulk RNA sequencing on sitafloxacin-treated SACs and delineate how the antibiotic changes the structure of the fibrin pseudocapsule. Defining the genes that respond to sitafloxacin and influence fibrin ring degradation will reveal novel targets for dispersing SACs to enhance current SOC for bone infection.

1) Cheng et al. FASEB J 25:3393-404 (2009), 2) Ren et al. Front Cell Infect Microbiol 12:910970 (2022), 3) Hofstee et al. Infect Immun. 88(11):e00293-2 (2020)

14th Annual Center for Musculoskeletal Research Symposium
October 17, 2024

Title: Development of an in vitro μSiM Platform to Study Bacterial Invasion of the Osteocyte Lacuno-Canalicular Network (OLCN)

Presenting Author: Arvind R. Srivatsava

Co-Author(s): Michael E. Klaczko, Gregory R. Madejski, Ann L. Gill, Steven R. Gill

Lab PI / Mentor: Hani A. Awad, James L. McGrath

ABSTRACT

Introduction.
Staphylococcus aureus infections contribute significantly to osteomyelitis, a ecting bone marrow, cortex, periosteum, and surrounding soft tissue, eventually leading to bone loss [1]. Osteomyelitis is characterized by recurrent and persistent infections in 40% of patient cases, exacerbated by S. aureus's intercellular persistence, immune system evasion, and robust antibiotic resistance [1]. Our previous work discovered S. aureus's ability to invade and colonize the osteocyte lacuno-canalicular network (OLCN), o ering a potential new mechanism of infection persistence [2]. Using the μSiM-CA (microdevice featuring a silicon-nitride membrane - canalicular array) model, we previously demonstrated that 1 μm-sized S. aureus can transit through sub-micron pores and identified penicillin-binding protein 4 (PBP4), a cell wall transpeptidase, as essential for OLCN-invasion [2].

Methods.
Building on our previous findings, we are now developing a high-throughput screen for drugs targeting PBP4. We employ e-beam lithography to create microenvironments that more accurately model the aspect ratio of cortical bone canaliculi. These precision structures feature several arrays of 2 - ~0.1 μm wide microchannels atop nanoporous membranes, enabling controlled introduction of antibiotics as S. aureus propagate through canalicular mimetics for future studies. USA300-GFP bacteria are sequestered in “loading-zones” using a negative pressure method and allowed to invade into microchannels. We use fluorescence live cell imaging of GFP-transfected-USA300 S. aureus transmission, visualizing bacterial growth and microchannel colonization after ~24 hours. In future investigations, we aim to examine conditions involving PBP4-mutant USA300-GFP strains, PBP4 inhibitors, and diverse antibiotic regimens.

Results.
Our new e-beam lithography-based platform successfully creates microenvironments that closely mimic the aspect ratio of cortical bone canaliculi. Initial observations using fluorescence live cell imaging show that USA300-GFP bacteria can be e ectively sequestered in loading zones and expand into the sub-micron channels. We intend to use this imaging approach for real-time visualization of bacterial growth and microchannel colonization, which will provide a more dynamic understanding of S. aureus proliferative behavior in these confined spaces.

Discussions.
This work demonstrates the versatility of our advanced tissue chip platform to create in vitro models to study the mechanisms of bone infection and to screen for drugs to treat osteomyelitis, particularly those targeting PBP4. The high-throughput nature of our current approach promises to accelerate the discovery of novel therapeutic strategies against persistent S. aureus infections in bone.

References.

1. Kavanagh, N., et al., Clin Microbiol Rev, 2018. 31(2).
2. Masters, E.A., et al., PLoS Pathog, 2020. 16(10): p. e1008988.

14th Annual Center for Musculoskeletal Research Symposium
October 17, 2024

Title: Quantitative Diagnosis of Murine Osteoarthritis by Geometric Indices of Micro-CT

Presenting Author: Churou Tang

Co-Author(s): Rong Duan, Lindsay Schnur and Zhenqiang Yao

Lab PI / Mentor: Zhenqiang Yao

ABSTRACT

Background. Osteoarthritis (OA) is the most common joint disease and one of the most common causes of physical disability among adults. But there is no disease-modifying therapy. The hallmarks of OA include articular cartilage degeneration, excessive ossification (osteophyte formation) and chronic synovial inflammation. Imaging is the golden method to diagnose OA, but it is challenging to quantify the pathological changes of OA in murine model.

Methods: The knee joints with medial meniscectomy (PTOA) and the opposite normal joints without injury (NJ) from one year-old C57Bl6 (WT) mice were scanned with micro-CT after 4 and 8 wks of surgery. Aimra software was used to detect the changes of geometric parameters in the distal femora and proximal tibia. The reliability (reality) and sensibility of the geometric indices in diagnosing OA were determined by their potential to represent golden parameters: articular cartilage damage and osteophyte formation and by comparing them with OARSI score, respectively. The responsiveness of the indices to clinical treatment was determined by their change after PTOA in WT vs. GM-CSF-/- mice, which have mitigated joint damage caused by collagenase. The reproducibility (repeatedly) was tested using age-related OA.

Results: The maximal height of secondary ossification center (2^{nd} Os.C) of tibia, representing tibial subchondral bone collapses caused by articular cartilage damage, was significantly decreased after 4 wks (0.767 ± 0.062 mm vs. 0.842 ± 0.032 mm of NJ, p= 0.025) and 8-wks (0.716 ± 0.052 mm vs. 0.823 ± 0.046 mm of NJ, p= 0.0025), resulting in significant reduction in the ratio of maximum height to width of 2^{nd} Os.C of tibiae at both time points. The length of distal femur (the distance between upper middle point of intercondylar groove and the intercondylar notch) was kept unchanged in WT OA joints after 4 and 8 wks, and thus can acts as a reference parameter. In contrast, the width of distal femur (distance between the edges of lateral and medial condyle, representing osteophyte) was increased in the WT OA joints after 4 wks (3.24 ± 0.14 mm vs. 2.9± 0.04 mm of NJ, p<0.001) and 8 wks (3.35 ± 0.13 mm vs. 2.87± 0.055 mm of NJ, p<0.001), resulting in the ratio of the width to length of distal femur largely increased in WT OA joints after 4 wks (1.36 ± 0.04 vs.1.22 ± 0.03 of NJ, p=0.000) and 8 wks (1.396 ± 0.045 vs.1.22 ± 0.013 of NJ, p=0.000). Interestingly, the ratio of maximum height to width of 2^{nd} Os.C of tibiae was not changed in GM-/- mice and the ratio value of width to length of distal femora was smaller in GM-/- mice than that in WT mice after 4 wks of surgery. In addition, 28-m-old aged male mice have increased ratio of length/width of distal femora (1.47±0.02 vs 1.23±0.03, p=0.016) and decreased ratio of max height/width of 2^{nd} Os.C of tibiae (0.26±0.03 vs 0.31±0.026, p=0.001) compared to 5-m-old adult mice. However, the aged mice have reduced subchondral bone volume (osteoporosis) compared to 5-month-old adult mice.

Discussions and Conclusions: The geometric indices of distal femur and proximal tibia can sensitively evaluate subchondral bone collapses caused by articular cartilage damage and osteophyte in both PTOA and aged-related OA in knee joint. The ratio of the length (height) to width is particularly useful to diagnose the cartilage damage and osteophyte formation because they would have little individual difference among the subjects. One issue is that the epiphysial plate is closed and the height of 2^{nd} Os.C cannot be measured in adult human. Thus, we should find the anatomic markers to measure the length (height) and width of distal femur and proximal tibia not only in human but also in murine so that the geometric parameters can be precisely measured and comparable by and among different investigators.

14th Annual Center for Musculoskeletal Research Symposium
October 17, 2024

Title: Real-Time Confocal Microscopy Assessment of PAD4-Mediated NETosis by S. aureus on Implants

Presenting Author: Allie Tay

Co-Author(s): Youliang Ren, Sashank Lekkala, Jason Weeks, Thomas Xue, Ye Shu, Shu-Chi A. Yeh, Edward M. Schwarz and Chao Xie

Lab PI / Mentor: Edward M. Schwarz, Chao Xie

ABSTRACT

Introduction: Implant-associated osteomyelitis remains a major risk of orthopaedic surgery. While it is known that surgical implantation of a foreign material in vivo is prone to bacterial attachment and colonization, the dynamics of host-pathogen interaction and host immunity mechanisms require more thorough characterization. A crucial aspect of neutrophil defense is NETosis, a process in which neutrophils release their DNA and antimicrobial peptides to create neutrophil extracellular traps (NETs) that aggregate and kill bacteria for subsequent phagocytosis. One of the key genes involved in NET formation is peptidyl arginase deiminase 4 (PAD4), which induces chromatin decondensation and the release of chromosomal DNA covered with antimicrobial molecules. Here, confocal microscopy techniques were combined with the development of a novel Catchup x PAD4-/- mouse model expressing the fluorescent protein tdTomato and with the PAD4 gene knocked out to study NETosis in the absence of PAD4. We hypothesized that Catchup neutrophils would form NETs consistent with the host PAD4-mediated response, while PAD4-deficient groups would fail to form NETs and hence fail to reduce the bacterial burden.

Methods: Longitudinal confocal fluorescent microscopy was used to image a co-culture system consisting of S. aureus-contaminated titanium pins and neutrophils for 6 hours. Catchup mice and PAD4-/- mice were obtained and crossbred. Catchup x PAD4-/- mice were genotyped to verify homozygosity for tdTomato +/+ and PAD4 -/-. Neutrophils were isolated from murine femurs and tibiae via density gradient centrifugation-separation. Prior to imaging, S. aureus (USA300 strain, EGFP+) was cultured overnight. Titanium pins were etched to guide robust nidus growth within a prospective region of interest (ROI), and were contaminated with S. aureus for 2.5 hours the morning of imaging and placed flat inside a cover glass-bottom culture dish. Isolated neutrophils were subsequently co-incubated with the contaminated pins at 5% carbon dioxide and 37°C for 6 hours under confocal microscopy. At 6 hours, SYTOX blue, a stain for extracellular DNA that penetrates cells with compromised membranes, was added to look for the presence of NETs. Quantification of bacterial volume, neutrophil volume, neutrophil swarming were performed in Imaris and Fiji following imaging.

Results: Pharmacological and genetic inhibition of PAD4 prevented NET formation, resulting in a robust bacterial biofilm. Catchup neutrophils incubated with S. aureus contaminated implants exhibited the expected neutrophil swarming response and reduced bacterial burden by 6 hours. SYTOX blue staining verified the presence of NET formation at the nidus for the control group. In contrast, addition of the PAD4 inhibitor GSK484 dramatically increased MRSA growth and static biofilm formation. No NETs were evident. The Catchup x PAD-/- group demonstrated low levels of extracellular DNA and no visible NET formation at the nidus; yet, interestingly exhibited a robust swarming response with a reduction in EGFP+ MRSA, similar to the Catchup control group.

Discussion: Elucidation of NET-forming mechanisms is crucial to understanding the host immune response during implant-associated infection and developing effective intervention as well as prevention strategies. Here, we verified the key role of PAD4 in mediating NETosis through pharmacological and genetic loss of function models, as well as visualized neutrophil swarming behavior using real-time confocal microscopy. While we confirmed that PAD4 is required for NET formation in response to MRSA, our preliminary findings demonstrate that PAD4-/- neutrophils are still able to effectively swarm to and clear bacterial on the implant. Future studies are warranted to track the long-term effects of NETs and illuminate the interplay between pro-NET and anti-NET formation factors, as well as confirm if neutrophil responses in vivo are consistent with in vitro findings.

14th Annual Center for Musculoskeletal Research Symposium
October 17, 2024

Title: ADI Is Associated With Depression Disparities at Minimum 1-Year Post-rTSA

Presenting Author: Kismat Touhid, BA

Co-Author(s): Jonathan Minto, MD, Andrew Jeong, MD, Patrick Castle, MD, Willian Zhuang, BS, Michaela Malin, BA, Sandeep Mannava, MD PhD

Lab PI / Mentor: Sandeep Mannava, MD PhD

ABSTRACT

Introduction:

Reverse total shoulder arthroplasty, or rTSA, have become increasingly popular in providing definitive treatment for rotator cuff arthropathy. Unfortunately, there is a lack of research exploring the role of social determinants of health (SDOH) on mediating long-term outcomes following rTSA. This study seeks to utilize Area Deprivation Index (ADI) as a surrogate for SDOH in elucidating how socioeconomics affect postoperative outcomes following rTSA as reported via PROMIS.

Methods:

This was a retrospective analysis of 112 patients that underwent unilateral, first-time rTSA between 2015-2021. CT included pre- and post-operative PROMIS scores for physical function, pain interference, depression, and upper extremity function. Demographic variables and ADI data were sourced from the University of Wisconsin's Neighborhood Atlas. Outcomes were compared across ADI quartiles using Chi-squared and Kruskal-Wallis tests for univariate analysis and mixed-effects models for adjusted analysis. Minimum clinically important difference, or MCID, was defined as a change in PROMIS scores exceeding 0.5 standard deviations from baseline.

Results:

At mean 18 months follow-up, ADI significantly influenced the likelihood of achieving MCID for depression. 30% of patients reported a significant clinical benefit to their mood in the most deprived quartile compared to 43% of patients in the least deprived quartile. After adjusting for covariates, the odds of reporting significant mood improvements were 6 times lower for patients in the higher deprivation quartiles compared to the lowest quartile ($p<0.05$). No other direct correlations were observed between ADI and pre- or post-operative PROMIS scores.

Discussion and Conclusion:

Our study demonstrates that ADI was correlated with long term mood improvements after rTSA. The most deprived patients were less likely to achieve MCID for depression. ADI was not correlated with achieving MCID for physical, pain, and upper extremity function. These results indicate that despite ADI, patients undergoing rTSA have improvements in physical function and pain. However, this study suggests that patients in the most deprived ADI quartiles undergoing rTSA may need additional counseling/support systems post-operatively.

14th Annual Center for Musculoskeletal Research Symposium
October 17, 2024

Title: Area Deprivation Index (ADI) Predicts Patient Reported Outcomes Following Total Shoulder Arthroplasty

Presenting Author: Kismat Touhid, BA

Co-Author(s): Jonathan Minto, MD, Andrew Jeong, MD, Patrick Castle, MD, Willian Zhuang, BS, Michaela Malin, BA, Sandeep Mannava, MD PhD

Lab PI / Mentor: Sandeep Mannava, MD PhD

ABSTRACT

Introduction:
Total shoulder arthroplasty (TSA) has been demonstrated to improve pain and functionality in patients with glenohumeral arthritis. While the literature indicates that social determinants of health (SDOH) influence patient outcomes after orthopedic procedures in general, assessing the aggregate impact of such variables on overall long-term outcomes remains a practical challenge. The purpose of this study is to explore the impact of area deprivation index (ADI) as a surrogate for the aggregate effect of SDOH on patient-reported outcomes after TSA.
Methods:
Retrospective analysis of 151 unilateral TSA patients at our institution between 2015-2023 with minimum 1-year follow up was performed. Data included pre- and post-operative PROMIS scores for physical function, pain interference, depression, upper extremity function, and demographic variables. ADI data were sourced from the University of Wisconsin's Neighborhood Atlas. Outcomes were compared across ADI quartiles using Chi-squared and Kruskal-Wallis tests for univariate analysis and mixed-effects models for adjusted analysis. Minimal clinically important difference, or MCID, was defined as a change in PROMIS exceeding 0.5 standard deviations from baseline. Results:
At mean follow-up of 18 months, higher ADI quartiles were significantly correlated with worse PI and UE scores. The most deprived cohort reported higher pain (+5.43 points) and lower UE function (-1.38 points) compared to the least deprived cohort. After adjusting for covariates, ADI remained the only independent predictor of postoperative pain, with the most deprived quartile predicting a 3.059 higher PI score compared to the least deprived cohort (95% CI [0.255, 5.862]). No significant differences in MCID achievement were observed.
Discussion:Our results convey how socioeconomic disadvantage is correlated to worse postoperative pain and upper extremity function following TSA. It also confirms the utility of ADI as a surrogate SDOH marker since it was the only variable that independently predicted postoperative pain. As no significant differences in rates of MCID achievement were detected, these data suggest that patients regardless of background experience comparable rates of achieving a minimum level of clinical benefit following TSA. However, there exists clear ADI-related disparities in the extent of that benefit, as evidenced by the divergence in final function scores.

14th Annual Center for Musculoskeletal Research Symposium
October 17, 2024

Title: Piloting ChatGPT in Summarizing Postoperative Rehab Progress Following Flexor Tendon Repair: A Validation Study

Presenting Author: Kismat Touhid, BA

Co-Author(s): Constantinos Ketonis, MD PhD

Lab PI / Mentor: Constantinos Ketonis, MD PhD

ABSTRACT

Introduction:
Large Language Models (LLMs) like ChatGPT have the potential to ameliorate the daily administrative burden hand surgeons face when querying the EMR for patient follow-up data. With information on postoperative range-of-motion (ROM) or strength scattered across tens of different progress notes, using GPT to automate the retrieval and synthesis of these data could be immensely useful if properly vetted. Given the risk of LLM "hallucination," it is critical to validate the usage of LLMs using real-life clinical data. This study, therefore, serves as a pilot case series that aims to assess the reliability of GPT4 in synthesizing patient rehabilitation data when given postoperative progress notes following flexor tendon repair (FTR).
Materials and Methods:
This is a retrospective validation study for five patients who underwent FTR 2019-2020. A standardized method of anonymization was developed and implemented for each patient note series. The data was converted into a .txt file for input to GPT-4-Turbo, with advanced data analysis enabled and memory and personalization features disabled. Iterative prompting informed the development of a standardized 4-prompt series using prompt engineering principles. 1 prompt was utilized to summarize qualitative clinical information, while a 3-step prompt series was developed for quantitative information that 1) identified all unique patient visits, 2) tabulated the relevant quantitative data, and 3) graphed the findings for easy visualization. The output was then cross-referenced with input for veracity. Accuracy rates of objectively verifiable data were recorded along with qualitative observational data to note potential pitfalls.
Results:
Approximately 29,000 words were analyzed across 95 office and PT/OT notes. Prompting GPT to identify unique visit dates prior to reporting ROM improvements enabled GPT to report on 100% of postoperative data. It accurately reported patient identifiers and presenting symptoms for every patient. There were no “hallucinated” quantitative data. GPT was 100% accurate when tabulating ROM for MCP, PIP, DIP, TAM, and strength. GPT was unable to interpret “extension/flexion” nomenclature for 20% of patients and could not graph extension ROM without further cueing. At baseline, GPT may omit information unless specifically prompted (e.g., only reporting unilateral hand grip values for the repaired side rather than bilateral values). GPT was 100% accurate in reporting discrete pain scores; if instead a range was recorded, it reported the range 80% of the time, or opted to report the current pain level 20% of the time. GPT accurately plotted ROM and discrete pain scores over time, but incorrectly coded for non-discrete values. Conclusions:
The results indicate that GPT4 may be a powerful tool to quickly assimilate pertinent patient data during chart review, with low risk of reporting false values, but a non-negligible risk of missing nuance when coding. In addition, there remains a non-negligible risk of omitting useful information, though specific instructions remedy this. Finally, GPT performs best when instructed to complete tasks in stepwise fashion. These findings suggest that GPT has the potential to accurately report and tabulate postoperative rehab progress, but idiosyncratic approaches are likely to yield higher utility.

14th Annual Center for Musculoskeletal Research Symposium
October 17, 2024

Title: Does preoperative serum glucose control affect the incidence of postoperative complications in diabetic patients undergoing primary total hip and total knee arthroplasty?

Presenting Author: Jonathan Umelo, MD

Co-Author(s): Ayodeji Jubril, MD; Pilomena Burger, BS; Janet Tran, BS; Benjamin F Ricciardi, MD

Lab PI / Mentor: Benjamin F Ricciardi, MD

ABSTRACT

Introduction:

This study examines the 1) risk factors for worse perioperative glucose control and 2) incidence of early postoperative complications in diabetic patients undergoing THA and TKA, comparing two groups: 1) stable diabetics (HbA1c 6.5%-8% for at least one year) and 2) labile diabetics (HbA1c >8% within the past year, improved to 6.5%-8% pre-surgery).

Methods:
This IRB-approved retrospective study analyzed data from diabetic patients who underwent primary THA or TKA between June 1, 2019, and June 1, 2022. Patients were categorized based on their HbA1c levels one year prior to surgery and their diabetic control regimen: diet-controlled, oral medications, insulin, or a combination of medications. The primary outcomes included perioperative glucose control (mean and maximum levels), length of hospital stay, postoperative complications, and reoperations. Exclusion criteria included patients without primary diagnosis of osteoarthritis, <1 year follow up, & no preop A1C. Multivariable regression models were used to assess the impact of HbA1c levels, Metformin use, and racial disparities on these outcomes.

Results:
585 patients met the inclusion criteria. Patients with A1C <8 were older than those with A1C ≥8 ($p = 0.023$), but there were no significant differences in gender or racial/ethnic distribution between the groups. Patients with A1C ≥8 had significantly higher mean (171.77 mg/dL vs. 159.39 mg/dL, $p = 0.000$) and maximum (239.91 mg/dL vs. 214.63 mg/dL, $p = 0.000$) perioperative glucose levels in the hospital postoperatively, indicating poorer early glucose control. The incidence of complications were similar between the two groups (22.56% vs. 15.91%) and reoperations (7.32% vs. 4.28%) was higher in the A1C ≥8 group, but these differences were not statistically significant ($p = 0.061$ and $p = 0.134$, respectively) and peak hemoglobin A1C in the year prior to surgery was not associated with complications or reoperations odds ratio 1.17 (95% CI 0.94-1.44) and 1.12 (95% CI 0.80-1.58) respectively. Preoperative HbA1c levels were found to be the strongest predictor of early perioperative glucose control, with a statistically significant difference in both mean ($p = 0.000$) and maximum ($p = 0.000$) perioperative glucose levels. However, perioperative glucose control did not seem to influence ultimate complications or the need for revision surgery in patients who were otherwise optimized preoperatively. No significant differences in perioperative glucose control were found among patients using oral medications, insulin, or a combination of both, indicating that the type of pharmacologic management may not critically impact perioperative glucose levels. Metformin use was associated with significantly lower postoperative complication rates (OR = 0.316, $p = 0.001$), though it did not significantly affect perioperative glucose control, length of stay, or reoperation rates. Black, Non-Hispanic patients had significantly higher odds of postoperative complications (OR = 2.319, $p = 0.021$) compared to White, Non-Hispanic patients, maybe highlighting the need for targeted interventions to address these disparities.

Discussion:

This study shows that preoperative hemoglobin A1C was the strongest predictor of early postoperative serum glucose control, highlighting the importance of preoperative HbA1c optimization in the DM population. Additionally, patients with previously uncontrolled DM did not have higher perioperative glucose levels, complications, or reoperations relative to controlled DM patients providing further support that DM is an optimizable risk factor in this patient population. While diet-controlled diabetes was associated with better glucose management, the choice between oral medications and insulin did not significantly influence outcomes. The protective effect of Metformin against complications suggests a potential benefit that warrants further investigation.

14th Annual Center for Musculoskeletal Research Symposium
October 17, 2024

Title: Is Socioeconomic Status Associated with Patient-Reported Outcomes Following Thumb Basal Joint Arthroplasty for Thumb Basal Joint Osteoarthritis?

Presenting Author: Giap Vu, MD

Co-Author(s): George Siodis

Lab PI / Mentor: Constantinos Ketonis, MD, PhD

ABSTRACT

Introduction: Osteoarthritis of the thumb basal joint is a highly prevalent diagnosis affecting approximately a third of the population by age 80 years. The severity of thumb basal joint arthritis exists on a spectrum, with patients on the high end of the spectrum usually requiring surgical intervention after failing non-operative management including hand therapy, bracing, and corticosteroid injections. Multiple studies across various disciplines demonstrated an association between socioeconomic status and treatment outcomes. This study aims to investigate the relationship between socioeconomic status and patient-reported outcomes following thumb basal joint arthroplasty (tBJA) for basal joint osteoarthritis of the thumb.

Methods: We retrospectively reviewed the medical records of all adult patients 18 years of age and above who underwent primary tBJA for thumb basal joint arthritis at a single institution between January 2015 and December 2023. Patient-reported outcomes were extracted retrospectively from the Patient-Reported Outcomes Measurement Information System (PROMIS) questionnaires completed by the patients during their office visits before and after the surgery. Patient's demographic and relevant clinical information were collected from the medical record. Area Deprivation Index (ADI) was extracted based on census block group based on home address using the Neighborhood Atlas (Center for Health Disparities Research, University of Wisconsin School of Medicine and Public Health). Linear mixed-effects models were employed to assess the association between ADI and PROMIS outcomes after tBJA, controlling for potential confounders.

Results: A total of 1552 unique patients with 1850 encounters for primary tBJA for thumb basal joint arthritis met the selection criteria. Higher ADI, which reflects greater socioeconomic disadvantage, was siginificantly associated with poorer self-reported upper extremity function (PROMIS Upper Extremity scale (UE), $p < 0.001$) and physical function (PROMIS Physical Function scale (PF), $p < 0.001$) as well as higher self-reported pain interference (PROMIS Pain Interference scale (PI), $p < 0.001$) and depression (PROMIS Depression scale (D), $p = 0.005$), before or after the surgery. Self-reported depression was overall significant reduced at weeks 27-53 postoperatively (-2.27, $p = 0.049$); this improvement however was independent of ADI ($p > 0.05$). Pain interference was significantly decreased at weeks 5-14, 14-27 and 27-53 postoperatively ($p < 0.001$); this change was also independent of ADI ($p > 0.05$). Self-reported physical function and upper extremity functions were significantly decreased at weeks 0-5 (-9.7, $p < 0.001$ for PF; -10, $p < 0.001$ for UE) and weeks 5-14 postoperatively (-3.7, $p < 0.001$ for PF; -4.6, $p < 0.001$ for UE), and not significantly different from the preoperative state at weeks 14-27 and 27-53 ($p > 0.05$). Interestingly, more socioeconomically disadvantaged patients reported a significantly greater increase in both physical ($p = 0.009$) and upper extremity function ($p < 0.001$) at weeks 0-5 compared to those who were more advantaged.

Discussions: Patients who came from more socioeconomically disadvantaged neighborhoods had overall worse self-reported function, pain, and depression related to thumb basal joint arthritis, compared to those coming from more advantaged areas. However, our results suggested that the former group experienced a significantly greater increase in self-reported upper extremity and overall physical functions after undergoing tBJA. This finding indicates that patients of disadvantaged background are not only at a higher risk of functional impairment due to thumb basal joint arthritis, but also would benefit from surgical intervention to a greater extent. Further studies and advocacy efforts are needed to improve the care and mitigate the disease burden of thumb basal joint arthritis in this vulnerable population.

14th Annual Center for Musculoskeletal Research Symposium
October 17, 2024

Title: Effects of hydroxybisphosphonate-conjugate sitafloxacin on fracture healing and skeletal growth in mice

Presenting Author: Hannah Wang

Co-Author(s): Youliang Ren, Thomas Xue, Sashank Lekkala, Allie Tay, Jason Weeks, Frank H. Ebetino, Jeffrey Neighbors, Shuting Sun, Edward M. Schwarz, and Chao Xie

Lab PI / Mentor: Edward Schwarz,Chao Xie

ABSTRACT

Introduction: The eradication of methicillin-resistant Staphylococcus aureus (MRSA) infections in bones requires targeting bacteria within the osteocyte-lacuna canalicular networks (OLCN) and Staphylococcal abscess communities (SACs), which cannot be achieved with standard of care (SOC) antibiotics. To overcome this, we developed hydroxy bisphosphonate-conjugated sitafloxacin (HBCS, BV63072) for "target-and-release" drug delivery at the site of bone infection, and demonstrated its effectiveness in murine models. Towards a Phase 1 clinical trial of HBCS in infected fracture patients, we aimed to demonstrate that HBCS is innocuous to bone cells and is noninferior to zoledronic acid (ZA) in a murine closed femur fracture model.

Methods: All animal studies were performed under IACUC-approved protocols. We utilized a stabilized, closed fracture mouse model on the mid-diaphyseal region of the right femur. A femoral fracture was established on day 0. The treatments included Group 1: ZA 0.1mg/kg i.p. (single dose); Group 2: HBCS (BV63072) 3.0mg/kg/48hr i.p. until sacrifice on days 14, 21, or 28. Calcein was injected 6 days and 1 day prior to sacrifice to evaluate the mineral apposition rate (MAR) and bone formation rate (BFR). Longitudinal X-rays were obtained on day 0 and every 7 days post-operation. Mice sacrificed on days 14 and 21 were euthanized via heart perfusion using lead chromate-based Microfil (MV120) under anesthesia. The femurs and tibiae were harvested and processed for micro-CT (n=5) and histological analysis (n=5). Samples from day 28 were also assessed through biomechanical testing (n=12). We conducted an additional non-fracture model to further assess the effects of HBCS. The groups included Group 1: Untreated control; Group 2: parenteral bisphosphonate (HPHBP) 3.0mg/kg/48hr i.p.; Group 3: HBCS 3.0mg/kg/48hr
i.p.; Group 4: ZA 0.1mg/kg i.p. (single dose). Mice were sacrificed on day 14, and the femurs and tibiae were harvested and processed for dynamic histomorphometry (n=3), micro-CT (n=3), and histology (n=3). Statistical analysis was performed using one-way ANOVA with $*P < 0.05$.

Results: Micro-CT and longitudinal X-ray analysis showed that HBCS and ZA treatment both increased bone callus and vessel volume, revealing no differences in radiographic healing at the fracture site (Figure 1; A). Histology at the fracture site showed no significant difference between ZA and HBCS groups in the cartilage area. Interestingly, at 2 weeks ZA and HBCS treated mice showed similar TRAP+ stain, while at 3 weeks HBCS treated mice showed decreased TRAP+ stain at the fracture site. The HBCS group had increased Yield Torque (YT) and Rotation at Yield (RY) compared to the ZA groups. Although similar bone remodeling was seen at the fracture site, micro-CT revealed ZA treatment increased the volume and density of the growth plate compared to HBCS at 2 and 3 weeks (Figure 1; B, Figure 2; A, B, C). Histology showed an increased cartilage area for ZA treatment while HBCS had no difference compared to untreated (Figure 2; D, E). However, ZA groups increased the TRAP+ area within the tibial growth plate while HBCS groups had decreased TRAP+ area compared to untreated and ZA groups (Figure 2; F). Although there was a significant difference between ZA and HBCS in cartilage area and osteoclast activity proximal to the growth plate, Calcein labeling revealed no differences in BFR and MAR in cortical and trabecular bone.

Discussion: While both HBCS and ZA are effective in promoting fracture healing and remodeling through increased fracture callus, vascular volume, and biomechanical fracture healing, their effects on osteoclasts and bone density differ. ZA increased bone density and volume and osteoclast numbers via inhibition of osteoclast activity, whereas HBCS increased YT and RY via an unknown mechanism. Further studies are needed to confirm these effects of ZA and HBCS on fracture healing and their mechanisms of action.

14th Annual Center for Musculoskeletal Research Symposium
October 17, 2024

Title: Femoral Head Osteochondral Allograft Transplantation with Simultaneous Periacetabular Osteotomy for Femoral Head Undercoverage – A Case Series

Presenting Author: Sarah Wegman

Co-Author(s): Hashim Shaikh MD, James Brodell MD, P. Christopher Cook MD, Brian D. Giordano MD

Lab PI / Mentor: Brian D. Giordano MD

ABSTRACT

Introduction

Untreated avascular necrosis (AVN) can lead to collapse of the femoral head, which ultimately requires total hip arthroplasty (THA). Osteochondral allograft transplantation (OATS) of the femoral head was designed to restore subchondral bone and articular cartilage in post-collapse AVN, ideally preventing or delaying the need for THA. Our cohort includes patients with hip dysplasia who underwent simultaneous periacetabular osteotomy (PAO) and OATS, the outcomes of which have not previously been described.

Methods

The OATS procedure involves a vessel-sparing hip dislocation for global femoral head exposure, removal of damaged articular cartilage and subchondral bone, and then press-fit implantation of a fresh femoral head allograft. Eleven patients have undergone this procedure at our institution, and we retrospectively collected information about their procedures and recovery. We also telephoned each patient to request updated physical function (PF), depression (D), and pain interference (PI) Patient-Reported Outcome Measurement Information System (PROMIS) data.

Results

Eleven patients had AVN of the femoral head. Six of them underwent simultaneous PAO and OATS, and all had ipsilateral hip dysplasia. Postoperatively, patients returned to s bearing by an average of 9.8 ± 5.6 weeks, and sports in 9.9 ± 2.9 months. Four patients did not return to sports due to unrelated health conditions. One patient had undergone THA at the time of follow-up, six years after the OATS procedure. Five patients provided PROMIS follow-up, and on average, PF and PI scores significantly improved ($p=0.01$). There were no significant differences between preoperative and follow-up PROMIS D scores ($p=0.31$).

Discussion

Our patient cohort included those who underwent OATS alone as well as an OATS/PAO combination. The patients recovered well, returning to weight bearing in 9.8 ± 5.6 weeks and sports in 9.9 ± 2.9 months. Both PROMIS PF and PI scores improved between preoperative and recent follow-up timepoints. The femoral head OATS procedure may be a reliable treatment that can delay or eliminate the need for THA. In patients with concomitant dysplasia, combined OATS and PAO may improve outcomes.

14th Annual Center for Musculoskeletal Research Symposium
October 17, 2024

Title: Trends in Female Authorship of Spine Literature from 2002 to 2022

Presenting Author: Sarah Wegman

Co-Author(s): Dominique Rinfret, Haseeb Goheer, Mina Botros, Gabriel Ramirez, Ram Haddas, Ashley Rogerson, Varun Puvanesarajah

Lab PI / Mentor: Varun Puvanesarajah, MD

ABSTRACT

Introduction

The goal of this cross-sectional bibliometric analysis was to characterize the change in first and senior female authors from 2002 to 2022 in prominent spine journals and assess the role of female senior authorship on authorship. While disparities in gender representation in research across surgical specialties have been extensively studied over the past decade, there remains a scarcity of information on gender-based differences in authorship within the field of spine surgery.

Methods

PubMed was searched to identify articles in journals predominantly focused on spine surgery. Articles published between Jan 2000 to December 2022 from the top fifteen spine journals were queried. Articles involving in vivo data, animal studies, or a primary language other than English were excluded. Gender API was then used to determine the gender of the first and last author of each article along with its % certainty. Names with below 90% certainty were excluded from the final analysis.

Results

Overall, 15,415 pairs of names (n = 30,830) were gendered by Gender API with over 90% certainty. Of the 1,697 publications with female senior authors, 18.4% were female first authors. Comparatively, of the 13,718 publications with male senior authors, 10.4% were female first authors. Female first authorship and senior authorship rates both significantly increased between 2000 to 2022, by 6.33% and 3.26% respectively. The increase in the adjusted proportion of female first authors with a female senior author was 1.6% greater than the corresponding increase for female first authors with a male senior author.

Discussion

First and senior female authorship rates have increased significantly from 2000 to 2022 in prominent spine journals. Further research into the role of training background, level of training, and productivity would characterize possible barriers and opportunities toward gender equity in female spine surgery publication rates.

14th Annual Center for Musculoskeletal Research Symposium
October 17, 2024

Title: Tendon Impingement Produces Regional Profiles of Intact and Fragmented Aggrecan

Presenting Author: Brian Wise

Co-Author(s):

Lab PI / Mentor: Mark Buckley, Ph.D., and Whasil Lee, Ph.D.

ABSTRACT

Tendon impingement generates a unique mechanical strain environment distinguished by elevated transverse compressive strains that sustain a localized fibrocartilage phenotype enriched with glycosaminoglycans (GAGs). While fibrocartilage is a normal feature in impinged regions of healthy tendon, excess GAG content is a hallmark feature of tendinopathy, a degenerative disease that disproportionately affects impinged tendons. As such, impingement is clinically recognized as an important extrinsic factor in tendinopathy pathogenesis. Despite this, the cellular and molecular basis of impingement mechanobiology is poorly described, in part due to a lack of experimental models. To fill this void, our lab has developed a novel murine hind limb explant model for studying the mechanobiology of Achilles tendon impingement. By preserving anatomical structures of the impinged region in situ, this model allows for controlled prescription of impingement via passive ankle dorsiflexion to reproduce multiaxial strain patterns that are measurable and well-characterized. Moreover, we have demonstrated that impingement produces collagen disorganization and significant change in GAG staining, consistent with fibrocartilage formation. In this study, we utilized our explant model to study how impingement impacts turnover of aggrecan, a large, GAG-rich proteoglycan upregulated in regions of fibrocartilage. Notably, prior studies have explicated dynamic aggrecan turnover in tendon fibrocartilage via constitutive ADAMTS catabolism, with evidence that simple uniaxial compression regulates both aggrecan biosynthesis and turnover. Nevertheless, aggrecan turnover within complex, spatially heterogeneous patterns of mechanical strain generated by impingement has yet to be described. We hypothesized that impingement elicits differential regional profiles of intact and fragmented aggrecan across the Achilles tendon insertion. Further, we hypothesized that these local changes in aggrecan integrity driven by impingement correlate with spatial patterns of micromechanical tissue properties. Explants were loaded into our platform to maintain impingement of the Achilles tendon insertion for 7 days, while contralateral limbs were cultured unloaded. Level-matched tissue sections from contralateral limbs were used to assess aggrecan turnover via immunofluorescence (IF) and micromechanical tissue properties using atomic force microscopy (AFM). For evaluation of aggrecan turnover, contralateral sections were incubated pairwise (i.e., simultaneously using the same antibody solutions) with anti-Aggrecan antibodies targeting epitopes in either the G2 domain or the chondroitin sulfate-2 (CS) domain. Given the landscape of aggrecan fragments isolated from fresh and cultured tendon tissue, we expect the G2 antibodies to label intact aggrecan and most prominent fragments, serving as a proxy for total aggrecan content. In contrast, the CS antibodies target a region spanning a high affinity site of ADAMTS-4,5 proteolysis that drives constitutive aggrecan turnover and are expected to label only intact aggrecan. Our data demonstrate significantly increased G2 labeling intensity in the distal region deep within the impinged tendon insertion, adjacent to the calcaneus, without accompanying change in CS labeling intensity. Thus, impingement triggers a local increase in total aggrecan with no change in intact aggrecan, suggesting accumulation of aggrecan fragments in a region where we have previously measured significantly elevated transverse compressive strain as well as significantly decreased collagen alignment. Collectively, our data support the hypothesis that spatial patterns of mechanical strain elicit differential regional patterns of aggrecan turnover at the impinged Achilles tendon insertion. Furthermore, our findings suggest aggrecan fragmentation driven by impingement may adversely impact collagen organization and micromechanical function.

14th Annual Center for Musculoskeletal Research Symposium
October 17, 2024

Title: Attraction and Efferocytosis of apoptotic neutrophils by mesenchymal stem cells

Presenting Author: Brooke Wise

Co-Author(s): Sandra Castillo, Emily Quarato, Laura Calvi, Roman Eliseev,

Lab PI / Mentor: Roman Eliseev

ABSTRACT

Introduction:
Bone marrow, the site of turnover and differentiation of hematopoietic cells is subject to musculoskeletal diseases such as osteoporosis upon aging. Cellular senescence, a major hallmark of the aging process along with mitochondrial dysfunction contributes to this disruption of homeostasis. Billions of apoptotic neutrophils (PMN) travel to the bone marrow to be removed by macrophages in a process termed efferocytosis. Our lab previously showed that mesenchymal stem/stromal cells (MSC) act as non-professional phagocytes and aid in the clearance of PMN. The efferocytotic capacity of macrophages declines with age increasing the efferocytotic load for MSCs with a cost of oxidative stress. We hypothesized that excessive efferocytosis leads to mitochondrial dysfunction and senescence of MSCs, thereby lowering their osteogenic potential and leading to bone loss. Our first goal was to elucidate the mechanism of PMN attraction by MSCs as RNAseq revealed increased *Cxcl12* and *Cxcl1* expression in MSCs post efferocytosis. Our second goal was to test if post-efferocytotic oxidative stress causes mitochondrial dysfunction and cell senescence.

Materials and Methods:
We used human PMN and MSCs as well as MSCs from mice expressing mitochondria-targeted catalase, a major antioxidant enzyme ($mCat^{TG}$). Mitochondrial isolation and western blot were performed to verify mCat expression. Transwell migration assays and flow cytometry were used to identify the mechanism of neutrophil attraction and MSC efferocytosis. Fluorescent probes DCFDA, TMRE, and DDAOG were used to access changes in cellular ROS, mitochondrial membrane potential, and cellular senescence, respectively. Some PMN were incubated with LPS to induce an immune challenge to access ROS production by PMN. To verify CXCL12 as the major cytokine involved in PMN attraction to MSCs we used its receptor, CXCR4, inhibitor and performed a magnetic depletion of the protein from hMSC conditioned media. To access the osteogenic differentiation potential of mouse and human MSCs post efferocytosis, alkaline phosphatase enzymatic/colorimetric assays were performed.

Results:
With regards to aim 1, using the inhibitor approach, we found that CXCL12 is the main cytokine attracting PMN to MSCs. Furthermore, immunodepletion of CXCL12 from the media abrogated PMN migration towards MSCs. With regards to aim 2, we observed that DCFDA (ROS) signal was highly expressed in human and mouse MSCs post efferocytosis of PMN, indicating a significant increase in cellular ROS. Interestingly, mCat expression did not prevent the observed ROS burst suggesting that it did not originate in MSC mitochondria. Later experiments with LPS induced PMN revealed that the majority of ROS can be attributed to PMN. Additionally, flow cytometry experiments revealed a change in mitochondrial membrane potential verified by increased TMRE expression in male mCAT MSCs, with no significant changes in DDAOG senescence signal.

Discussion:
The increase in TMRE signal indicates increase oxidative phosphorylation in mCAT MSCs suggesting that catalase transgene has protective effects on mitochondria. Additionally, while cellular ROS was significantly reduced across male and female mCAT MSCs, we attribute that to the aPMN as a source as they produce ROS via NOX enzymes. Future studies will utilize NOX inhibitor, N-ethylmaleimide (NEM), to observe how NEM affects efferocytosis by MSCs, and B-galactosidase colorimetric assays to access cellular senescence post efferocytosis.

14th Annual Center for Musculoskeletal Research Symposium
October 17, 2024

Title:
Evaluation of PROMIS Outcomes in patients undergoing cubital tunnel release with and without transposition

Presenting Author:
Justin Wong, MPH

Co-Author(s):
Dominique Rinfret, BS, Thomas Carroll, MD

Lab PI / Mentor:
Constantinos Ketonis, MD/PhD

ABSTRACT

Introduction
Transposition during cubital tunnel release (CuTR) is frequently performed for the relief of symptomatic ulnar neuropathy at the surgeon's discretion. We hypothesize that patients who underwent transposition would have less severe EMG classifications and an equal change in pre-operative and post-operative PROMIS scores compared to patients with an in situ release.

Methods
A single institution, retrospective chart review of all patients who underwent a CuTR between 2015 to 2023 was conducted, yielding 1899 patients. Exclusion criteria were concomitant procedures, age <18 or >75, traumatic injury, or prior elbow surgeries. Only patients with available pre-operative and <60 days post-operative PROMIS scores were included for comparison.

Results
In total, 143 patients met the inclusion criteria (transposed: 102, in situ: 41). The groups were not statistically di erent by age, BMI, and race; however, the transposed group contained a significantly larger proportion of males and patients who underwent CuTR on the right. The EMG severity classifications, complication, and revision rates were also not significantly di erent between the in situ and transposition groups.

In the in situ group at the 2 week follow-up, there were no significant changes in PROMIS physical function (PF), pain interference (PI), and upper extremity (UE) scores compared to baseline, but there was a significant improvement in depression (DEP) scores. By the 6 week follow-up, in situ PI scores showed significant improvement.

Meanwhile, in the transposition group, there were no significant changes in PI, DEP, and UE scores at the 2 week follow-up. PF scores significantly decreased from pre-op to the 2 week follow-up but at 6 weeks, physical function scores returned to baseline as there was no longer a significant di erence from pre-op to the 6-week follow-up PF scores.

Discussion
EMG severity classification was not predictive of whether patients received in situ decompression or transposition. In the in situ group, patient depression scores and pain interference scores significantly improved at the 2- and 6-week follow-up intervals, respectively. In the transposition group, physical function scores significantly decreased from pre-op to the 2 week follow-up, then returned to baseline at the 6 week follow-up. Overall, there were minimal di erences between pre-op and post-op PROMIS scores in both the in situ and transposition groups.

14th Annual Center for Musculoskeletal Research Symposium
October 17, 2024

Title:
Factors Influencing Ulnar Nerve Transposition in Cubital Tunnel Release and Revision Surgery

Presenting Author:
Justin Wong, MPH

Co-Author(s):
Dominique Rinfret, BS, Thomas Carroll, MD

Lab PI / Mentor:
Constantinos Ketonis, MD/PhD

ABSTRACT

Introduction
Cubital tunnel release (CuTR) can be performed with or without ulnar nerve transposition, often depending on nerve instability. We hypothesize that patients who received an ulnar nerve transposition were more likely to have nerve enlargement or instability on pre-op ultrasound (US) or clinical examination but less severe EMG than in situ release patients.

Methods
Patients who underwent CuTR between 2015-2023 at a single academic institution were retrospectively analyzed. Patient demographics, clinical examination, pre-operative EMG severity classification, ulnar nerve cross-sectional area (CSA), and transposition indications were compared with either Chi-Squared and t-test.

Results
491 patients met inclusion criteria, with 335 patients in the in situ group and 156 that underwent transposition. Between the groups, race, laterality, EMG severity classifications, and complication rates were not significantly di erent, however, the transposition group was significantly younger, had a greater male percentage, and lower operative BMI. (Figure 1). The in situ group had a higher revision rate (7.2% vs. 3.2%, p = 0.12), with the main indications of recurrence and subluxation.

In patients with available pre-op US, nerve enlargement (transposed: 77.5%; in situ: 78.3%, p = 0.32) and mean CSA (Transposed: 14.8 mm2; In situ14.3 mm2; p= 0.64) did not di er between groups (Figure 2). Furthermore, within this same cohort, nerve instability was detected with ultrasound in 13.3% (n =75) of patients who underwent transposition and in 2.0% (n = 101) of patients who underwent in situ decompression (Figure 2).

Of all patients, 10.2% had a pre-operative clinical assessment of nerve instability and 23.6% had intraoperative instability, of which 90.0% and 95.7% were transposed, respectively. Overall, 72.4% of transposed patients and 1.5% of in situ patients had instability noted pre-operatively, intra-operatively, or both. When instability was not noted, reasons listed in operative notes for transposition included the severity of motor and sensory deficits and prior transposition on the contralateral limb.

Conclusion
The ultrasound CSA, EMG severity classification, and complication rates were not significantly di erent between groups. 72.4% of transposed vs. 1.5% of in situ patients had noted instability pre-operatively, intraoperatively, or both. A minority (6.4%) of transposed patients had instability noted on US.

14th Annual Center for Musculoskeletal Research Symposium
October 17, 2024

Title: Quantification of micro-CT based union ratio to characterize bone graft healing mediated by tissue-engineered periosteum

Presenting Author: Hao Wu[1]

Co-Author(s): Alyson March[2], Danielle S.W. Benoit[2]

Lab PI / Mentor: Regine Choe[2]

[1]The Institute of Optics, University of Rochester, Rochester, NY
[2]Department Of Biomedical Engineering, University of Rochester, Rochester, NY

ABSTRACT

Introduction: Decellularized cadaveric allografts are widely recognized as the "gold standard" for treating critically sized bone defects. However, they still face a significant failure rate of approximately 60% within 10 years post-surgery, primarily due to the absence of periosteum, which is crucial for bone regeneration. To enhance the healing process of these allografts, we developed the approach by coating allografts with poly(ethylene glycol) (PEG)-based hydrogels designed to mimic periosteum function. Our hypothesis was that the degradability of matrix metalloproteinases (MMPs), which are cell secreted enzymes, and the adhesiveness of ligand of this tissue-engineered periosteum (TEP) would promote the healing of grafts. To evaluate our hypothesis, we employed the union ratio, a parameter that reflects the connection area between the host callus and the graft, serving as a critical indicator of successful healing. This parameter could be obtained from analyzing micro-computed tomography (μCT) images.

Methods: A MATLAB graphical user interface (GUI) developed by David Reynolds, which enables users to manually trace the outer and inner contours of the graft for each μCT slice, is used. A semi-automated algorithm was employed to refine the contours, which are first snapped to the periosteum through edge detection, and then dilated into the darker regions (soft tissue) of the μCT images to identify the area of connection between the host callus and the graft. For each graft, the union ratio was calculated separately for its proximal and distal parts. The overall union ratio of the graft was determined by taking the minimum value between these two parts, ensuring a conservative estimate of graft healing. This method was applied to analyze μCT images of femoral bones from 40 mice at 6 and 9 weeks post-surgery. These bones include autografts, allografts, and TEP-allografts, with three variations of TEP. The union ratios of these bone grafts were statistically compared using the two-way ANOVA and Tukey's honestly significant difference test.

Results: In the first set of data, we compared the union ratios of allografts coated by
group 1: MMP-degradable TEP with adhesive RGD ligand,
group 2: MMP-degradable TEP with non-adhesive RGE control,
group 3: Non-degradable TEP with adhesive RGD ligand,
at different times (6 weeks and 9 weeks post-surgery), where RGD is Arginine-Glycine-Aspartic acid, and RGE is Arginine-Glycine-Glutamic acid. Two-way ANOVA test showed significant difference between 6 weeks and 9 weeks post-surgery, where 9 weeks has higher union ratio. However, there is no significant difference between the three groups with different degradability and adhesiveness. Despite the lack of statistical significance, contrast in union ratio is still noticeable between groups at 9 weeks post-surgery, where group 1 shows a higher average union ratio 10.23% compared to groups 2 and group 3, which had average union ratios of 5.72% and 5.26%, respectively.

Discussion: The results highlight the potential effect of MMP-degradability and ligand adhesiveness in TEP to improve the healing of allografts. To date, only the subset of μCT data of allografts that investigates the effect of degradability and adhesiveness has been analyzed. Work in progress includes evaluation of autografts and allografts, along with additional TEP variations, to provide a more comprehensive understanding of graft and TEP performance.

14th Annual Center for Musculoskeletal Research Symposium
October 17, 2024

Title: NanoString GeoMx Digital Spatial Profiling of Auto and Allo Bone Graft Healing in a Murine Segmental Femoral Bone Defect Model

Presenting Author: Xiaojie Xing

Co-Author(s): Tianfeng Miao, Samantha Mill

Lab PI / Mentor: Xinping Zhang

ABSTRACT

Autograft and allograft are commonly used in reconstruction of large bone defect caused by trauma, tumor resection and congenital conditions. Autografts demonstrate better healing than allografts, largely due to the robust osteogenic and angiogenic activities elicited by the living cells in periosteum and in autograft bone tissue. Utilizing a murine segmental femoral bone graft transplantation model, our previous studies highlight the key differences between autograft and allograft healing. Autografts exhibit enhanced periosteum-mediated endochondral bone formation and rapid bone remodeling, while allografts show suboptimal angiogenesis and a persistence of fibrotic tissue. To further elucidate the molecular and cellular mechanisms underlying the distinct healing dynamics of autografts and allografts, this study employed the NanoString GeoMx Digital Spatial Profiling technology, which allowed molecular profiling across various locations and cell types during bone graft healing. To facilitate cell type specific analyses at the site of long bone defect repair, a Col1(2.3)GFP; AplnCreER; Ai14 (tdTomato) which enabled fluorescence labeling of osteoblasts with GFP and endothelial cells (ECs) with tdTomato RFP was further used in bone graft transplantation model. Samples were harvested at weeks 1, 2, and 5 post-surgery and processed for GeoMx DSP RNA assays. About 2000-8000 DEGs in the selected ROIs were identified and used to perform gene ontology and gene enrichment analyses. Comparing bone forming ROIs in auto and allografts, genes associated with endochondral bone formation (Col 2a1, Col10a2, Ihh, and sp7) were significantly higher in autografts than in allografts at weeks 1 and 2 post-op ($p<0.05$). Gene associated with glycolysis was higher at week 1 while genes associated with oxidative phosphorylation and mitochondrion were higher in bone forming ROIs in autograft at weeks 2. When comparing bone forming ROIs with fibrotic ROIs, osteogenic genes were markedly enriched in bone forming ROIs while inflammatory genes namely IL1b, IL6 as well as IL-17 signaling were enriched in fibrotic ROIs at weeks 1, 2 and 5. The genetic labeling of osteoblasts and sprouting EC allowed us to further compare differentially expressed genes in GFP+ OB and EMCN+ EC at different ROIs in auto and allograft healing. Our analyses showed significantly enriched marker genes of osteoblasts and endothelial cells as well as disparate expression of GFP and RFP genes. Our data further revealed that compared to GFP+ OB in allografts, GFP+ OB in autografts had augmented enhanced osteogenic genes. The EMCN+ ECs coupling with osteoblasts had higher level of PDGFb and enriched PI3K-AKT pathway. In comparison, ECs in fibrotic tissue had enriched IL17 pathway genes and higher-level expression of inflammatory response genes namely IL-6 and IL-1b. Further ssGSEA analyses demonstrated higher expression of gene sets associated with oxidative phosphorylation and fatty acid metabolism in bone forming ROIs in autografts than in allografts. Consistently, gene sets of inflammatory response were higher in ECs at fibrotic ROIs of allograft and lower in bone forming ROIs of auto or allografts. Taken together, our current study revealed a heightened mitochondrial function and metabolic reprogramming in bone forming ROIs, suggesting a critical role of energy metabolism and higher demand for oxygen at the site of bone repair and remodeling. These findings align with the known high metabolic activity required for osteoblast function and bone tissue regeneration. In addition, our study also revealed the enhanced inflammatory genes and pathways in areas of persistent fibrotic tissue formation during allograft healing, providing insights into the challenges of bone allograft integration. Further analyses are needed to validate the potential targets for therapeutic intervention aimed at reducing fibrotic tissue formation and promoting better integration.

14th Annual Center for Musculoskeletal Research Symposium
October 17, 2024

Title: Do Patients with Lumbosacral Radiculopathy Require Different Ergonomic Accommodations? A Biomechanical Lifting Analysis

Presenting Author: Phillip T. Yang

Co-Author(s): Haseeb E. Goheer, Gabriel Ramirez, Andrew Megas, Ashley Rogerson, Varun Puvanesarajah, Ram Haddas

Lab PI / Mentor: Ram Haddas

ABSTRACT

INTRODUCTION: Low back pain (LBP) is a highly prevalent pathology, afflicting over 600 million people globally and accounting for 3% of emergency department visits in the United States. It is estimated that direct costs associated with LBP in the United States exceed $250 billion annually. Lumbosacral radiculopathy is a common cause of LBP; in this condition, nerve roots in the lumbosacral spine are compressed (typically due to spinal stenosis or herniated discs), contributing to weakness, pain, and muscle atrophy. As a result, lumbosacral radiculopathy can lead to altered gait mechanics and lower limb hyporeflexia. However, there has been limited exploration into the impact of this pathology on performance of physical activities and joint range of motion (RoM). Thus, the aim of this study was to compare disability between patients with lumbosacral radiculopathy and healthy controls during lifting. The findings from this effort may provide insight into the ergonomic adjustments and biomechanical effects of lumbosacral radiculopathy, as well as improve future care for patients with the condition.

METHODS: This was a retrospective cohort study of patients with symptomatic lumbosacral radiculopathy (LSR) and healthy controls (H) between 2023 and 2024 at a single institution. Inclusion criteria included: age between 30 and 70 years, presence of symptomatic degeneration in the radiculopathy cohort, and ability to stand and walk without assistance. Patients were fitted with a full-body external reflective marker set for a three-dimensional analysis of the lifting performance of the lower extremities and trunk. Each patient completed nine lifting tasks where a box weighing no more than 10% of body weight was lifted onto a one-meter-high table: three trials were completed with the box to the right, three with the box to the left, and three with the box placed centrally. Linear mixed-effects regression models were estimated with a random intercept at the subject level and only the group as a categorical independent variable. Groups were then compared using post-estimation comparisons using Stata 16.1, StataCorp, College Station TX. Statistical significance was set at $p < 0.05$.

RESULTS: Thirty-one patients with LSR and 33 controls were included in this study. The mean age of the LSR cohort was 58.0 (15.9) years, and 64.5% were female. The mean age of the control cohort (H) was 45.1 (15.0) years, and 55% were female. Patients with LSR presented with significant ergonomic differences including reduced hip flexion (asymmetry: LSR: 79.0° vs H: 90.7°, $p<0.001$; symmetry: LSR: 63.9° vs H: 72.2°, $p<0.001$), pelvic rotation (asymmetry: LSR: 45.6° vs H: 52.1°, $p=0.014$;), and lumbar spine RoM (asymmetry: LSR: 63.6° vs H: 70.8°, $p=0.004$;) compared to controls. Additionally, reduced hip (asymmetry: LSR: 90.6° vs H: 99.5°, $p=0.003$; symmetry: LSR: 90.1° vs H: 96.9°, $p=0.035$), and increase in lumbar spine (Asymmetry: LSR: 62.0° vs H: 47.9°, $p=0.038$;) angles in the sagittal plane was observed in patients with LSR compared to controls.

DISCUSSION: The results of this study support that patients with lumbosacral radiculopathy may present with varying ergonomic profiles. Patients with LSR experienced reduced hip flexion, pelvic rotation, lumbar spine RoM, and hip angles in the sagittal plane compared to controls. Thus, it appears that LSR alters the biomechanics of asymmetric and symmetric lifting, which may provide targetable interventions for physical therapy and rehabilitation to reduce the risk of worsening LSR. Future studies should continue to assess individual biomechanics in order to improve understanding of the ergonomic impacts of LSR.

SIGNIFICANCE: This study provides insight into risk factors for worsening LSR in patients completing lifting activities. Our results could lead to earlier diagnoses and improved clinical outcomes.

14th Annual Center for Musculoskeletal Research Symposium
October 17, 2024

Title: Assessing Major Osteoporotic Fracture Risk through Metacarpal Cortical Index in a Human Cadaveric Model

Presenting Author: Tony Yosick

Co-Author(s): Sophia Turbide MD

Lab PI / Mentor: Hani Awad PhD

ABSTRACT

INTRODUCTION: Osteoporosis is often called a silent bone disease because, without screening and diagnosis, bone mineral density (BMD) degradation will reduce the strength and integrity of bone and manifest as a fracture. Fracture risk can be estimated through dual-energy X-ray absorptiometry (DXA) T-Score and individual health history through FRAX. While an established clinical standard for osteoporotic fracture risk, FRAX is limited in describing limits of biomechanical energy at these fracture locations. In a review of additional quantitative methods, metacarpal cortical index (MCI) is particularly appealing due to its accessibility and ease of measurement from hand x-rays. Our objective is to understand the relationship between major osteoporotic fracture risk and energy at the fracture site and to investigate the potential of leveraging MCI to estimate BMD and predict major osteoporotic fracture risk.

METHODS: 10 female non-paired human cadaver arms (disarticulated at the elbow) were obtained through Anatomy Gifts Registry (AGR). Specimen BMD category was determined by DXA scan by Advanced Radiology on a Horizon Ci DXA System (Hologic) of the 1/3 radius. Biomechanical wrist fracture induction was performed. Specimens were dissected to expose the radius and ulna and embedded into self-curing acrylic with the forearm in pronation and a 15-degree radial abduction. Biomechanical testing was conducted using an Instron Electroplus10000 by applying a pre-load followed by a compressive load to the palm at a rate of 3.3 mm/s to simulate a fall on an outstretched hand. Following fracture induction, full hand radiographs were collected on the UltraFocus Faxitron X-Ray system (Hologic). Radiographs were analyzed to calculate the MCI. Using a linear regression fit between MCI and actual distal radius BMD, a predicted BMD was calculated. Major osteoporotic fracture risk was calculated through FRAX using patient health history and actual and predicted specimen BMDs. Results are analyzed using linear regression and descriptive statistics (R^2) to illustrate the correlation between variables and an F-test to assess the overall significance of the linear model.

RESULTS: Forearm specimens included 10 female human cadaveric donors with an average age of 80.8±13.1 years and an average BMI of 22.6±7.0 kg/m^2. All specimens were analyzed for biomechanical measurements but only 8 specimens were analyzed for FRAX measurements, as two were excluded due to age exceeding 90 years. Fracture energy displayed a modest correlation to major osteoporotic fracture risk but increased when compared against the MCI achieving R^2 values of 0.462 and 0.693, respectively. A stronger correlation is displayed when analyzing MCI against distal radius BMD with an R^2 value of 0.730. A strong correlation is seen between the actual and predicted major osteoporotic fracture risk with an R^2 of 0.902.

DISCUSSION: This study has demonstrated the potential of utilizing MCI calculated at a peripheral location to predict a distal radius BMD and major osteoporotic fracture risk. We observed modest associations between energy and major osteoporotic fracture risk that displayed with an anticipated inverse relationship. While this study illustrates the potential application of an accessible radiographic screening method, it is limited in the pilot cohort sample size, BMD distribution, fracture locations investigated, and comprehensiveness of health histories. Medical history review is limited by medications listed at time of death (not comprehensive), familial history of fracture not indicated, and variance of quantification of smoking and alcohol consumption. Calculation of FRAX values was completed using the distal radius BMD, which presents a possible limitation due to discordance from the femoral neck. Our future studies plan to expand our sample size with equal distribution across BMD categories and include analysis of another major osteoporotic fracture site, the femur.

14th Annual Center for Musculoskeletal Research Symposium
October 17, 2024

Title: Mitochondrial Metabolism Determines Mesenchymal Stem Cell Fate

Presenting Author: Yu, Chen

Co-Author(s): Sautchuk, Rubens; Eliseev, Roman A

Lab PI / Mentor: Eliseev, Roman A

ABSTRACT

Introduction: Aging-related changes in bone marrow stromal (a.k.a. mesenchymal stem) cells (BMSCs) shift cell fate away from osteogenesis and towards adipogenesis. This leads to lower bone formation and higher bone marrow fat content. The mechanism(s) underlying such changes are not completely understood. Mitochondria are important cell organelles that not only produce energy but also determine cell behavior by regulating metab-olism, signaling, calcium homeostasis, apoptosis, and other cellular processes. We have previously shown that mitochondrial activation is important during osteogenesis of BMSCs. Such activation is in large part due to a decrease in the activity of the mitochondrial permeability transition pore (mPTP) caused by downregulation of its positive regulator, cyclophilin D (CypD). We also found that in aged bone tissue, there is pathological opening of the mPTP which leads to mitochondrial dysfunction. Adipogenesis is an alternative fate for BMSCs, and the goal of our study was to determine how CypD and mPTP are regulated during this process and whether they play a role in BMSC fate shift.

Methods: RT-qPCR and western blot were performed to measure CypD expression in C3H10T1/2, a mouse embryonic mesenchymal cell line, and primary mouse BMSCs during adipogenesis. Live-cell mitochondria-spe-cific fluorescent staining and Seahorse bioenergetic profiling were used to evaluate mitochondrial morphology and function, respectively. We used CypD gene, Ppif, promoter luciferase reporter assay and ChIP-PCR to study CypD transcriptional regulation during adipogenesis. To evaluate the effect of CypD deletion or overexpression in BMSCs on bone marrow fat, we used Prx1Cre-mediated Ppifff or caPpifTG mouse models, respectively, and osmium tetroxide staining, histology analysis and immunofluorescence staining analysis.

Results: We observed that during adipogenesis, BMSCs significantly upregulate glycolysis and increase CypD expression and mPTP activity. Confocal imaging shows that mitochondria are rounded and fragmented during this process, consistent with high mPTP activity. Ppif promoter analysis reveals multiple binding sites for adipo-genic C/EBP and inflammatory NF-κB transcription factors. Luciferase assay and ChIP-PCR analysis confirm C/EBPα as a transcriptional activator of CypD. NF-κB p65 translocates to the nucleus during adipogenesis and shows synergistic effect with C/EBPα in inducing Ppif expression, suggesting a potential link between 'inflam-maging' and altered BMSC fate. In vitro CypD overexpression enhances, whereas CypD knockdown impairs adipogenesis in C3H10T1/2 cells and primary mBMSCs. Pharmacological inhibition of CypD by NIM811 also impairs adipogenesis in vitro. In vivo, Prx1Cre-mediated CypD overexpression in caPpifTG mice impairs cortical bone and, contrary to our initial hypothesis, decreases bone marrow fat in 12-month-old mice. This may be due to the observed decrease in viability of BMSCs in these mice. Currently we are investigating the potential mech-anisms of these changes in Prx1Cre;caPpifTG mice. We are also pursuing the effect of Prx1Cre-mediated CypD conditional knockout in Prx1Cre; Ppifff mice at 4-months or 12 months of age.

Discussion: BMSCs upregulate CypD expression during adipogenesis leading to increased mPTP activity, ac-tivated glycolysis and low mitochondrial function. It is consistent with the observation of fragmented and rounded mitochondria in mature adipocytes, thus establishing a metabolic profile that appears to be favorable for adipo-genic lineage. Aging and age-related diseases are associated with chronic inflammation within tissues and in-creased intracellular inflammatory signaling. Transcriptional regulation of Ppif expression by C/EBPα and NF-κB p65 suggests a potential mechanism for age-related change of differentiation capacity in BMSCs.

14th Annual Center for Musculoskeletal Research Symposium
October 17, 2024

Title: TAM Inhibitor LDC1267 Blocks Bone Marrow Stromal Cell Efferocytosis and Rescues Osteoblastic Differentiation

Presenting Author: Jane Zhang

Co-Author(s): Ronald Lakony, Emily R. Quarato, Lizz Lamere, Adam Tyrlik, Catherine Caballero, Zhiming Jin, Chunmo Chen, Nataliia Vdovichenko, Swachi Patel

Lab PI / Mentor: Laura Calvi

ABSTRACT

BACKGROUND: Osteoporosis, a loss of bone density, is heavily associated with aging and age-related processes. Bone marrow stromal cells (BMSCs), a population with osteoblastic di erentiation capacity, are key bone marrow microenvironmental regulators and help maintain skeletal integrity and bone growth. They act as non-professional phagocytes within the bone marrow, and in the setting of aging, have been shown to upregulate e erocytosis, the clearance of apoptotic cells. This process leads to increased BMSC senescence and decreased osteoblastic di erentiation. BMSC e erocytosis is initiated by the TAM receptors, for which small-molecule inhibitors have been developed. This project assesses the e ect of LDC1267, a pan-TAM inhibitor, on BMSC e erocytosis and osteoblastic di erentiation.

METHODS: Primary cells were cultured and treated with LDC1267 and analyzed for e erocytic activity and di erentiation capacity. 3-month-old C57BL/6 mice received LDC1267 (20mg/kg/day) or vehicle for 6 days and were irradiated to increase apoptotic cell burden to mimic loads seen in aging. Stained end-stage human neutrophils (PMNs) were injected into mice and bone marrow was collected and analyzed using flow cytometry 24hrs post injection.

RESULTS: In-vitro assays showed decreased e erocytosis in LDC1267-treated primary BMSCs, with limited toxicity. When BMSCs have decreased e erocytic activity they have shown increased di erentiation capacity. No significant di erence in cellular viability was seen between LDC1267 and vehicle-treated mice in the respective irradiation groups. A decrease in the percentage of e erocytic BMSCs out of all live cells was seen in LDC1267 vs vehicle-treated irradiated mice (<0.0011) without a change in e erocytic e iciency ($p<0.7228$) as measured by mean fluorescent intensity (MFI).

CONCLUSIONS: Overall, we found that despite decreased cell count due to irradiation, there was a significant decrease in BMSC e erocytosis after LDC1267 treatment in an irradiated model, mimicking the aged apoptotic cell burden in the bone marrow. Next steps include quantifying osteoblastic di erentiation in-vivo to assess the impact of the drug on skeletal formation.


1850
MELIORA
UR
MEDICINE